Multi-resonant Electromagnetic Shunt in Base Isolation for Vibration Damping and Energy Harvesting

Yalu Pei

Thesis submitted to the faculty of
Virginia Polytechnic Institute and State University
in partial fulfillment of the requirements for the degree of

Master of Science
in
Mechanical Engineering

Lei Zuo, Chair
Shashank Priya,
Muhammad R. Hajj,

Dec. 6, 2016
Blacksburg, Virginia

Multi-resonant Electromagnetic Shunt in Base Isolation for Vibration Damping and Energy Harvesting

Yalu Pei

ABSTRACT

The objective of this thesis is to develop a dual-functional approach to effectively mitigate the earthquake induced vibrations of low- or mid-rise buildings, and at the same time to efficiently harvest utility-scale energy by using an optimally configured multi-resonant electromagnetic shunt in base isolation. In this research, two multi-resonant shunt configurations, parallel and series, were proposed and optimized based on the H_2 criteria when the base isolation system is subjected to ground acceleration excitations. The performance of the proposed multi-resonant electromagnetic shunt was compared with traditional multiple tuned mass dampers (TMDs) applied to the base isolation system. It shows that, for multiple TMDs and multi-resonant electromagnetic shunt dampers with 5% total stiffness ratio, the parallel shunt electromagnetic shunt can achieve the best vibration mitigation performance among other types of multi-resonant dampers, including parallel TMDs, series TMDs and the series electromagnetic shunt damper.

Case study of a base-isolated structure was analyzed to investigate the effectiveness of the proposed multi-resonant electromagnetic shunt. It shows that both multi-mode shunt circuits outperform single mode shunt circuit by suppressing the primary and the second vibration modes simultaneously. Comparatively, the parallel shunt circuit is more effective in vibration mitigation and energy harvesting, and is also more robust in parameter mistuning than the series shunt circuit. The time history response analysis shows that, under the recorded Northridge earthquake, the instant peak power and total average power capable to be harvested by the multi-resonant shunt can reach up to 1.18 MW and 203.37KW, respectively.

This thesis further experimentally validated the effectiveness of the multi-resonant electromagnetic shunt on a scaled-down base-isolated building. The impact hammer test shows that the multi-resonant electromagnetic shunt can achieve enhanced vibration suppression by

reducing the first resonant peak by 27.50dB and the second resonant peak by 22.57dB regarding the primary structure acceleration. The shake table test shows that under scaled Kobe and Northridge earthquake signals, the electromagnetic shunt can effectively reduce the vibration resonant peak value by 38.92% and 66.61%, respectively. The voltage simultaneously generated in the multi-mode shunt circuit was also obtained, which demonstrated the dual functions of the multi-resonant electromagnetic shunt in base isolation.

Multi-resonant Electromagnetic Shunt in Base Isolation for Vibration Damping and Energy Harvesting

Yalu Pei

GENERAL AUDIENCE ABSTRACT

This thesis investigated multi-resonant electromagnetic shunt with application to base isolation for dual-functional vibration damping and energy harvesting. Two multi-mode shunt circuit configurations, namely in parallel and in series, were proposed and optimized based on the H_2 criteria, with physical meaning to minimize the RMS relative displacement for the concern of building safety subjected to broad bandwidth ground acceleration excitations. The performance of the proposed multi-resonant electromagnetic shunt was compared with traditional multiple tuned mass dampers applied to the base isolation system. It shows that, for multiple TMDs and multi-resonant electromagnetic shunt dampers with 5% total stiffness ratio, the parallel shunt electromagnetic shunt can achieve the best vibration mitigation performance among other types of multi-resonant dampers, including parallel TMDs, series TMDs and the series electromagnetic shunt damper. Case study of a base-isolated structure is analyzed in both the frequency and the time domain to investigate the effectiveness of the multi-mode electromagnetic shunt resonances. It is found that both multi-mode resonant shunt circuits outperform single mode resonant shunt circuit by suppressing the primary and the second vibration modes simultaneously. In addition, under the same stiffness ratio, parallel shunt circuit is more effective in energy harvesting and vibration suppression. And parallel shunt circuit is also more robust to parameter mistuning than series shunt circuit. This thesis further experimentally validated the effectiveness of the multi-mode electromagnetic resonances for vibration damping and energy harvesting using recorded earthquake signals on a scaled-down building.

Acknowledgments

I would like to express my thanks to everyone who helped me in this endeavor. This thesis would not have been possible without their support.

First and foremost, I would like to express my sincere gratitude to my advisor, Dr. Lei Zuo, for his support, guidance and encouragement throughout the thesis. With his valuable ideas and suggestions, I was able to overcome the major difficulties in my research work. His enthusiasm and dedication to the research motivates me to put forth my best effort. I would also like to thank Professor Muhammad R. Hajj and Professor Shashank Priya for serving on my thesis committee. Thank Dr. Alfred L. Wicks for attending my thesis defense and providing helpful comments and suggestions.

Thanks to Dr. Matthew Eatherton in Department of Civil and Environmental at Virginia Tech, for his generous assistance to the experimental testing. I also wish to expand my thanks to Dr. Kevin Kochersberger and Dr. Corina Sandu, for their kind support and encouragement during the most difficult time in my graduate program.

I thank my fellow labmates, Yilun Liu, Changwei Liang, Yue Yuan, Sijing Guo, Xiaofan Li, Yu Pan and Mincan Cao, for their assistance and discussions. They made my time at Virginia Tech more positive and enjoyable.

My deepest gratitude goes to my family for their continuous support and encouragement.

Contents

List of figures

List of tables

1. Introduction

1.1 Motivation

Civil structures, such as buildings and bridges, are very susceptible to the dynamic loadings of wind, earthquake, traffic, and human motions. Large vibration amplitudes can damage the structure or cause discomfort to its human occupants. In extreme cases, severe wind or earthquake-induced excitations may even destroy the building structure, causing significant property damage and loss of life. Over the past decades, the research on structural vibration control has mainly focused on "energy dissipation" strategy using various dampers [1]. In most situations, the mechanical energy is converted to heat, and thus energy dissipation is often associated with undesirable self-heating. Meanwhile, energy harvesting from ambient vibration sources has emerged as a prominent research area [2]. Considering the great amount vibrational energy existed in civil structures, energy harvesting damper, which is capable of converting structural vibration energy into electricity, provides a better way for structural vibration control and hazard mitigation. The green and regenerative energy harvested can serve as an alternative power supply to the seismic response monitoring system or wireless sensing networks in civil structures [3].

Electromagnetic shunt damping is a promising technique suitable for the applications in civil structures in view that structural dynamic responses typically ranges from 0.1 Hz to 20 Hz [4]. Moreover, electromagnetic shunt damper is capable of realizing structural vibration damping and energy harvesting simultaneously [5]. For high-rise buildings, the original viscous tuned mass damper (TMD) can be replaced by the electromagnetic shunt damper, which can achieve enhanced effectiveness and robustness without introducing additional mass. Besides, the electromagnetic shunt circuit can also simultaneously harvest energy, which was originally wasted by classic TMD, for potential uses [6]. For low- and mid-rise buildings, the most widely used seismic protection system is base isolation [7]. However, the base-isolated building is generally considered as a two degrees of freedom system. Traditional electromagnetic shunt circuit with single resonance is not capable of suppressing two separate vibration modes at the same time. Therefore, electromagnetic shunt with multiple resonances is required for the application in base isolation.

Inspired by multi-mode shunt damping in piezoelectric applications [8], various multi-resonant electromagnetic shunt dampers have been proposed [9]. However, the coupling effect bettwen

multi circuit branches complicates the task of implementing the required circuits. Besides, for low structural vibration frequency, large inductance values in the order of tens or hundreds of Henrys may be needed. Negative resistance may also occur due to the relatively large internal resistnace of the electromanetic transducer. In these cases, virtual inductors and resistors have to be used which are difficult to tune and sensitive to component characteristics [10]. Thus, it becomes crucial to determine the optimal circuit parameters and find a more systematic way to design the multi-resonant electromagnetic shunt damper.

1.2 Objectives of the Thesis

The objective of this thesis is to develop a dual-functional approach to effectively mitigate the earthquake induced vibrations of low- and mid-rise buildings, and at the same time to efficiently harvest utility-scale energy by using an optimally configured multi-resonant electromagnetic shunt in base isolation. Specifically,

1. Develop multi-resonant electromagnetic shunts for the base isolation system. Propose multi-mode shunt circuits to suppress both the first and second vibration modes when the system is subjected to wind force or ground motion excitations, and simultaneously harvest the vibrational energy for potential uses.

2. Optimize the proposed multi-resonant electromagnetic shunt circuits. Formulate the optimization problem for the base isolation system with multi-mode electromangetic shunts. Determine the optimal circuit parameters and find a systematic way to design the multi-resonant electromagnetic shunt circuit.

3. Conduct case study of the base isolation system with multi-resonant electromagnetic shunts. Investigate the effectiveness and robustness of the proposed multi-resonant electromangetic shunt under real earthquake excitations. Estimate the potential power that can be harvested using the proposed shunt circuits.

4. Experimentally verify the effectivensss of the multi-resonant electromagnetic shunt. Develop a multi-resonant electromagnetric shunt for an experimental base-isolated building structure using the proposed optimization method. Demonstrate dual functions in both vibration damping and energy harvesting through experimental tests.

1.3 Literature Review

1.3.1 Base isolation

Base isolation is one of the most widely used techniques for seismic isolation in civil infrastructures, such as bridges and buildings [11]. Inserted between the base of a structure and the ground, as shown in Figure 1.1, a base isolation system decouples the building structure from ground motions, effectively protecting it from external excitations, such as strong winds or unexpected earthquakes. In last few decades, base isolation has been thoroughly studied and the available technique is becoming mature and well established. Due to the ability to alter the characteristic of the structure from rigid to flexible, base isolation is more applicable to high stiffness, mid- or low-rise buildings [12]. Nowadays, an increasing number of buildings to be isolated reveals the fact that base isolation is gradually getting accepted as a proven technique in structural vibration control and hazard mitigation.
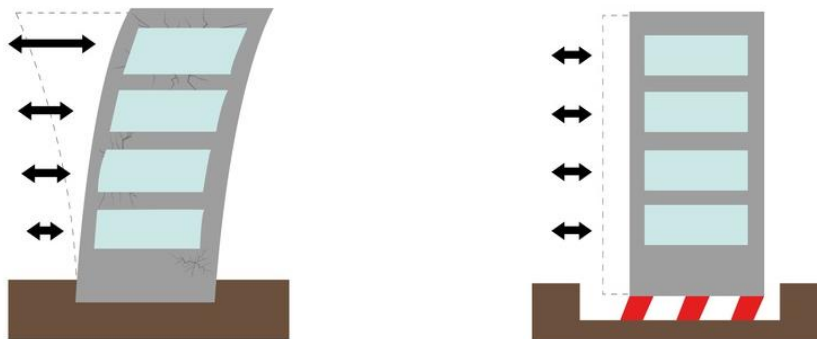
Figure 1.1 Two types of building structures: fixed-base building and base-isolated building [13]

The concept of base isolation is to shift the fundamental frequency of the combined building-isolation system to a lower value, moving away from the dominant frequency ranges of earthquakes [14]. Assuming a traditional fixed-base building, with a fundamental period of 1.0 sec or smaller, is isolated, the fundamental period is able to be enlarged to the range of 1.5 sec to 2.5 sec [15]. Because the base-isolated building has a larger fundamental period than of the corresponding fixed-base building, the first vibration mode of the isolated building only involves deformation of the base while the superstructure remains almost rigid. In addition, the isolation system can dissipate the kinetic energy so that the vibration of the primary structure can be largely

reduced [16]. Therefore, by employing base isolation technique in buildings, the structure can be essentially uncoupled from ground motions thus achieve effective seismic protection.

There are two basic components in practical base isolation systems, bearings and dampers. Bearings provide the flexibility so that the vibration period of the building structure can be increased sufficiently to reduce the system response. These bearings are usually manufactured using synthetic or natural rubbers bounded between steel plates. There are six major types of bearings which are widely used in base isolation, including ball and roller bearing, elastomeric bearing, sliding bearing, lead rubber bearing, pendulum bearing and high damping bearing [17]. In addition to a flexible mounting, dampers are also necessary in base isolation so as to enhance isolation and control the relative deflection between the structure and the ground to a practical level. The dampers in base isolation can be classified into velocity type dampers and hysteretic type dampers. The velocity type damper includes viscous damper and oil damper. The hysteretic damper includes friction damper, lead damper and steel damper [18].

Many post-earthquake studies have been conducted to assess the performance of real base-isolated buildings. S. Nagarajaiah and X. Sun [19] evaluated the effectiveness of base isolation system in buildings in the 1994 Northridge earthquakes. One of the objective is an USC hospital located in Los Angeles, California, which is an 8-storey steel braced building with 68 lead rubber isolators and 81 elastomeric isolators. Figure 1.2 shows peak responses of the story drift and shear of the building floors compared with the result assuming the building were to be fixed. The comparison clearly reflects the effectiveness of the base isolation strategy. In view of the excellent performance of base isolation, engineers are also devoted to develop detailed design and construction criteria used in base-isolated structures [20].
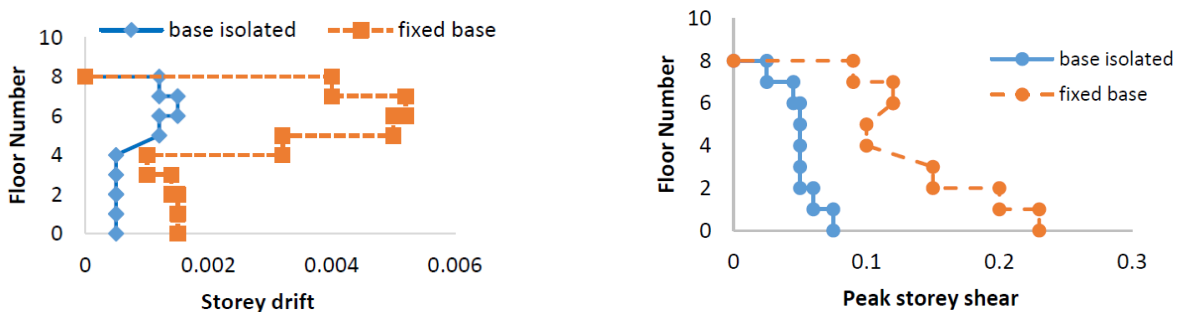
Figure 1.2 Comparison of base-isolated and fixed-base building structures: Normalized peak story shear and drift [20]

Base isolation is generally regarded as a passive method in building structural control. There are several disadvantages, for example, large seismic gaps and poor adaptability. In particular, base isolation systems are not suitable for the site with soft soil conditions [21]. To solve these problems, smart base isolation systems have been proposed and attracted increasing attention in recent years. To limit the base drift, Spencer and Sain [22] studied the combination of active control devices to the base isolation system. Reinhorn and Riley [23] experimentally verified the active control strategy used in base isolation systems. Besides, smart dampers, also called semi-active dampers, are developed for use in the base isolation which work more effectively than traditional dampers [24]. Compared with passive base isolation systems, the smart base isolation is able to realize enhanced effectiveness and robustness for different soil conditions and various ground motion excitations. Although smart base isolation strategy possesses these advantages, it also has several drawbacks, such as the complexity to implement and the additional requirement for power sources and controllers [25].

In order to further enhance the structural control performance of smart base isolation systems, a number of new base isolation systems with innovative damping devices have been proposed in recent years. V.A. Matsagar and R.S. Jangid [26] employed viscoelastic dampers in base isolation and placed them between adjacent structures, which achieves enhanced effectiveness in reducing large bearing displacements. H. Yoshioka, J. C. Ramallo and B. F. Spencer Jr. [27] proposed the use of magnetorheological damper between the base and the ground, realizing controllable damping for the building system. S. Etedali, M.R. Sohrabi and S. Tavakoli [28] studied the piezoelectric friction damper and semi-active control strategy to dissipate the excessive kinetic energy is the building structure, validated by using different earthquake inputs. Recently, electromagnetic shunt damping has become a popular technique [29]. In this thesis, a unique approach is proposed to provide enhanced structural response suppression by converting the dissipated vibration energy into electricity by using an optimally configured electricity-generating electromagnetic shunt damper.

1.3.2 Electromagnetic shunt damper

The traditional method to dissipate vibrational energy of structures is through damping devices, such as viscous dampers, friction dampers and magneto-rheological fluid dampers. The kinetic energy is converted to heat in most cases, resulting in undesirable self-heating. In recent years, energy harvesting from ambient sources has become a promising research topic. Various energy harvesting strategies, including electromagnetic and piezoelectric method, have been explored [30]. The excessive kinetic energy of structures is able to be converted into sustainable electrical energy. In civil structures, the large-scale vibrational energy provides a potential regenerative energy which can be collected for powering sensing networks or structural control systems [31]. Considering the considerable value of energy harvesters, the traditional damping devices may not be the optimal way for structural control.
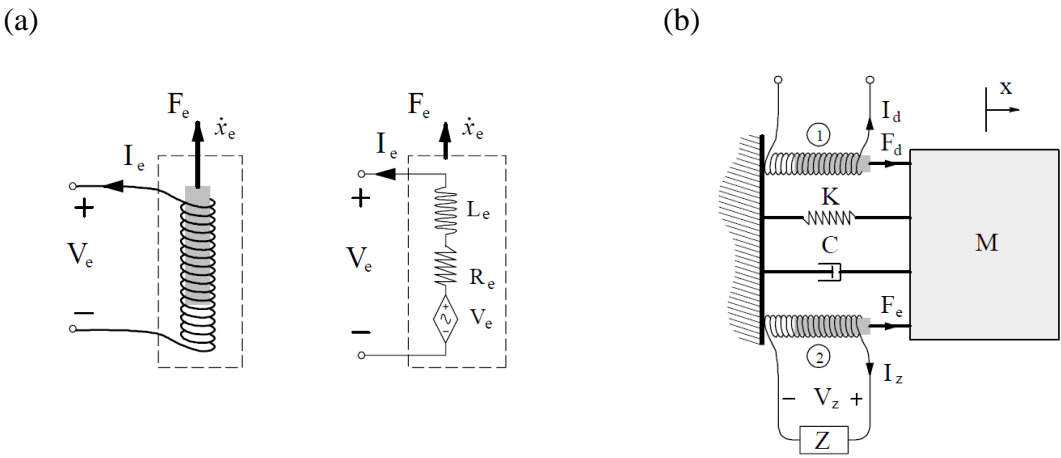
Figure 1.3 Electromagnetic shunt damper. (a) Electromagnetic transducer; (b) An electromagnetic shunted spring-mass-damper system [32]

Electromagnetic transducer, as shown in Figure 1.3(a), is basically consisted of a coil and a moving magnet. The relative motion of the magnet and the coil will generate a voltage across on the terminal of the coil. Due to the inherent inductance and internal resistance of the coil, the electromagnetic transducer is usually modelled as a dependent voltage source in series with an inductor and a resistor. Electromagnetic transducer can be employed as conventional sensors or actuators. Electromagnetic shunt damping is a technique which uses both sensing and actuating functions for structural vibration control. The relative motion between the coil and the magnet can

be mitigated by connecting an electrical impedance to the electromagnetic transducer. Figure 1.3(b) shows a simple mass-spring-damper system which is combined with an electromagnetic transducer. When the mechanical system is excited, a voltage will be generated which is proportional to the velocity of the mass. A corresponding electro-motive-force will also be induced in the electromagnetic transducer. By connecting a shunt impedance to the terminal of the electromagnetic transducer, the vibrational energy of the mechanical system can be effectively dissipated [32].

In addition to shunt damping, electromagnetic transducer can also be used for simultaneous energy harvesting. By connecting the terminals of the transducer to a power conditional circuit, the structural vibration energy can be extracted as electrical energy which can be further delivered to the energy storage element for potential uses. By properly designing the electrical circuit, the transducer is capable of suppressing the mechanical vibration significantly, and at the same time harvesting the energy otherwise dissipated by traditional dampers [33]. For civil structures, the structural responses ranges from 0.1 Hz to 20 Hz which is suitable for use of electromagnetic transducers. It can provide shunt damping for protection of building structures when subjected to wind or earthquake induced vibrations. The scavenged electrical energy can be further provided to the building when the regular power is not available in extreme situations.

Piezoelectric transducers have similar electromechanical properties. However, there are significant differences between piezoelectric and electromagnetic transducers regarding their physical and electrical characteristics [34]. One major distinction is that the electromagnetic transducer usually has a much larger stroke than the piezoelectric transducer. For applications where piezoelectric transducers cannot be applied because of the limited stroke, the electromagnetic transducer can be considered a feasible alternative. Electromagnetic shunt devices can be made at the micro-scale for MEMS uses [35], or at a very large scale such as a 50kN electrodynamic shaker [36]. Beyond the robustness, electromagnetic transducer is also much easier to drive because of its resistive-inductive characteristics.

Electromagnetic shunt damping technique has been the subject of intense research in the recent decade. Behrens et al. [37] proposed the electromagnetic shunt damping technique, validated on a basic electromagnetic mass spring system. Inoue et al. [9] optimized the parameters of a single mode electromagnetic shunt circuit by using the fixed point method to acheive the effect of tuned

vibration absorbers. Electromagnetic shunt dampers are able to be used in passive, semi-active or active modes. Palomera Arias [38] used an electromagnetic shunt device as a passive damper and investigated the influence of damping coefficients in the application of building structural control. Cheng and Oh [39] proposed a semi-active electromagnetic shunt which is capable of effectively suppressing multi-mode vibrations of a cantilever beam. Zhang and Ou [40] conducted comprehensive study in active vibration control of building structures by employing an electromagnetic shunt damper. Zuo and Cui [41] proposed the series electromagnetic tuned mass damper for dual-functional vibration control and energy harvesting, which can achieve enhanced effectiveness and robustness without suffering from large motion stroke of the series TMD. Tang et al [42] proposed closed-form H_2 and H_∞ optimal solutions of the electromagnetic resonant circuit for both vibration damping and energy harvesting. Later, Liu et al. [43] presented the exact optimal tuning laws for the energy harvesting series electromagnetic TMD and verified its effectiveness in experiments. Without introducing additional mass, electromagnetic resonant shunt method provides a convenient way realizing the vibration damping for low and middle rise buildings which are not suitable to implement large TMDs. Additionally, the vibrational energy simultaneously harvested by the shunt circuit may also be extremely valuable for providing electrical power to structural sensing and control systems .

Provided that electricity energy is properly stored in energy storage elements, e.g. supercapacitors and rechargeable batteries, Electromagnetic dampers can provide a green and regenerative power supply to portable and wireless devices at the building sites, and can serve as a superior structural element with both vibration control and energy harvesting functions. This thesis proposed a multi-mode electromagnetic shunt damper, which is supposed to be connect to the building's or structure's power grid, and will develop a complete semi-active self-powered vibration control system. When earthquake happens, the electromagnetic damper could effectively suppression the vibration and may simultaneously harvest tens of megawatts level energy, which will be extremely valuable to the vibration control and hazard mitigation.

1.3.3 Resonant shunt circuit

Resonant shunt circuit, also called shunt network, usually consists of inductors, capacitors and resistors [44]. It is able to realize effective vibration control by providing large modal damping to the mechanical system. Resonant shunt circuit can be divided into two categories, single mode shunt circuit and multi-mode shunt circuit. Single mode circuit is simple to implement, but it can only damp one vibration mode of the structure. Two examples of the single mode circuit employed in piezoelectric shunt damping are shown in Figure 1.4(a). Multi-mode circuit is capable of damping multiple vibration modes simultaneously. However, the circuit order may increase rapidly with the number of modes to be damped, making the task of implementing the circuit complicated. Two examples of the multi-mode circuit are shown in Figure 1.4(b) [45].

(a)
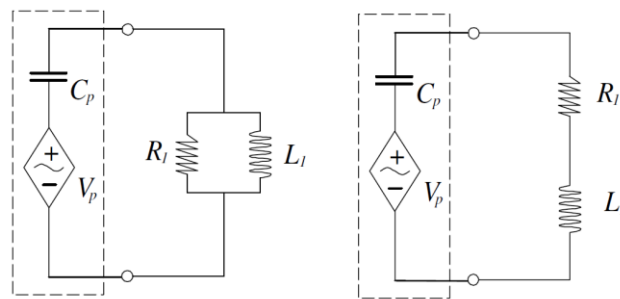
(b)
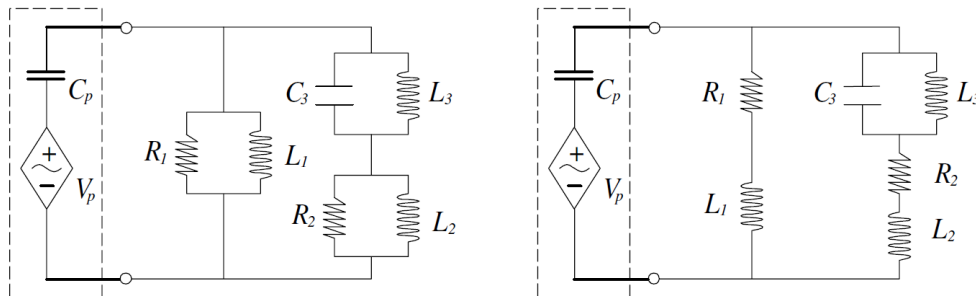
Figure 1.4. Electrical resonant shunt circuits. (a) Single-mode shunt circuits; (b) multi-mode shunt circuits [45]

The electrical resonant shunt circuit with different configurations for shunt damping and vibration control was reviewed in [46]. The first shunt circuit is proposed by Forward in 1979 [47], in which he employed an inductive (LC) shunting to mitigate resonant mechanical responses. Later,

Hagood and von Flotow [48] interpreted the behavior of the resonant shunt circuit as an analogous to a mechanical vibration absorber. The electrical resonance of the circuit can be tuned to a specific resonance frequency of the mechanical system by selecting the inductance and capacitance appropriately. Besides, when a resistive element is added, the resonant shunt will become an *RLC* circuit. By adopting a proper value of the resistance, the resonant response at the tuned frequency can be reduced.

When implementing resonant shunt circuit, one difficulty is how to determine the optimal values for the electrical elements. There are a number of techniques can be employed. One approach is to form an optimization problem to minimize the H_2 norm of a transfer function related to the mechanical system as a function of the electrical parameters [49]. Another way is to use a pole placement method, which is introduced in [48]. When properly adopted, it will result in the placement of poles with enlarged structural damping. Another difficulty, as pointed out in [8], is the need for very large inductors, maybe up to thousands of henry. Virtual grounded inductor is usually required to implement such inductive elements. In [50], Edberg et al. introduced the synthetic inductor for use in the resonant shunt circuit, in which the inductance can be adjusted by varying resistors in the network.

Multi-mode shunt damping technique, which is capable of suppressing multiple structural vibration modes simultaneously, has been the subject of intense research in recent decades. Wu et al. [51] first introduced the multi-mode shunt technique by using an RL shunt for each individual mode. He proposed the current-blocking circuit which can decoupled the multi-mode shunt by inserting additional LC circuit inside each circuit branch. Hollkamp [52] developed a multi-mode shunt circuit which is consisted of a number of parallel RLC shunt. The circuit is applied to a cantilever beam, realizing vibration suppression for several vibration modes. To simplify the implementation of multi-mode shunt circuits, the current-flowing shunt circuit was proposed in [53], in which the current-flowing network in each circuit branch is tuned to approximate a short circuit at the target resonance frequency. To reduce the values of the required inductors, a series-parallel resonant shunt is proposed in [54], which combines a current-blocking circuit and a parallel single-mode damping circuit in each sub-network. In practical applications, the sensitivity of the multi-mode shunt circuit may influence the damping performance. To solve this problem, Niederberger [55] proposed a new technique for the online adaptation of the multi-mode shunt

circuit, in which the circuit component values can be optimally tuned online, thus maintaining the good damping performance.

Inspired by multi-mode shunt damping in piezoelectric applications, researchers also introduced the multi-mode shunt circuit in electromagnetic area to achieve enhanced structural damping and vibration control. Cao and Zuo [56] proposed a two-mode electromagnetic shunt circuit, in which a current-flowing LC network is employed to decouple the influence of circuit branches on each other. The required external resistance is estimated by using the fixed point method. To simplify the implementation of the multi-mode electromagnetic shunt circuit, Cheng and Oh [57] proposed a modified current flowing multi-mode circuit for electromagnetic shunt damping of cantilever beams. The circuit configuration is concise and requires less circuit elements, however, the optimal vibration suppression performance is not achieved due to unoptimized circuit parameters. Due to the relatively large inherent inductance and internal resistance of the electromagnetic transducer, the optimal electrical parameters for the multi-mode shunt circuit may not even be achieved. To solve this problem, Zhang et al. [58] proposed a novel multi-mode shunted electromagnetic damping technique with negative inductances and resistances, which is able to cancel the inductance and resistance of the electromagnet, making it feasible to control the multi-mode vibration of the system.

Resonant shunt circuit requires less space and is more flexible to tune than classic tuned mass dampers. The circuit can be further expanded not only for structural vibration control but also for simultaneous energy harvesting functions. Multi-mode electromagnetic shunt is a promising technique allowing for multiple-mode vibration suppression. Based on the review of current research in this field, the design and implementation of the multi-mode shunt circuit needs to be further investigated. It is also crucial to find a more systematic way to determine the optimal circuit parameters for the multi-mode electromagnetic shunt circuit.

1.4 Contributions of the Thesis

The research accomplished in this thesis includes:

1) Dynamics and modeling of the base isolation with the multi-resonant electromagnetic shunt. Two multi-mode resonant shunt circuit configurations, parallel and series, were proposed. Both of the shunt circuits are capable of simultaneously mitigating both vibration modes of the base isolated structure. The performance of the multi-resonant electromagnetic shunt is compared with its equivalent multiple tuned mass dampers.

2) Design and optimization of the proposed multi-mode electromagnetic shunt circuits. The optimal parameters of the electrical circuit are obtained by optimizing the vibration mitigation performance based on the H_2 criteria. The root-mean-square value of the relative displacement between the base and the primary structure is minimized. Both the wind force excitation and earthquake ground motion excitation are considered.

3) Case study of the effectiveness of the multi-resonant electromagnetic shunt applied in a base-isolated structure under real recorded earthquake signals. The proposed parallel and series shunt circuits are analyzed and compared regarding their performance in vibration suppression and capability in energy harvesting. The sensitivity of circuit parameters for both parallel and series shunt circuits is also analyzed.

4) Experiment verification of dynamics of a designed base isolation system and optimization of the multi-mode shunt circuit. The effectiveness of the proposed multi-resonant electromagnetic shunt is validated using shake table test with scaled earthquake signals. The voltages simultaneously generated in two branches of the multi-mode shunt circuit were also obtained, which demonstrated the dual functions of the multi-resonant electromagnetic shunt in base isolation.

The research in this thesis has several scientific values. (1) The proposed research is multi-disciplinary as it blends concepts of structural, mechanical, power system, and electrical engineering for designing an optimal system for energy harvesting to enhance sustainability in structural designs, and for controlling structures to enhance their safety and reliability. (2) It has the potential to revolutionize the approach of vibration mitigation from energy dissipation to

electricity generation. The harvested energy can be utilized to provide a valuable alternative power source to seismic response monitoring or structural control systems, especially considering the possible power outage during and after earthquakes. (3) The concept of multi-resonant electromagnetic shunt can be extended to conventional base isolation for protection of the precision machine and instrumentations. By dissipating the energy induced by ambient oscillations, the damper is capable of ensuring the safety and functionality of vibration sensitive equipment.

1.5 Thesis Organization

This thesis is organized as follows. Chapter 1 presents the introduction of the thesis. Chapter 2 introduces the concept and modeling of the multi-resonant electromagnetic shunt in base isolation. Two shunt circuit configurations, parallel and series, are proposed and optimizaed based on the H_2 optimization criteria. The optimal parameters for the electromagnetic shunt circuits are determined. Chapter 3 compares the electromagnetic shunt damper with equivalent tuned mass dampers regarding their vibration mitigtion performance. Chapter 4 conducts numerical analysis for a case study, in which recorded earthquake signals are applied to a base-isolated building structure. The performance of multi-resonant electromagnetic shunt is studied and compared with single mode electromagnetic shunt. The effectiveness and robustness of parallel and series shunt circuits are investigated. In Chapter 5, a scaled-down building base isolation system is established. Both impact hammer testing and shake table testing are conducted to verify the effectiveness of the proposed multi-resonant electromagnetic shunt. The dual functions of the electromagneric shunt in both vibration damping and energy harvesitng are demonstrated. Chapter 6 gives conclusions of the thesis and recommendations for future research.

2. Modeling and Optimization of the Base Isolation System with Multi-resonant Electromagnetic Shunt Dampers

2.1 Chapter Introduction

This chapter introduces the multi-resonant electromagnetic shunt damper applied in the building base isolation system. Two multi-mode shunt circuit configurations, namely in parallel and in series, are proposed, the working principle of which is similar with traditional tuned mass dampers. The overall dynamics of the base isolation system with multi-resonant electromagnetic shunt is obtained. Both wind force excitation and earthquake ground motion excitations are considered. Since the inductance and internal resistance of the electromagnetic transducer usually could not be ignored, the way to simplify the resonant circuit while considering the influences is provided. Later, the optimization method used to optimize the design parameters of the multi-resonant electromagnetic shunt circuits is discussed. Since the wind force or earthquake ground motion excitations are of broad bandwidth, H_2 norm is employed to minimize the RMS value of the relative displacement between the base and the primary structure with the main concern of structural damage control and building safety. By minimizing the performance index regarding the vibration mitigation performance, the optimal electrical circuit parameters of the multi-resonant electromagnetic shunt can be obtained. In this chapter, the detailed design and optimization process for the parallel shunt circuit and the series shunt circuit is provided. In addition, both the wind loads and seismic excitations are considered, providing a guidance for the design of the multi-resonant shunt circuit in base isolation system under various ambient loadings. For multi-mode shunt, the circuit branches are coupled with each other. The proposed optimization method provides a systematic way to design the electrical circuit parameters thus to achieve the most effective performance for vibration mitigation.

2.2 Concept and Modeling of the Base Isolation System with Multi-resonant Electromagnetic Shunt Dampers

The concept of base isolation system with multi-resonant electromagnetic shunt is to replace the traditional oil damper in base isolation with an electromagnetic machine and shunt it with a multiple resonant circuit. The resonances of the electrical circuit can be tuned based on the vibration mitigation performance of the base isolation system when subjected to wind force or ground motion excitations. The shunt circuit also includes elements for simultaneous energy harvesting, e.g. AC-DC converter, DC-DC converter and energy storage elements. In this thesis, all the energy regulation and storage package is modeled as a pure external resistive load [59]. The energy dissipated in resistors is regarded as the harvested energy. Although resistor circuit is not a practical energy harvesting circuit, the behaviors of energy harvesters connected with resistor circuits are widely investigated for understanding their fundamental principles and optimal design rules. In this section, two multi-mode resonant shunt circuit configurations, namely, in parallel and in series, are proposed and modeled.

2.2.1 Base isolation system with electromagnetic parallel shunt damper

Figure 2.1 Base isolation system with electromagnetic parallel shunt circuit

Figure 2.1 shows the base isolation system with multi-resonant electromagnetic parallel shunt circuit. The base-isolated structure is modeled as a two degrees of freedom system moving in the

15

horizontal direction. An electromagnetic motor with inductance L_0 and internal resistance R_0 is placed between the base and the ground. The parallel shunt circuit, similar with the modified current flowing multi-mode resonant circuit in [39], is consisted of two RLC resonant circuit in parallel. The parallel shunt circuit itself behaves similarly as two TMDs in parallel, as shown in Figure 2.2.
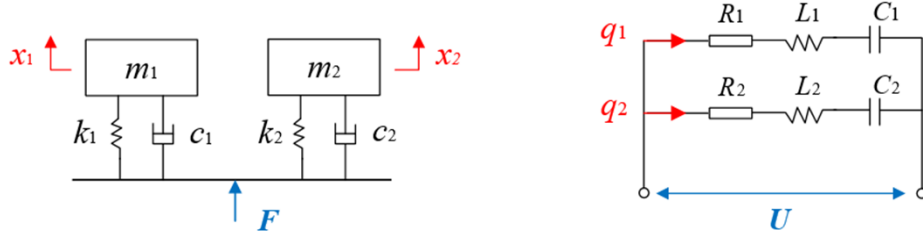
Figure 2.2 Parallel TMDs and analogous electrical parallel shunt circuit

The differential equations of the two parallel systems are of the same form as shown in Eq. (2.1) and Eq. (2.2).

$$m_i \ddot{x}_i + c_i \dot{x}_i + k_i x_i = F \tag{2.1}$$

$$L_i \ddot{q}_i + R_i \dot{q}_i + \frac{1}{C_i} q_i = U \tag{2.2}$$

where m_i, c_i, k_i (i=1~2) are mass, damping and stiffness parameters of the two TMDs. F is the applied force. L_i, R_i, C_i (i=1~2) are inductance, resistance and capacitance of the electrical resonant circuit. U is the induced voltage.

Although parallel shunt circuit is equivalent to the parallel TMDs, when combined into a vibration system, the electromagnetic shunt circuit is not exactly the same as the class TMD [14]. Thus, the performance of the multi-resonant electromagnetic shunt circuit needs to be further analyzed considering the primary system.

When the base isolation system is excited by wind force F_w or ground motion acceleration $\ddot{x}_g$, the base motion produces an induce voltage, e_{EMF}, which is proportional to the base velocity $\dot{x}_b$. At the same time, the electrical current in the electromagnetic transducer will produce a force f_{EMF}, which is proportional to the electrical current. Thus,

$$e_{EMF} = k_v \dot{x}_b, \qquad f_{EMF} = k_f i \tag{2.3}$$

where the proportional gain k_v [V/(m/s)] and k_f [N/A] is the voltage constant and the force constant of the electromagnetic transducer, respectively. Usually $k_v=k_f$ is assumed for an ideal transducer without energy loss.

The overall dynamic equations of the base isolation system with multi-resonant electromagnetic parallel shunt circuit are given by,

$$m_b\ddot{x}_b + k_b x_b - k_s(x_s - x_b) - c_s(\dot{x}_s - \dot{x}_b) - k_f(\dot{q}_1 + \dot{q}_2) = -m_b\ddot{x}_g$$

$$m_s\ddot{x}_s + k_s(x_s - x_b) + c_s(\dot{x}_s - \dot{x}_b) = F_w - m_s\ddot{x}_g$$

$$k_v\dot{x}_b + L_1\ddot{q}_1 + R_1\dot{q}_1 + \frac{1}{C}q_1 = 0$$

$$L_1\ddot{q}_1 + R_1\dot{q}_1 + \frac{1}{C_1}q_1 = L_2\ddot{q}_2 + R_2\dot{q}_2 + \frac{1}{C_2}q_2 \tag{2.4}$$

where x_s and x_b are the displacement of primary structure and the base. $\dot{q}_1$ and $\dot{q}_2$ are the electrical current in each circuit branch. m_s and m_b are the mass of the primary structure and the base. c_s is the damping coefficient of the primary structure. k_s and k_b are the stiffness of the primary structure and the base. L_1, C_1, R_1 and L_2, C_2, R_2 are the inductance, capacitance and resistance of the first and second branch of the parallel circuit.

To simplify the multi-mode shunt circuit design, the inductance L_0 and internal resistance R_0 is neglected during the dynamic modeling. After optimal electrical elements in the parallel shunt circuit are determined, the actual required values of the inductances and resistances can be obtained by considering the equivalent circuit as shown in Figure 2.3.
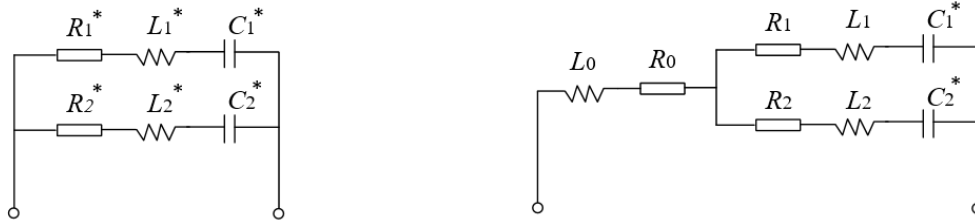
Figure 2.3 Equivalent circuit with inductance L_0 and resistance R_0 of the electromagnetic motor

According to the total impedance of the circuit, by setting the two resonant frequencies of the circuit be the same, the following equations can be obtained.

$$L_0L_1 + L_0L_2 + L_1L_2 = L_1^*L_2^*$$

$$L_0(R_1 + R_2) + L_1(R_0 + R_2) + L_2(R_0 + R_1) = L_1^*R_2^* + L_2^*R_1^*$$

$$C_1^*(R_0 + R_1) + C_2^*(R_0 + R_2) = C_1^*R_1^* + C_2^*R_2^*$$

$$L_0(C_1^* + C_2^*) + L_1C_1^* + L_2C_2^* + C_1^*C_2^*(R_0R_1 + R_0R_2 + R_1R_2) = C_1^*L_1^* + C_2^*L_2^* + C_1^*C_2^*R_1^*R_2^* \quad (2.5)$$

Eq. (2.5) can be numerically solved after the optimal electrical circuit elements $C_1^*, R_1^*, C_2^*, R_2^*$ are determined. The actual required inductance and resistance L_1, L_2, R_1, R_2 for the parallel shunt circuit can thus be obtained. This provides an easier and systematic way to design the multi-mode shunt circuit when the inductance L_0 and internal resistance R_0 of the electromagnetic motor is considered.
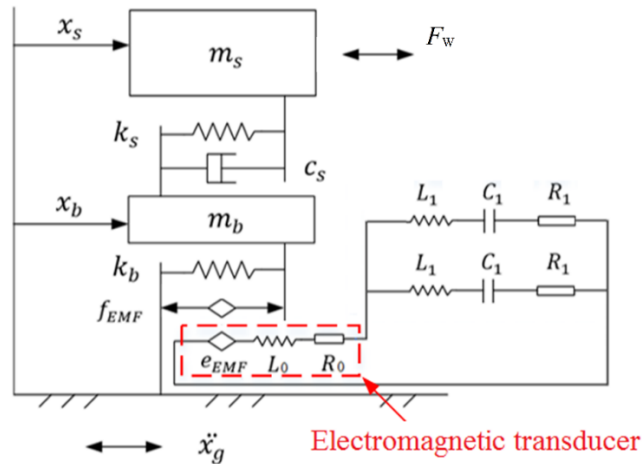
2.2.2 Base isolation system with electromagnetic series shunt damper
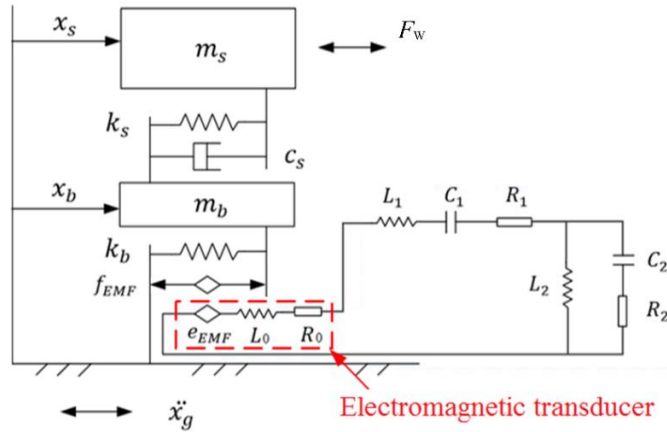
Figure 2.4 Base isolation system with electromagnetic series shunt circuit

Figure 2.4 shows the base isolation system with electromagnetic series shunt circuit, which is proposed based on the concept of series multiple TMDs. According to [60], series multiple TMDs are more effective than all the other types of TMDs of the same mass ratio. Besides, series two TMDs are more robust to parameters change in the absorbers than parallel two TMDs. Since the resonant shunt circuit behaves similarly with equivalent TMDs, the effectiveness and robustness of series shunt circuit in base isolation system will be investigated. In electromagnetic shunt damping, the stiffness ratio (the electromagnetic mechanical coupling stiffness k_vk_f/L divided by the stiffness

k_s of the original system) plays a similar role as the mass ratio in multiple TMDs [43]. Thus, we expect to find the performance of the series shunt circuit when compared to the parallel shunt circuit with the same stiffness ratio. In addition, as both parallel and series shunt circuit are capable of harvesting vibration energy simultaneously, the potential power that can be collected by the two shunt circuits will also be analyzed.
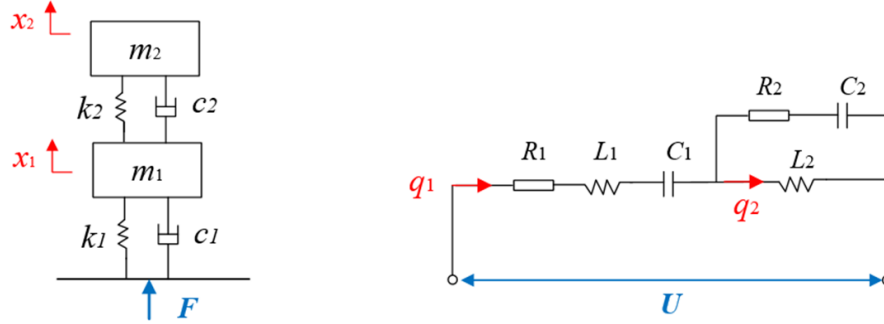
Figure 2.5 Series TMDs and analogous electrical series shunt circuit

As shown in Figure 2.5, the series shunt circuit is proposed according to series multiple TMDs based on the electrical-mechanical analogies [61]. The two series systems are of the same form dynamic equations as shown in Eq. (2.6) and Eq. (2.7).

$$\begin{bmatrix} m_1 & 0 \\ 0 & m_2 \end{bmatrix} \begin{bmatrix} \ddot{x}_1 \\ \ddot{x}_2 \end{bmatrix} + \begin{bmatrix} c_1 + c_2 & -c_2 \\ -c_2 & c_2 \end{bmatrix} \begin{bmatrix} \dot{x}_1 \\ \dot{x}_2 \end{bmatrix} + \begin{bmatrix} k_1 + k_2 & -k_2 \\ -k_2 & k_2 \end{bmatrix} \begin{bmatrix} x_1 \\ x_2 \end{bmatrix} = \begin{bmatrix} F \\ 0 \end{bmatrix} \tag{2.6}$$

$$\begin{bmatrix} L_1 & 0 \\ 0 & L_2 \end{bmatrix} \begin{bmatrix} \ddot{q}_1 \\ \ddot{q}_2 \end{bmatrix} + \begin{bmatrix} R_1 + R_2 & -R_2 \\ -R_2 & R_2 \end{bmatrix} \begin{bmatrix} \dot{q}_1 \\ \dot{q}_2 \end{bmatrix} + \begin{bmatrix} \frac{1}{C_1} + \frac{1}{C_2} & -\frac{1}{C_2} \\ -\frac{1}{C_2} & \frac{1}{C_2} \end{bmatrix} \begin{bmatrix} q_1 \\ q_2 \end{bmatrix} = \begin{bmatrix} U \\ 0 \end{bmatrix} \tag{2.7}$$

The overall dynamic equations of the base isolation system with electromagnetic series shunt circuit are given by,

$$m_b \ddot{x}_b + k_b x_b - k_s(x_s - x_b) - k_f \dot{q}_1 = -m_b \ddot{x}_g$$

$$m_s \ddot{x}_s + k_s(x_s - x_b) = -m_s \ddot{x}_g$$

$$k_v \dot{x}_b + L_1 \ddot{q}_1 + R_1 \dot{q}_1 + \frac{1}{C} q_1 + L_2 \ddot{q}_2 = 0$$

$$L_2 \ddot{q}_2 = R_2(\dot{q}_1 - \dot{q}_1) + \frac{1}{C_2}(q_1 - q_2) \tag{2.8}$$

All parameters remain the same as those in the modeling of parallel shunt circuit. Specifically, $\dot{q}_1$ and $\dot{q}_2$ are the electrical current flowing across the inductors in the primary branch and side branch, respectively. L_1, C_1, R_1 and L_2, C_2, R_2 are the inductance, capacitance and resistance of the main and side branch of the series circuit.

In the modeling, the inductance L_0 and internal resistance R_0 of the electromagnetic motor are also not considered. For series shunt circuit, when the optimal electrical elements are determined, the actual required inductance and resistance for the side circuit branch remains the same $L_2 = L_2^*$ and $R_2 = R_2^*$, while for the main circuit branch, the inductance and resistance can be obtained by,

$$L_1 = L_1^* - L_0, \ \ R_1 = R_1^* - R_0 \tag{2.9}$$

where L_1^*, L_2^* are optimal inductances for the series shunt circuit. L_1, L_2 are actual required inductances. R_1^*, R_2^* are optimal resistances for the sereis shunt circuit, R_1, R_2 are actual required resistances.

2.3 Optimization of the Base Isolation System with Multi-resonant Electromagnetic Shunt Dampers

2.3.1 Optimization problem formulation

The optimization problem of the base isolation system with multi-resonant electromagnetic shunt is how to tune the electrical circuit parameters of the multi-mode resonant circuit to minimize the building's vibration when the primary structure is subjected to wind- or earthquake-induced excitations. In practical terms, the optimization problem is how to choose optimal capacitances C_1, C_2 and resistances R_1, R_2 of the multi-mode resonant circuit to minimize the vibration of the base isolation system for the given base-isolated structure m_s, k_s, m_b, k_b, with selected electromagnetic motor k_v, k_f and inducors L_1, L_2. Or equivalently, how to optimize dimensionless parameters of the electrical tuning ratios f_{e1}, f_{e2} and the electrical damping ratios ξ_{e1}, ξ_{e2} for the given mechanical mass ratio μ, frequency ratio f_b, and stiffness ratios μ_{k1}, μ_{k2} so that the performance index *PI* regarding the vibration mitigation of the building is minimized. The dimensionless parameters are defined as,

$$\mu = \frac{m_b}{m_s}, \ f_b = \frac{\omega_b}{\omega_s}, \ \mu_{k1} = \frac{k_v k_f}{L_1 k_b}, \ \mu_{k2} = \frac{k_v k_f}{L_2 k_b}$$

$$f_{e1} = \frac{\omega_{e1}}{\omega_s} = \frac{\sqrt{1/(L_1 C_1)}}{\sqrt{k_s/m_s}}, \ f_{e2} = \frac{\omega_{e2}}{\omega_s} = \frac{\sqrt{1/(L_2 C_2)}}{\sqrt{k_s/m_s}}$$

$$\xi_{e1} = \frac{R_1}{2L_1 \omega_{e1}} = \frac{R_1}{2\sqrt{L_1/C_1}}, \ \xi_{e2} = \frac{R_2}{2L_2 \omega_{e2}} = \frac{R_2}{2\sqrt{L_2/C_2}} \tag{2.10}$$

As mentioned above, the dimensionless parameters μ_{k1}, μ_{k2} are also called electromagnetic mechanical coupling coefficient, which play similar roles as the mass ratio in TMDs.

2.3.2 H_2 optimization for the force excitation system

The wind-induced force excitation is of broad bandwidth. H_2 norm is better for evaluating the system performance since it is the root mean square (RMS) value of the performance under unit Gaussian white noise input [42]. The performances of building include building safety, people comfort (equipment protection) and energy harvesting, which are related to the relative displacement between the base and primary structure, the absolute acceleration of the primary structure and the electrical current in the harvesting circuit, respectively. In practice, building safety is normally the highest priority under extreme external excitations. Thus, in this paper, we minimize the H_2 norm form the ground acceleration $\ddot{x}_g$ to the relative displacement x_r to achieve the best effectiveness on improving the performance of building safety. The performance index (*PI*) for force excitation is defined as,

$$PI_f = \left\| H_f^r(\alpha) \right\|_2^2 = \frac{1}{2\pi} \int_{-\infty}^{\infty} \left| \frac{X_r(j\alpha)}{F_w(j\alpha)/k_s} \right|^2 d\alpha = \frac{1}{2\pi} \int_{-\infty}^{\infty} \left| \frac{Num(j\alpha)}{Den(j\alpha)} \right|^2 d\alpha \tag{2.11}$$

where $\frac{X_r(j\alpha)}{F_w(j\alpha)/k_s}$ is the normalized transfer function $H_f^r(\alpha)$ from $F_w(j\alpha)/k_s$ to x_r, which can be expressed as: $\frac{Num(j\alpha)}{Den(j\alpha)}$, in which,

$$Num(j\alpha) = (j\alpha)^6 + A_5(j\alpha)^5 + A_4(j\alpha)^4 + A_3(j\alpha)^3 + A_2(j\alpha)^2 + A_1(j\alpha) + A_0$$

$$Den(j\alpha) = (j\alpha)^8 + B_7(j\alpha)^7 + B_6(j\alpha)^6 + B_5(j\alpha)^5 + B_4(j\alpha)^4 + B_3(j\alpha)^3 + B_2(j\alpha)^2 + B_1(j\alpha) + B_0$$

For the parallel shunt circuit, the parameters A_i (i=0~5) and B_j (j=0~7) are determined by,

$$A_0 = f_b^2 f_{e1}^2 f_{e2}^2$$

$$A_1 = f_b^2 (2\xi_{e1} f_{e1} f_{e2}^2 + 2\xi_{e2} f_{e2} f_{e1}^2)$$

$$A_2 = f_{e1}^2 f_{e2}^2 + f_b^2 (f_{e1}^2 + f_{e2}^2 + \mu_{k1} f_{e2}^2 + \mu_{k2} f_{e1}^2 + 4\xi_{e1} f_{e1} \xi_{e2} f_{e2})$$

$$A_3 = 2\xi_{e1} f_{e1} (f_{e2}^2 + f_b^2 + \mu_{k2} f_b^2) + 2\xi_{e2} f_{e2} (f_{e1}^2 + f_b^2 + \mu_{k1} f_b^2)$$

$$A_4 = f_{e1}^2 + f_{e2}^2 + f_b^2 (1 + \mu_{k1} + \mu_{k2}) + 4\xi_{e1} f_{e1} \xi_{e2} f_{e2}$$

$$A_5 = 2\xi_{e1} f_{e1} + 2\xi_{e2} f_{e2}$$

$$B_0 = f_b^2 f_{e1}^2 f_{e2}^2$$

$$B_1 = f_b^2 (2\xi_{e1} f_{e1} f_{e2}^2 + 2\xi_{e2} f_{e2} f_{e1}^2)$$

$$B_2 = f_b^2 (f_{e1}^2 + f_{e2}^2 + \mu_{k1} f_{e2}^2 + \mu_{k2} f_{e1}^2 + f_{e1}^2 f_{e2}^2) + f_{e1}^2 f_{e2}^2 \left(1 + \frac{1}{\mu}\right) + 4\xi_{e1} f_{e1} \xi_{e2} f_{e2} f_b^2$$

$$B_3 = 2\xi_{e1} f_{e1} \left(f_b^2 + \mu_{k2} f_b^2 + f_{e2}^2 + \frac{f_{e2}^2}{\mu} + f_{e2}^2 f_b^2\right) + 2\xi_{e2} f_{e2} \left(f_b^2 + \mu_{k1} f_b^2 + f_{e1}^2 + \frac{f_{e1}^2}{\mu} + f_{e1}^2 f_b^2\right)$$

$$B_4 = f_{e1}^2 \left(1 + \frac{1}{\mu} + f_b^2 + \mu_{k2} f_b^2 + f_{e2}^2\right) + f_{e2}^2 \left(1 + \frac{1}{\mu} + f_b^2 + \mu_{k1} f_b^2\right) + f_b^2 (1 + \mu_{k1} + \mu_{k2})$$

$$+ 4\xi_{e1} f_{e1} \xi_{e2} f_{e2} (1 + \frac{1}{\mu} + f_b^2)$$

$$B_5 = 2\xi_{e1} f_{e1} \left(1 + \frac{1}{\mu} + f_b^2 + f_{e2}^2 + \mu_{k2} f_b^2\right) + 2\xi_{e2} f_{e2} \left(1 + \frac{1}{\mu} + f_b^2 + f_{e1}^2 + \mu_{k1} f_b^2\right)$$

$$B_6 = f_{e1}^2 + f_{e2}^2 + f_b^2 (1 + \mu_{k1} + \mu_{k2}) + 1 + \frac{1}{\mu} + 4\xi_{e1} f_{e1} \xi_{e2} f_{e2}$$

$$B_7 = 2\xi_{e1} f_{e1} + 2\xi_{e2} f_{e2}$$

For the series shunt circuit, the form of Eq. (2.11) remains the same. The parameters A_i (i=0~5) and B_j (j=0~7) are determined by,

$$A_0 = f_b^2 f_{e1}^2 f_{e2}^2$$

$$A_1 = f_b^2 (2\xi_{e1} f_{e1} f_{e2}^2 + 2\xi_{e2} f_{e2} f_{e1}^2)$$

$$A_2 = f_{e1}^2 f_{e2}^2 + f_b^2 (f_{e1}^2 + f_{e2}^2 + \mu_{k1} f_{e2}^2) + 4\xi_{e1} f_{e1} \xi_{e2} f_{e2} f_b^2$$

$$A_3 = 2\xi_{e1} f_{e1} (f_b^2 + f_{e2}^2) + 2\xi_{e2} f_{e2} (f_b^2 + f_{e1}^2 + \mu_{k1} f_b^2) + 2\xi_{e2} f_{e2} f_b^2 \mu_{k1} / \mu_{k2}$$

$$A_4 = f_{e1}^2 + f_{e2}^2 + f_b^2 + \mu_{k1}f_b^2 + 4\xi_{e1}f_{e1}\xi_{e2}f_{e2}$$

$$A_5 = 2\xi_{e1}f_{e1} + 2\xi_{e2}f_{e2} + \frac{2\xi_{e2}f_{e2}\mu_{k1}}{\mu_{k2}}$$

$$B_0 = f_b^2 f_{e1}^2 f_{e2}^2$$

$$B_1 = f_b^2(2\xi_{e1}f_{e1}f_{e2}^2 + 2\xi_{e2}f_{e2}f_{e1}^2)$$

$$B_2 = f_b^2(f_{e1}^2 + f_{e2}^2 + \mu_{k1}f_{e2}^2 + f_{e1}^2 f_{e2}^2) + f_{e1}^2 f_{e2}^2\left(1 + \frac{1}{\mu}\right) + 4\xi_{e1}f_{e1}\xi_{e2}f_{e2}f_b^2$$

$$B_3 = 2\xi_{e1}f_{e1}\left(f_b^2 + f_{e2}^2 + \frac{f_{e2}^2}{\mu} + f_{e2}^2 f_b^2\right) + 2\xi_{e2}f_{e2}\left(f_b^2 + \mu_{k1}f_b^2 + f_{e1}^2 + \frac{f_{e1}^2}{\mu} + f_{e1}^2 f_b^2 + \frac{f_b^2\mu_{k1}}{\mu_{k2}}\right)$$

$$B_4 = f_b^2 + \mu_{k1}f_b^2 + f_{e1}^2\left(1 + \frac{1}{\mu} + f_b^2 + f_{e2}^2\right) + f_{e2}^2\left(1 + \frac{1}{\mu} + f_b^2 + \mu_{k1}f_b^2\right) + 4\xi_{e1}f_{e1}\xi_{e2}f_{e2}(1 + \frac{1}{\mu} + f_b^2)$$

$$B_5 = 2\xi_{e1}f_{e1}\left(1 + \frac{1}{\mu} + f_b^2 + f_{e2}^2 + \mu_{k2}f_b^2\right) + 2\xi_{e2}f_{e2}\left(1 + \frac{1}{\mu} + f_b^2 + f_{e1}^2 + \frac{\mu_{k1}}{\mu_{k2}} + \frac{f_b^2\mu_{k1}}{\mu_{k2}} + \frac{\mu_{k1}}{\mu\mu_{k2}}\right)$$

$$B_6 = f_{e1}^2 + f_{e2}^2 + f_b^2 + 1 + \frac{1}{\mu} + 4\xi_{e1}f_{e1}\xi_{e2}f_{e2} + \mu_{k1}f_b^2$$

$$B_7 = 2\xi_{e1}f_{e1} + 2\xi_{e2}f_{e2}(1 + \mu_{k1}/\mu_{k2})$$

The integral in Eq. (2.11) can be solved using the residue theorem, the general formula of which can be found in the appendix. Hence, the performance index PI_g can be obtained explicitly as a function of the four design parameters $f_{e1}, \xi_{e1}, \xi_{e2}, f_{e2}$ and given parameters, $\mu, f_b, \mu_{k1}, \mu_{k2}$. By using numerical algorithms for the constrained global optimization problem, which is directly available in numerous commercial software optimization packages, the minimum value of the performance index PI_g can be obtained, and optimal dimensionless tuning parameters $f_{e1}^{opt}, \xi_{e1}^{opt}, f_{e2}^{opt}, \xi_{e2}^{opt}$ can thus be determined.

After obtaining optimal dimensionless tuning parameters, the corresponding optimal value for the electrical circuit elements C_i^{opt}, R_i^{opt} (i=1~2) can be obtained by,

$$C_i^{opt} = \frac{\mu_{ki}k_b}{k_v k_f f_{ei}^{opt^2}\omega_s^2}, \quad R_i^{opt} = \frac{2k_v k_f f_{ei}^{opt}\xi_{ei}^{opt}\omega_s}{\mu_{ki}k_b} \tag{2.12}$$

2.3.3 H_2 optimization for the ground excitation system

For the base isolation system with ground excitation, the performance index is defined as,

$$PI_g = \left\| H_g^r(\alpha) \right\|_2^2 = \frac{1}{2\pi} \int_{-\infty}^{\infty} \left| \frac{X_r(j\alpha)}{\ddot{X}_g(j\alpha)/\omega_s^2} \right|^2 d\alpha = \frac{1}{2\pi} \int_{-\infty}^{\infty} \left| \frac{Num(j\alpha)}{Den(j\alpha)} \right|^2 d\alpha \qquad (2.13)$$

where $\frac{X_r(j\alpha)}{\ddot{X}_g(j\alpha)/\omega_s^2}$ is the normalized transfer function $H_g^r(\alpha)$ from $\ddot{x}_g/\omega_s^2$ to x_r, which can also be expressed as: $\frac{Num(j\alpha)}{Den(j\alpha)}$, in which,

$$Num(j\alpha) = A_4(j\alpha)^4 + A_3(j\alpha)^3 + A_2(j\alpha)^2 + A_1(j\alpha) + A_0$$

$$Den(j\alpha) = (j\alpha)^8 + B_7(j\alpha)^7 + B_6(j\alpha)^6 + B_5(j\alpha)^5 + B_4(j\alpha)^4 + B_3(j\alpha)^3 + B_2(j\alpha)^2 + B_1(j\alpha) + B_0$$

For the parallel shunt circuit, the parameters A_i ($i=0\sim4$) and B_j ($j=0\sim7$) are determined by,

$$A_0 = f_b^2 f_{e1}^2 f_{e2}^2$$

$$A_1 = f_b^2(2\xi_{e1}f_{e1}f_{e2}^2 + 2\xi_{e2}f_{e2}f_{e1}^2)$$

$$A_2 = f_b^2 f_{e1}^2(1 + \mu_{k2}) + f_b^2 f_{e2}^2(1 + \mu_{k1}) + 4\xi_{e1}f_{e1}\xi_{e2}f_{e2}f_b^2$$

$$A_3 = 2\xi_{e1}f_{e1}f_b^2(1 + \mu_{k2}) + 2\xi_{e2}f_{e2}f_b^2(1 + \mu_{k1})$$

$$A_4 = f_b^2(1 + \mu_{k1} + \mu_{k2})$$

$$B_0 = f_b^2 f_{e1}^2 f_{e2}^2$$

$$B_1 = f_b^2(2\xi_{e1}f_{e1}f_{e2}^2 + 2\xi_{e2}f_{e2}f_{e1}^2)$$

$$B_2 = f_{e1}^2 f_{e2}^2\left(1 + \frac{1}{\mu} + f_b^2\right) + f_b^2(f_{e1}^2 + f_{e2}^2 + f_{e1}^2\mu_{k2} + f_{e2}^2\mu_{k1} + 4\xi_{e1}f_{e1}\xi_{e2}f_{e2})$$

$$B_3 = 2\xi_{e1}f_{e1}\left(f_b^2 + f_b^2\mu_{k2} + \frac{f_b^2 f_{e2}^2 + f_{e2}^2 + f_{e2}^2}{\mu}\right) + 2\xi_{e2}f_{e2}\left(f_b^2 + f_b^2\mu_{k1} + \frac{f_b^2 f_{e1}^2 + f_{e1}^2 + f_{e1}^2}{\mu}\right)$$

$$B_4 = f_{e1}^2\left(1 + \frac{1}{\mu} + f_b^2 + f_{e2}^2 + \mu_{k2}f_b^2\right) + f_{e2}^2\left(1 + \frac{1}{\mu} + f_b^2 + \mu_{k1}f_b^2\right) + 4\xi_{e1}f_{e1}\xi_{e2}f_{e2}\left(1 + \frac{1}{\mu} + f_b^2\right)$$
$$\quad + f_b^2(1 + \mu_{k1} + \mu_{k2})$$

$$B_5 = 2\xi_{e1}f_{e1}\left(1 + \frac{1}{\mu} + f_b^2 + f_{e2}^2 + \mu_{k2}f_b^2\right) + 2\xi_{e2}f_{e2}\left(1 + \frac{1}{\mu} + f_b^2 + f_{e1}^2 + \mu_{k1}f_b^2\right)$$

$$B_6 = f_{e1}^2 + f_{e2}^2 + 1 + \frac{1}{\mu} + f_b^2(1 + \mu_{k1} + \mu_{k2}) + 4\xi_{e1}f_{e1}\xi_{e2}f_{e2}$$

$$B_7 = 2\xi_{e1}f_{e1} + 2\xi_{e2}f_{e2}$$

For the series shunt circuit, the form of Eq. (2.13) remains the same. The parameters A_i ($i=0\sim4$) and B_j ($j=0\sim7$) are determined by,

$$A_0 = f_b^2 f_{e1}^2 f_{e2}^2$$

$$A_1 = f_b^2(2\xi_{e1}f_{e1}f_{e2}^2 + 2\xi_{e2}f_{e2}f_{e1}^2)$$

$$A_2 = f_b^2 f_{e1}^2 + f_b^2 f_{e2}^2\left(1 + u_{k1} + \frac{u_{k1}}{u_{k2}}\right) + 4\xi_{e1}f_{e1}\xi_{e2}f_{e2}f_b^2$$

$$A_3 = 2\xi_{e1}f_{e1}f_b^2 + 2\xi_{e2}f_{e2}f_b^2\left(1 + u_{k1} + \frac{u_{k1}}{u_{k2}}\right)$$

$$A_4 = f_b^2(1 + u_{k1})$$

$$B_0 = f_b^2 f_{e1}^2 f_{e2}^2$$

$$B_1 = f_b^2(2\xi_{e1}f_{e1}f_{e2}^2 + 2\xi_{e2}f_{e2}f_{e1}^2)$$

$$B_2 = f_b^2 f_{e1}^2 + f_{e1}^2 f_{e2}^2\left(1 + \frac{1}{\mu} + f_b^2\right) + f_b^2 f_{e2}^2\left(1 + u_{k1} + \frac{u_{k1}}{u_{k2}}\right) + 4\xi_{e1}f_{e1}\xi_{e2}f_{e2}f_b^2$$

$$B_3 = 2\xi_{e1}f_{e1}f_b^2 + 2\xi_{e1}f_{e1}f_{e2}^2\left(1 + \frac{1}{\mu} + f_b^2\right) + 2\xi_{e2}f_{e2}f_{e1}^2\left(1 + \frac{1}{\mu} + f_b^2\right) + 2\xi_{e2}f_{e2}f_b^2\left(1 + u_{k1} + \frac{u_{k1}}{u_{k2}}\right)$$

$$B_4 = f_b^2(1 + u_{k1}) + f_{e1}^2\left(1 + \frac{1}{\mu} + f_b^2 + f_{e2}^2\right) + f_{e2}^2\left(\frac{u_{k1}}{u_{k2}} + \frac{1}{\mu} + \frac{u_{k1}}{\mu u_{k2}}\right) + f_b^2 f_{e2}^2\left(1 + u_{k1} + \frac{u_{k1}}{u_{k2}}\right)$$

$$\qquad + 4\xi_{e1}f_{e1}\xi_{e2}f_{e2}\left(1 + 1/\mu + f_b^2\right)$$

$$B_5 = 2\xi_{e1}f_{e1}\left(1 + \frac{1}{\mu} + f_b^2 + f_{e2}^2\right) + 2\xi_{e2}f_{e2}(1 + f_{e1}^2 + f_b^2 + f_b^2 u_{k1} + f_b^2\frac{u_{k1}}{u_{k2}} + \frac{u_{k1}}{u_{k2}} + \frac{1}{\mu} + \frac{u_{k1}}{\mu u_{k2}})$$

$$B_6 = 1 + \frac{1}{\mu} + f_b^2(1 + \mu_{k1}) + f_{e1}^2 + f_{e2}^2(1 + \frac{u_{k1}}{u_{k2}}) + 4\xi_{e1}f_{e1}\xi_{e2}f_{e2}$$

$$B_7 = 2\xi_{e1}f_{e1} + 2\xi_{e2}f_{e2}(1 + \frac{u_{k1}}{u_{k2}})$$

The integral in Eq. (9) can also be solved according to the general formula in the appendix. Similar with the force excitation system, the performance index can be numerically minimized by optimiing the four parameters $f_{e1}, \xi_{e1}, \xi_{e2}, f_{e2}$ with the given parameters $\mu, f_b, \mu_{k1}, \mu_{k2}$. The optimal capacitances and resistances C_1, C_2, R_1, R_2 of the multi-mode shunt circuit can thus be

determined according to Eq. (2.12). It should be noted that, to simplify the optimization problem, the inductance and internal resistance of the electromagnetic motor are not considered. After the optimal value of $C_1^{opt}, C_2^{opt}, R_1^{opt}, R_2^{opt}$ are determined. The actual required capacitances and resistances for the multi-resonant electromagnetic shunt can be calculated according to Eq. (2.5) for the parallel shunt circuit and Eq. (2.9) for the series shunt circuit.

2.4 Chapter Summary

This chapter introduces the concept of multi-resonant electromagnetic shunt damper and establishes the dynamic model of the base isolation system with the proposed parallel and series shunt circuits. For both circuit configurations, the electrical resonances can be tuned to the natural frequencies of the base-isolated building structure, thus achieve enhanced vibration suppression effectiveness by mitigating the first and second vibration modes simultaneously. Besides, the electromagnetic shunt circuit is capable of harvesting the vibrational energy at the same time. For both parallel and series shunt circuit, the electrical parameters are optimized using the H_2 criteria to minimize root mean square values of the relative displacement between the base and primary structure with the consideration of building safety. The optimal performance index for vibration mitigation under force and ground excitations are provided, respectively. According to the design, with selected stiffness ratio parameters for a certain base-isolated structure with mass ratio μ, frequency ratio f_b, four dimensionless parameters, namely electrical tuning ratio f_{e1}, f_{e2} and electrical damping ratio ξ_{e1}, ξ_{e2}, can be determined. The optimal capacitances and resistances of the multi-mode resonant shunt circuit can thus be obtained. The optimization process provides a schematic way to design and determine the optimal parameters for the multi-resonant electromagnetic shunt circuits.

3. Comparison of Electromagnetic Shunt Dampers and Tuned Mass Dampers Used in the Base Isolation System

3.1 Chapter Introduction

This chapter compares the effectiveness of traditional tuned mass dampers with electromagnetic shunt dampers regarding the vibration suppression of the primary system when subjected to ground motion excitations. Basic models of the classic TMD and the electromagnetic shunt damper are established and optimized using the H_2 optimization method to obtain the optimal tuning parameters when connected with the primary system. Later, four multi-resonant mode dampers, including parallel TMDs, series TMDs, electromagnetic parallel shunt damper and electromagnetic series shunt damper, are developed and compared with each other regarding the vibration mitigation performance when combined into a SDOF system. The frequency responses of the primary system with optimized multiple TMDs and multi-resonant electromagnetic shunt dampers of total stiffness ratio 5% are obtained and compared with each other. Since the base-isolated building system is generally considered as a two-DOF system, the effectiveness of multi-resonant mode dampers in suppressing the vibration of the two-DOF system is investigated. With the main consideration of building safety, the vibration mitigation performance is optimized using the H_2 criteria to minimize the root-mean-square values of the relative displacement between the base and the primary structure. The optimal tuning parameters are numerically obtained for the four multi-resonant mode dampers. The effectiveness of the dampers are studied by comparing the frequency responses of the 2-DOF system with the optimized multiple TMDs and multi-resonant electromagnetic shunt dampers of 5% total stiffness ratio. For both the SDOF and 2-DOF system, the influence of the mass ratio distribution in multiple TMDs and the stiffness ratio distribution in multi-resonant electromagnetic shunt dampers are considered.

3.2 Single DOF System with Single Resonant Mode Dampers

3.2.1 Classic TMD and single resonant electromagnetic shunt damper

(a)   (b)
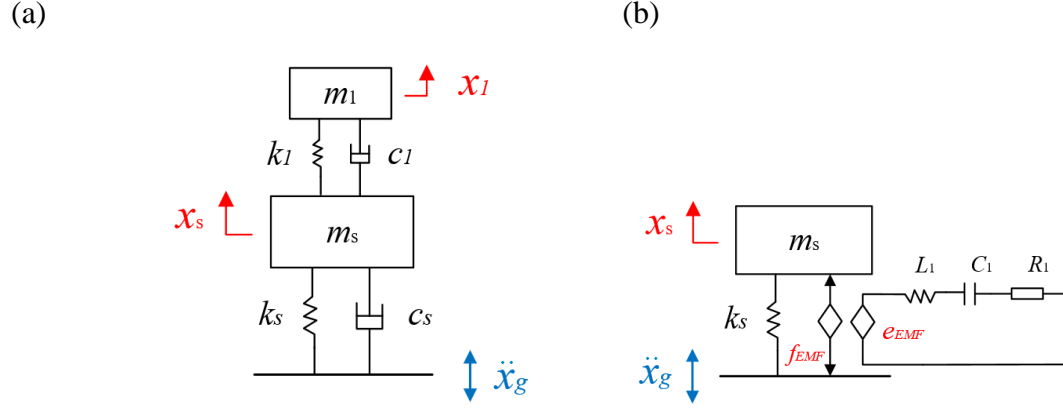
Figure 3.1 Single DOF system with single resonant mode dampers. (a) Classic TMD; (b) single resonant electromagnetic shunt damper

The classic TMD is consisted of a single DOF mass with a spring and a damper, as shown in Figure 3.1(a). When connected to the primary system, the dynamic equations are given by,

$$m_s\ddot{x}_s + c_1\dot{x}_s - c_1\dot{x}_1 + (k_1 + k_s)x_s - k_1 x_1 = -m_s\ddot{x}_g$$

$$m_1\ddot{x}_1 - c_1\dot{x}_s + c_1\dot{x}_1 - k_1 x_s + k_1 x_1 = -m_1\ddot{x}_g \qquad (3.1)$$

where m_s k_s, c_s are the mass, stiffness and damping of the primary structure; m_1, k_1, c_1 are the mass, stiffness and damping of the TMD; x_s, x_1 is the displacement of the primary structure and the TMD, respectively; $\ddot{x}_g$ is the ground motion acceleration.

The transfer function from $\ddot{x}_g$ to x_s can be written as,

$$TF = \left|\frac{X_s}{\ddot{X}_g}\right| = \frac{s^2 + (\frac{c_1}{m_1} + \frac{c_1}{m_s})s + \frac{k_1}{m_1} + \frac{k_1}{m_s}}{s^4 + (\frac{c_1}{m_1} + \frac{c_1}{m_s})s^3 + (\frac{k_1}{m_1} + \frac{k_1}{m_s} + \frac{k_s}{m_s})s^2 + \frac{k_s c_1}{m_s m_1}s + \frac{k_s k_1}{m_s m_1}} \qquad (3.2)$$

The dimensionless form of which is given by,

$$\left|\frac{X_s}{\ddot{X}_g/\omega_s^2}\right| = \frac{(j\alpha)^2+2\xi_m f_m(1+\mu)(j\alpha)+f_m^2(1+\mu)}{(j\alpha)^4+2\xi_m f_m(1+\mu)(j\alpha)^3+(1+f_m^2+f_m^2\mu)(j\alpha)^2+2\xi_m f_m(j\alpha)+f_m^2} \tag{3.3}$$

where $\mu = m_1/m_s$ is the mass ratio; α is the excitation frequency ratio, $\alpha = \omega/\omega_s$; $f_m = \omega_1/\omega_s$ is the frequency tuning ratio, $\xi_m = c_1/(2\omega_1 m_1)$ is the damping tuning ratio; $\omega_s = \sqrt{k_s/m_s}$, $\omega_1 = \sqrt{k_1/m_1}$ is the natural frequency of the primary structure and the TMD, respectively.

Suppose the system is under random ground motion excitation, H_2 optimization method can be used to minimize the root-mean-square (RMS) vibration of the primary structure. The performance index is expressed as,

$$PI = \frac{1}{2\pi}\int_{-\infty}^{\infty}\left|\frac{X_r(j\alpha)}{\ddot{X}_g(j\alpha)/\omega_s^2}\right|^2 d\alpha \tag{3.4}$$

The integral of Eq. (3.4) can be solved using residue theorem. The general solution can be found in Reference [62]. The performance index can then be obtained as a function of the frequency tuning ratio f_m and the damping ratio ξ_m.

$$PI = \frac{A_4\mu^4+A_3\mu^3+A_2\mu^2+A_1\mu+A_0}{4\mu\xi_m f_m} \tag{3.5}$$

in which,

$$A_0 = 1 - 2f_m^2 + 4f_m^2\xi_m^2 + f_m^4$$

$$A_1 = 4f_m^4 + 12f_m^2\xi_m^2 - 3f_m^2$$

$$A_2 = 6f_m^4 + 12f_m^2\xi_m^2$$

$$A_3 = 4f_m^4 + 4f_m^2\xi_m^2 + f_m^2$$

$$A_4 = f_m^4$$

By minimizing the performance index, the optimal tuning ratio f^{opt} and optimal damping ratio ξ^{opt} can be obtained. The corresponding optimal values for the stiffness and damping of the TMD can thus be determined.

The electromagnetic resonant shunt damper, as shown in Figure 3.1(b), is consisted of an electromagnetic transducer shunted with an RLC circuit. Similar with classic TMD, the electromagnetic shunt damper can also provide a resonance coupled with the primary structure. The governing equations of the system are given by,

$$m_s \ddot{x}_s + k_s x_s - k_f \dot{q} = -m_s \ddot{x}_g$$

$$k_v \dot{x}_s + L \ddot{q} + R \dot{q} + \frac{1}{C} q = 0 \tag{3.6}$$

where k_s is the stiffness of the primary structure; x_s is the displacement of the primary structure; k_v, k_f are the voltage constant and force constant of the electromagnetic transducer, L, C, R are the inductance, capacitance and resistance of the resonant shunt circuit; $\dot{q}$ is the electrical current in the circuit; $\ddot{x}_g$ is the ground motion acceleration.

The transfer function from $\ddot{x}_g$ to x_s can be written as,

$$TF = \left| \frac{X_s}{\ddot{X}_g} \right| = \frac{s^2 + \frac{R}{L}s + \frac{1}{LC}}{s^4 + \frac{R}{L}s^3 + \left(\frac{1}{LC} + \frac{k_s}{m_s} + \frac{k_v k_f}{m_s L}\right)s^2 + \frac{k_s R}{m_s L}s + \frac{k_s}{m_s LC}} \tag{3.7}$$

The dimensionless form of which is given by,

$$\left| \frac{x_s}{\ddot{x}_g / \omega_s^2} \right| = \frac{(j\alpha)^2 + 2\xi_e f_e (j\alpha) + f_e^2}{(j\alpha)^4 + 2\xi_e f_e (j\alpha)^3 + (1 + f_e^2 + \mu_k)(j\alpha)^2 + 2\xi_e f_e (j\alpha) + f_e^2} \tag{3.8}$$

where $f_e = \omega_e / \omega_s$ is the frequency tuning ratio, $\xi_e = R/(2\omega_e L)$ is the damping tuning ratio, and $\omega_e = \sqrt{1/(LC)}$ is the resonance frequency of the shunt circuit.

Based on the H_2 optimization method, the performance index can thus be determined as,

$$PI = \frac{f_e^4 + 4\xi_e^2 f_e^2 + \mu_k f_e^2 - 2f_e^2 + 1}{4\mu_k \xi_e f_e} \tag{3.9}$$

where μ_k the stiffness ratio which plays a similar role as the mass ratio μ in the class TMD.

By minimizing the performance index, the optimal tuning ratio f_e^{opt} and optimal damping ratio ξ_e^{opt} can be obtained. The corresponding optimal values for the inductance, capacitance and resistance of the electromagnetic shunt circuit can thus be determined.

3.2.2 Comparison of TMD and electromagnetic shunt

For both the classic TMD and the electromagnetic shunt damper, the optimal tuning rule can be obtained by making the derivative of PI be equal to zero in respect to the frequency tuning ratio and damping ratio, which means, $(\partial PI/\partial f) = 0$ and $(\partial PI/\partial \xi) = 0$. By solving these equations, the H_2 optimal tuning rule can be obtained. The optimal tuning ratio f^{opt}, the optimal damping ratio ξ^{opt}, and the optimal performance index PI^{opt} for the class TMD and the electromagnetic shunt circuit are summarized in Table 3.1.

Table 3.1 H_2 tuning laws for the classic TMD and the electromagnetic shunt damper

Optimum parameters	Classic TMD	Shunt Circuit
Tuning ratio f^{opt}	$\dfrac{\sqrt{2(2-\mu)}}{2(1+\mu)}$	$\sqrt{\dfrac{2-\mu_k}{2}}$
Damping ratio ξ^{opt}	$\dfrac{1}{2}\sqrt{\dfrac{\mu(\mu-4)}{2(\mu+1)(\mu-2)}}$	$\sqrt{\dfrac{\mu_k^2-4\mu_k}{8\mu_k-16}}$
Performance index PI^{opt}	$\dfrac{(4+3\mu)\sqrt{1+\mu}}{2\sqrt{\mu(4-\mu)}}$	$\dfrac{4-\mu_k}{2\sqrt{\mu_k(4-\mu_k)}}$

For the classic TMD, the optimal parameters can also be expressed regarding the stiffness ratio μ_k, defined as, $\mu_k = k_1/k_s$. From above H_2 tuning laws, the relationship between between μ and μ_k can be defined as,

$$\mu = \frac{1-2\mu_k-\sqrt{1-6\mu_k}}{1+2\mu_k} \tag{3.10}$$

Thus, the optimal parameters f^{opt} and ξ^{opt} for the classic TMD can also be expressed as,

31

$$f^{opt} = \frac{\sqrt{(1+2\mu_k)(6\mu_k+\sqrt{1-6\mu_k}+1)}}{\sqrt{2}(2-\sqrt{1-6\mu_k})} \tag{3.11}$$

$$\xi^{opt} = \frac{1}{2}\sqrt{\frac{(6\mu_k+1)\sqrt{1-6\mu_k}-5\mu_k+10\mu_k^2-1}{(6\mu_k-1)\sqrt{1-6\mu_k}-18\mu_k-1}} \tag{3.12}$$

To compare the effectiveness, we investigate the cases when the primary structure is connected with a class TMD and an electromagnetic shunt damper, both with 5% stiffness ratio. The optimal tuning ratio f^{opt}, damping ratio ξ^{opt}, and the minimal H_2 norm value are listed in Table 3.2.

Table 3.2 Optimal parameters for class TMD and electromagnetic shunt circuit

	H_2 norm	f^{opt}	ξ^{opt}
Classic TMD	2.121	0.9318	0.1175
Shunt Circuit	2.108	0.9874	0.1125

Figure 3.2 shows the frequency response of the primary structure with the optimized TMD and the electromagnetic shunt damper, both with 5% stiffness ratio. It shows that the electromagnetic shunt damper can achieve slightly better vibration suppression performance compared with the classic TMD. In addition to the effectiveness, the electromagnetic shunt damper is able to save more space than the classic TMD which has large motion stroke.
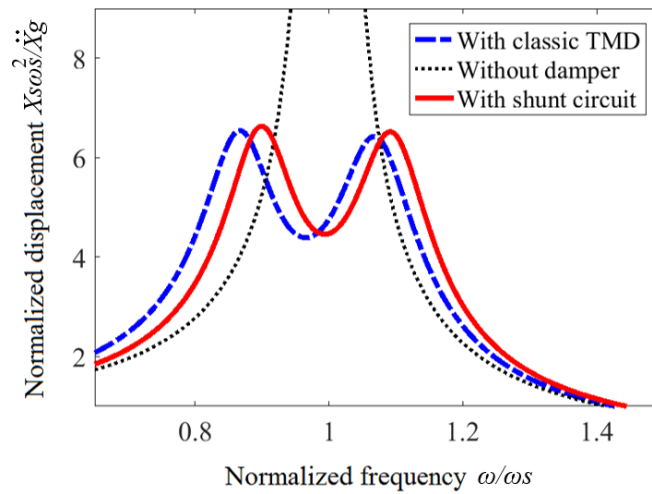
Figure 3.2 Frequency responses of the classic TMD and the electromagnetic shunt damper of stiffness ratio μ_k=5%

3.3 Single DOF System with Multi-resonant Mode Dampers

3.3.1 Multiple TMDs and multi-resonant electromagnetic shunt damper

To achieve enhanced vibration suppression performance, multiple TMDs have been proposed which can be connected with the primary structure either in parallel or in series. According to the [60], series multiple TMDs can achieve much better effectiveness and robustness than parallel TMDs and all other types TMDs. To explore the performance of the electromagnetic shunt damper with multi-mode resonances, parallel shunt circuit and series shunt circuit are proposed and combined with the primary system. The parallel shunt circuit, as shown in Figure 3.3(c), is consisted of two RLC circuit in parallel, which behaves similarly as parallel TMDs. The series shunt circuit, as shown in Figure 3.3(d), is developed based on series multiple TMDs by using the mechanical-electrical analogy.
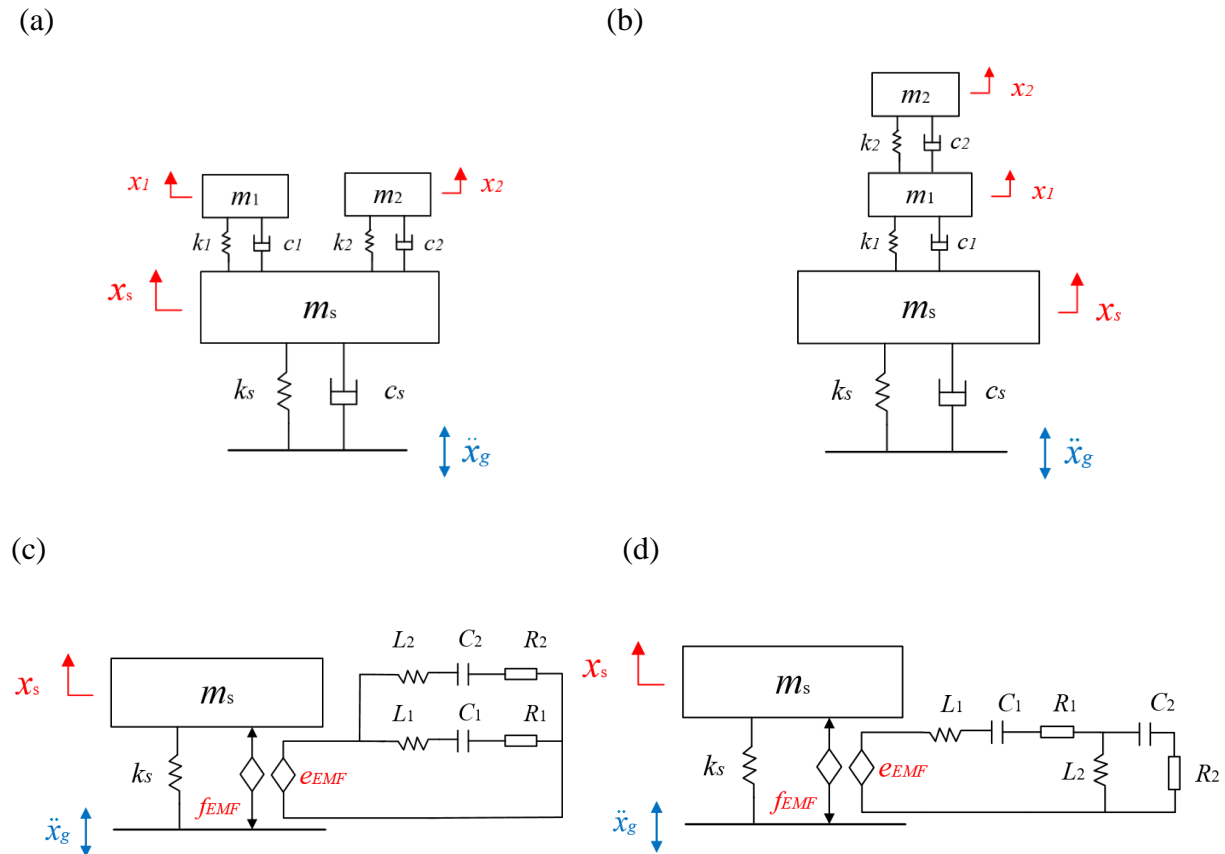
Figure 3.3 Single DOF system with multi-resonant mode dampers. (a) Parallel TMDs; (b) series TMDs; (c) parallel shunt circuit; (d) series shunt circuit

For the system with parallel TMDs shown in Figure 3.3(a), the dynamic equations are given by,

$$m_s\ddot{x}_s + (c_1 + c_2)\dot{x}_s - c_1\dot{x}_1 - c_2\dot{x}_2 + (k_s + k_1 + k_2)x_s - k_1x_1 - k_2x_2 = -m_s\ddot{x}_g$$

$$m_1\ddot{x}_1 + c_1\dot{x}_1 - c_1\dot{x}_s + k_1x_1 - k_1x_s = -m_1\ddot{x}_g$$

$$m_2\ddot{x}_2 - c_2\dot{x}_s + c_2\dot{x}_2 - k_2x_s + k_2x_2 = -m_2\ddot{x}_g \tag{3.13}$$

where m_s, k_s are the mass and stiffness of the primary structure; m_i, c_i, k_i (i=1~2) are mass, damping and stiffness parameters of the two TMDs; x_s, x_1, x_2 are the displacement of the primary structure and the TMDs; $\ddot{x}_g$ is the ground motion acceleration.

For the system with series TMDs shown in Figure 3.3(b), the dynamic equations are given by,

$$m_s\ddot{x}_s + c_1\dot{x}_s - c_1\dot{x}_1 + (k_s + k_1)x_s - k_1x_1 = -m_s\ddot{x}_g$$

$$m_1\ddot{x}_1 - c_1\dot{x}_s + (c_1 + c_2)\dot{x}_1 - c_2\dot{x}_2 - k_1x_s + (k_1 + k_2)x_1 - k_2x_2 = -m_1\ddot{x}_g$$

$$m_2\ddot{x}_2 - c_2\dot{x}_1 + c_2\dot{x}_2 + k_2x_2 - k_2x_1 = -m_2\ddot{x}_g \tag{3.14}$$

in which the parameters are defined the same as parallel TMDs.

To effectively suppress the vibration of the primary structure, the H_2 norm from the ground motion acceleration $\ddot{x}_g$ to the deformation of the primary structure x_s can be minimized by optimizing the tuning parameters of the multiple TMDs. The performance index is defined as,

$$PI = \frac{1}{2\pi}\int_{-\infty}^{\infty}\left|\frac{X_s(j\alpha)}{\ddot{X}_g(j\alpha)/\omega_s^2}\right|^2 d\alpha \tag{3.15}$$

The integral of Eq. (3.15) can be solved using residue theorem. The general solution for six-order systems can be found in Reference [62]. For given mass ratios of the TMDs, the performance index PI can be obtained as a function of the frequency tuning ratios $f_1 = \omega_1/\omega_s$, $f_2 = \omega_2/\omega_s$, and damping tuning ratios $\xi_1 = c_1/(2\omega_1 m_1)$, $\xi_2 = c_2/(2\omega_2 m_2)$. By minimizing the performance index, the optimal parameters for the multiple TMDs can be determined.

For the system with parallel shunt circuit, the overall dynamic equations are given by,

$$m_s\ddot{x}_s + k_s x_s - k_f(\dot{q}_1 + \dot{q}_2) = -m_s\ddot{x}_g$$

$$k_v\dot{x}_s + L_1\ddot{q}_1 + R_1\dot{q}_1 + \frac{1}{C_1}q_1 = 0$$

$$L_1\ddot{q}_1 + R_1\dot{q}_1 + \frac{1}{C_1}q_1 = L_2\ddot{q}_2 + R_2\dot{q}_2 + \frac{1}{C_2}q_2 \qquad (3.16)$$

where L_i, R_i, C_i (i=1~2) are inductance, resistance and capacitance of the electrical resonant circuit. $\dot{q}_1$ and $\dot{q}_2$ are the electrical current in each circuit branch.

For the system with series shunt circuit, the dynamic equations are given by,

$$m_s\ddot{x}_s + k_s x_s - k_f\dot{q}_1 = -m_s\ddot{x}_g$$

$$k_v\dot{x}_s + L_1\ddot{q}_1 + R_1\dot{q}_1 + \frac{1}{C_1}q_1 + L_2\ddot{q}_2 = 0$$

$$L_2\ddot{q}_2 = R_2(\dot{q}_1 - \dot{q}_2) + \frac{1}{C_2}(\dot{q}_1 - \dot{q}_2) \qquad (3.17)$$

where L_1, C_1, R_1 and L_2, C_2, R_2 are the inductance, capacitance and resistance of the main and side branch of the series circuit. $\dot{q}_1$ and $\dot{q}_2$ are the electrical current flowing across the inductors in the primary branch and side branch.

Similar with multiple TMDs, the optimal parameters for the electromagnetic shunt damper can be obtained for vibration mitigation of the primary system subjected to random ground motion excitations by using the H_2 optimization method. The performance index can also be expressed as Eq. (3.15). By minimizing the H_2 norm, the optimal frequency tuning ratios f_{e1}, f_{e2} and damping ratios ξ_{e1}, ξ_{e2} can be determined for a given stiffness ratio μ_k of the system. The optimal element values for the electrical shunt circuit can thus be obtained.

3.3.2 Comparison of multi-mode TMDs and electromagnetic shunts

To compare the effectiveness of multiple TMDs with multi-resonant electromagnetic shunt dampers, we first investigate the cases when the primary structure is connected with: (a) parallel TMDs of 5% total mass ratio; (b) series TMDs of 5% total mass ratio; (c) parallel shunt circuit of 5% total stiffness ratio; (d) series shunt circuit of 5% total stiffness ratio.

Different from the system with single resonant mode damper, the mass ratio distribution in multiple TMDs and the stiffness ratio distribution in the multi-resonant electromagnetic shunt have a significant influence on the vibration suppression performance. Here, the mass ratio distribution in TMDs is defined as $\mu_1/(\mu_1 + \mu_2)$, in which $\mu_1 = m_1/m_s$, $\mu_2 = m_2/m_s$ and the stiffness ratio distribution in shunt circuit is defined as $\mu_{k1}/(\mu_{k1} + \mu_{k2})$, in which $\mu_{k1} = k_v k_f/L_1 k_s$, $\mu_{k2} = k_v k_f/L_2 k_s$. For comparison, the minimal H_2 norm value as a function of the mass or stiffness ratio distribution of the four multi-resonant mode dampers are presented in Figure 3.4.
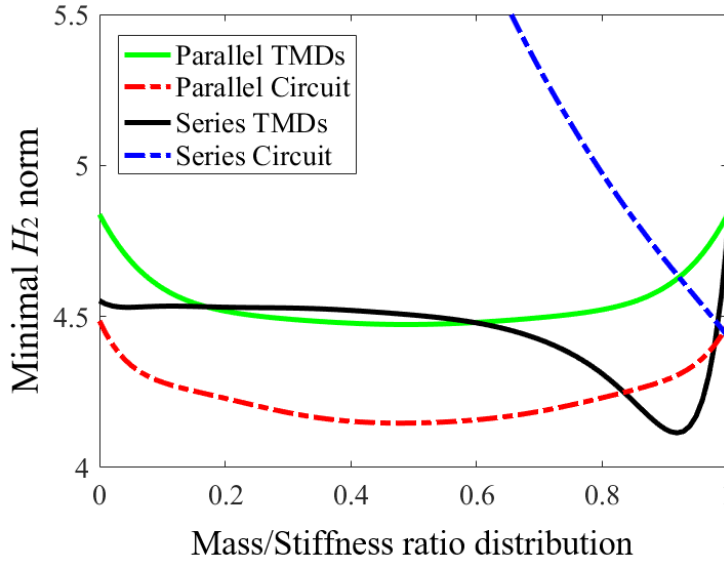
Figure 3.4 Minimal H_2 norm value as a function of the mass ratio distribution in multiple TMDs and the stiffness ratio distribution in multi-resonant electromagnetic shunt damper.

Figure 3.4 shows that, for parallel TMDs and parallel shunt circuit, both curves are symmetric to the center when the mass or stiffness ratio distribution is equal to 0.5. Parallel shunt circuit can achieve much smaller H_2 norm value than parallel TMDs, which indicates better vibration suppression performance. For series TMDs, the optimal mass ratio distribution is 0.91, which can provide a smaller H_2 norm value than all other cases. For the series shunt circuit, there is no local minimum value, the minimal H_2 norm is achieved when the stiffness ratio distribution tends towards 1, turning into a single resonant electromagnetic shunt damper.

For multiple TMDs and multi-resonant electromagnetic shunt dampers with 5% total stiffness ratio, under the optimal mass or stiffness ratio distribution for each case, the optimal tuning ratio

f^{opt}, the optimal damping ratio ξ^{opt}, and the minimal H_2 norm value are obtained and listed in Table 3.3.

Table 3.3 Optimal parameters for multi-mode TMDs and electromagnetic shunt damper

	H_2 norm	f_1^{opt}	f_2^{opt}	ξ_1^{opt}	ξ_2^{opt}
Parallel TMDs	2.070	1.02	0.88	0.068	0.070
Series TMDs	2.031	1.01	0.92	0	0.18
Parallel Circuits	2.037	0.92	1.07	0.076	0.064
Series Circuits	2.114	0.99	0.004	0.11	0.0026

Figure 3.5 shows the frequency response of the primary structure with optimized multiple TMDs and multi-resonant electromagnetic shunt dampers. It shows that parallel shunt circuit can achieve better vibration suppression performance than parallel TMDs, while series TMDs can achieve the best performance compared with all other cases.
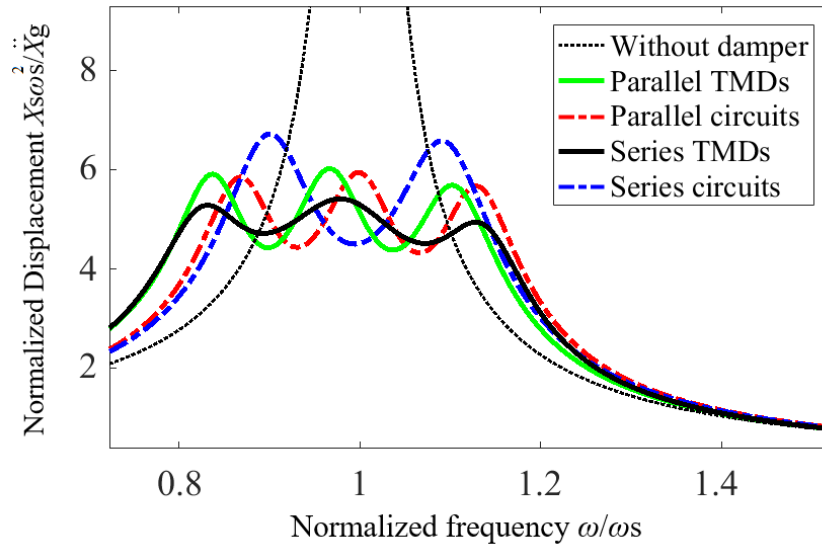
Figure 3.5 Frequency responses of the primary system with multiple TMDs and multi-resonant electromagnetic shunt dampers of total stiffness ratio $\mu_k=5\%$.

3.4 Base Isolation System (Two-DOF) with Multi-resonant Mode Dampers

3.4.1 Multiple TMDs and multi-resonant electromagnetic shunt damper

Base-isolated buildings can be regarded as two-DOF systems, resulting in two separate vibration modes when subjected to ground motion excitations. Multi-resonant mode dampers can be considered to suppress the two vibration modes simultaneously thus achieve enhanced vibration mitigation performance than single resonant mode damper. For multiple TMDs, both parallel TMDs and series TMDs can be installed on the base structure, as shown in Figure 3.6(a) and 3.6(b). For multi-resonant electromagnetic shunt dampers, the electromagnetic transducer can be placed between the base structure and the ground, and then shunted with the parallel circuit or the series circuit, as shown in Figure 3.6(c) and 3.6(d).
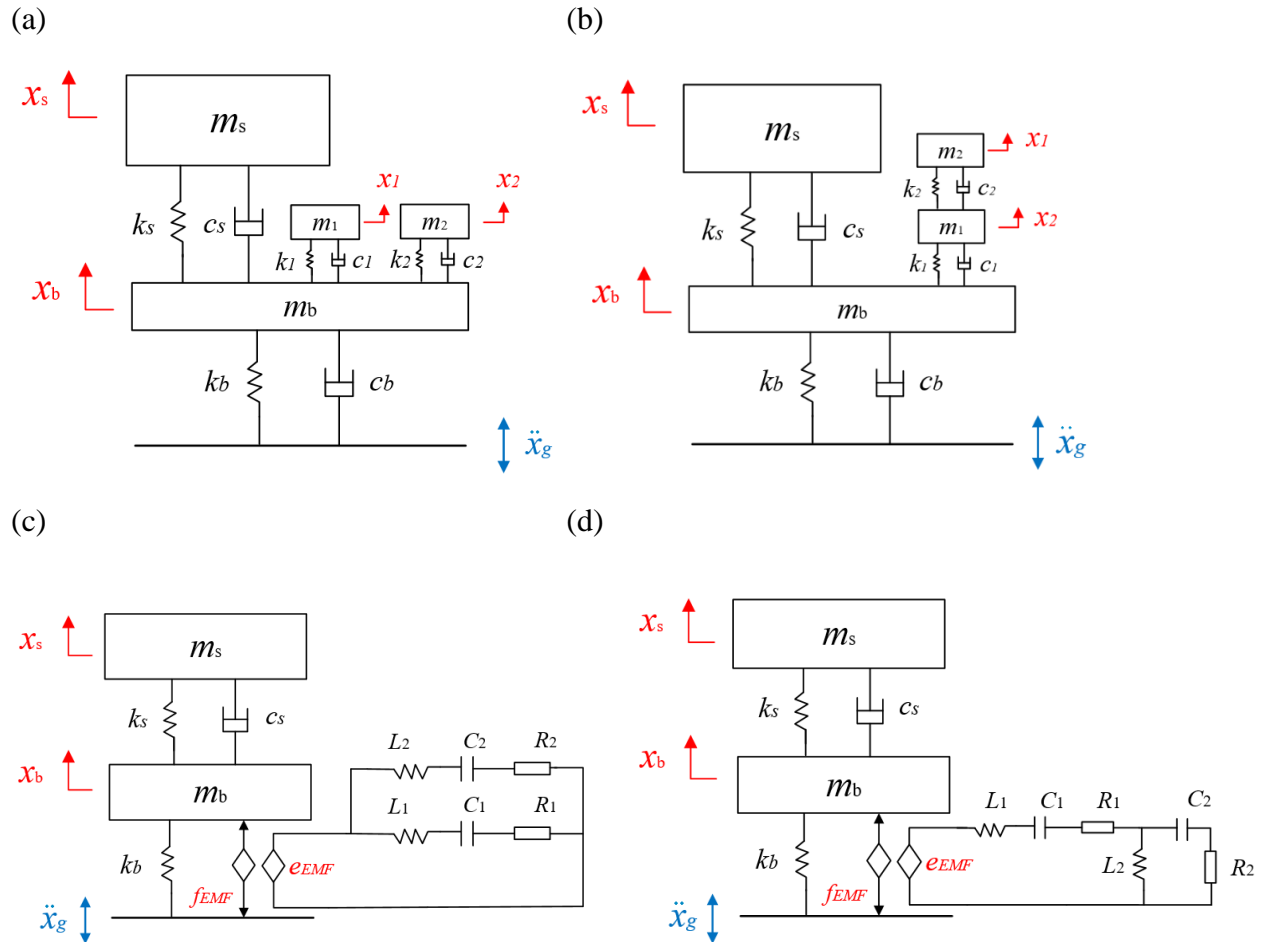
Figure 3.6 Two-DOF system with multi-resonant mode dampers. (a) Parallel TMDs; (b) series TMDs; (c) parallel shunt circuit; (d) series shunt circuit.

For the two-DOF system with parallel TMDs, the overall dynamic equations are given by,

$$M_{Tp}\ddot{X} + C_{Tp}\dot{X} + K_{Tp}X = F \tag{3.18}$$

where the vector $X = [x_s, x_b, x_1, x_2]^T$, $F = \left[-m_s\ddot{x}_g, -m_b\ddot{x}_g, -m_1\ddot{x}_g, -m_2\ddot{x}_g\right]^T$ and

$$M_{Tp} = \begin{bmatrix} m_s & 0 & 0 & 0 \\ 0 & m_b & 0 & 0 \\ 0 & 0 & m_1 & 0 \\ 0 & 0 & 0 & m_2 \end{bmatrix}, \quad C_{Tp} = \begin{bmatrix} 0 & 0 & 0 & 0 \\ 0 & c_1 + c_2 & -c_1 & -c_2 \\ 0 & -c_1 & c_1 & 0 \\ 0 & -c_2 & 0 & c_2 \end{bmatrix},$$

$$K_{Tp} = \begin{bmatrix} k_s & -k_s & 0 & 0 \\ -k_s & k_s + k_b + k_1 + k_2 & -k_1 & -k_2 \\ 0 & -k_1 & k_1 & 0 \\ 0 & -k_2 & 0 & k_2 \end{bmatrix}$$

where m_s, k_s are the mass and stiffness of the primary structure; m_b, k_b are the mass and stiffness of the base; m_i, c_i, k_i (i=1~2) are mass, damping and stiffness parameters of the two TMDs; x_s, x_b, x_1, x_2 are displacements of the primary structure, the base and two TMDs; $\ddot{x}_g$ is the ground motion acceleration.

For the two-DOF system with series TMDs, the dynamic equations are given by,

$$M_{Ts}\ddot{X} + C_{Ts}\dot{X} + K_{Ts}X = F \tag{3.19}$$

where the vector $X = [x_s, x_b, x_1, x_2]^T$, $F = \left[-m_s\ddot{x}_g, -m_b\ddot{x}_g, -m_1\ddot{x}_g, -m_2\ddot{x}_g\right]^T$ and

$$M_{Tp} = \begin{bmatrix} m_s & 0 & 0 & 0 \\ 0 & m_b & 0 & 0 \\ 0 & 0 & m_1 & 0 \\ 0 & 0 & 0 & m_2 \end{bmatrix}, \quad C_{Tp} = \begin{bmatrix} 0 & 0 & 0 & 0 \\ 0 & c_1 & -c_1 & 0 \\ 0 & -c_1 & c_1 + c_2 & -c_2 \\ 0 & 0 & -c_2 & c_2 \end{bmatrix},$$

$$K_{Tp} = \begin{bmatrix} k_s & -k_s & 0 & 0 \\ -k_s & k_s + k_b + k_1 & -k_1 & 0 \\ 0 & -k_1 & k_1 + k_2 & -k_2 \\ 0 & 0 & -k_2 & k_2 \end{bmatrix}$$

where the parameters are defined the same as parallel TMDs.

To effectively mitigate the vibration and achieve the best performance in improving the building safety, the H_2 norm regarding the response from the ground acceleration $\ddot{x}_g$ to the relative displacement between the base and the primary structure x_r can be minimized by optimizing the tuning parameters of the multiple TMDs. The performance index is defined as,

$$PI = \frac{1}{2\pi} \int_{-\infty}^{\infty} \left| \frac{X_r(j\alpha)}{\ddot{X}_g(j\alpha)/\omega_s^2} \right|^2 d\alpha = \frac{1}{2\pi} \int_{-\infty}^{\infty} \left| \frac{X_s(j\alpha)-X_b(j\alpha)}{\ddot{X}_g(j\alpha)/\omega_s^2} \right|^2 d\alpha \qquad (3.20)$$

The integral of Eq. (3.20) can be solved using residue theorem. The general solution for eight-order systems can be found in the Appendix. For a certain Two-DOF system, with given mass ratios of the TMDs, the performance index PI can be determined as a function of the frequency tuning ratios $f_1 = \omega_1/\omega_s$, $f_2 = \omega_2/\omega_s$, and damping tuning ratios $\xi_1 = c_1/(2\omega_1 m_1)$, $\xi_2 = c_2/(2\omega_2 m_2)$. By minimizing the performance index PI, the optimal stiffness and damping of the multiple TMDs can be obtained.

For the system with parallel shunt circuit, the overall dynamic equations can be expressed in the matrix form,

$$M_{Ep}\ddot{X} + C_{Ep}\dot{X} + K_{Ep}X = F \qquad (3.21)$$

where the vector $X = [x_s, x_b, q_1, q_2]^T$, $F = \left[-m_s\ddot{x}_g, -m_b\ddot{x}_g, 0,0\right]^T$ and

$$M_{Ep} = \begin{bmatrix} m_s & 0 & 0 & 0 \\ 0 & m_b & 0 & 0 \\ 0 & 0 & L_1 & 0 \\ 0 & 0 & L_1 & -L_2 \end{bmatrix}, \quad C_{Ep} = \begin{bmatrix} c_s & -c_s & 0 & 0 \\ -c_s & c_s & -k_f & -k_f \\ 0 & k_v & R_1 & 0 \\ 0 & 0 & R_1 & -R_2 \end{bmatrix},$$

$$K_{Ep} = \begin{bmatrix} k_s & -k_s & 0 & 0 \\ -k_s & k_s + k_b & 0 & 0 \\ 0 & 0 & 1/C_1 & 0 \\ 0 & 0 & 1/C_1 & -1/C_2 \end{bmatrix}$$

in which x_s and x_b are the displacement of primary structure and the base. $\dot{q}_1$ and $\dot{q}_2$ are the electrical current in each circuit branch. L_1, C_1, R_1 and L_2, C_2, R_2 are the inductance, capacitance and resistance of the first and second branch of the parallel circuit.

For the system with parallel shunt circuit, the overall dynamic equations can be expressed in the matrix form,

$$M_{Es}\ddot{X} + C_{Es}\dot{X} + K_{Es}X = F \tag{3.22}$$

where the vector $X = [x_s, x_b, q_1, q_2]^T$, $F = \left[-m_s\ddot{x}_g, -m_b\ddot{x}_g, 0, 0\right]^T$ and

$$M_{Ep} = \begin{bmatrix} m_s & 0 & 0 & 0 \\ 0 & m_b & 0 & 0 \\ 0 & 0 & L_1 & L_2 \\ 0 & 0 & 0 & L_2 \end{bmatrix}, \quad C_{Ep} = \begin{bmatrix} c_s & -c_s & 0 & 0 \\ -c_s & c_s & -k_f & -k_f \\ 0 & k_v & R_1 & 0 \\ 0 & 0 & -R_2 & R_2 \end{bmatrix},$$

$$K_{Ep} = \begin{bmatrix} k_s & -k_s & 0 & 0 \\ -k_s & k_s + k_b & 0 & 0 \\ 0 & 0 & 1/C_1 & 0 \\ 0 & 0 & -1/C_2 & 1/C_2 \end{bmatrix}$$

The optimal parameters for the multi-resonant electromagnetic shunt damper can also be obtained for vibration mitigation in protection of the building structure by using the H_2 optimization method. Similar with multiple TMDs, the performance index can be expressed as Eq. (3.20). By minimizing the H_2 norm, the optimal electrical tuning ratios f_{e1}, f_{e2} and electrical damping ratios ξ_{e1}, ξ_{e2} can be obtained for a given two-DOF system with an electromagnetic shunt of stiffness ratios μ_{k1}, μ_{k2} . The optimal elements for the shunt circuit can thus be determined.

3.4.2 Comparison of multi-mode TMDs and electromagnetic shunts

To investigate the performance of multiple TMDs with multi-resonant electromagnetic shunt dampers in the two-DOF base isolation system, we first compare the cases when the primary structure is connected with: (a) parallel TMDs of 5% total mass ratio; (b) series TMDs of 5% total mass ratio; (c) parallel shunt circuit of 5% total stiffness ratio; (d) series shunt circuit of 5% total stiffness ratio. For simplicity, both the mass ratio and frequency ratio in the two-DOF system are assumed as 1. The influence of mass ratios in multiple TMDs and stiffness ratios in the multi-resonant electromagnetic shunt is considered. Figure 3.7 shows the minimal H_2 norm value as a function of the mass or stiffness ratio distribution of the four multi-resonant mode dampers.
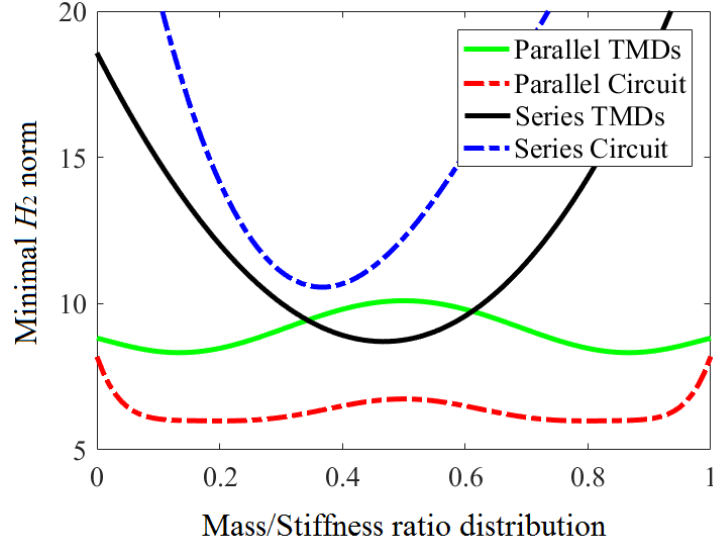
Figure 3.7 Minimal H_2 norm value as a function of the mass ratio distribution in multiple TMDs and the stiffness ratio distribution in multi-resonant electromagnetic shunt damper.

Figure 3.7 shows that, for parallel TMDs, the minimal H_2 norm value is achieved when the mass ratio distribution is equal to 0.1 or 0.9 due to the symmetric structure. Parallel shunt circuit can achieve much smaller value when the stiffness ratio equals 0.17 or 0.83. For series TMDs, the optimal mass ratio is 0.44, while for the series circuit, the optimal stiffness ratio is 0.38. Comparatively, the parallel shunt circuit can achieve the smallest H_2 norm value, indicating the best vibration suppression performance among the four multi-mode dampers. With 5% total stiffness ratio, the optimal tuning ratio f^{opt}, the optimal damping ratio ξ^{opt}, and the minimal H_2 norm value for each case are obtained and listed in Table 3.4.

Table 3.4 Optimal parameters for multi-mode TMDs and electromagnetic shunt damper

	H_2 norm	f_1^{opt}	f_2^{opt}	ξ_1^{opt}	ξ_2^{opt}
Parallel TMDs	2.546	1.63	0.62	0.030	0.057
Series TMDs	3.041	1.39	0.74	0	0.098
Parallel Circuits	2.445	1.63	0.63	0.024	0.088
Series Circuits	3.393	0.84	1.20	0.062	0.0083

Figure 3.8 shows the frequency response regarding of the relative displacement between the base and the primary structure, with the optimized multiple TMDs and multi-resonant electromagnetic shunt dampers of 5% total stiffness ratio.

(a)
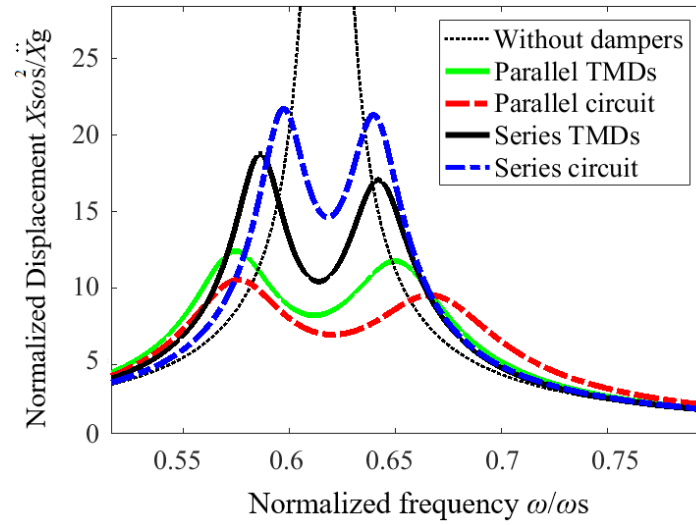
(b)
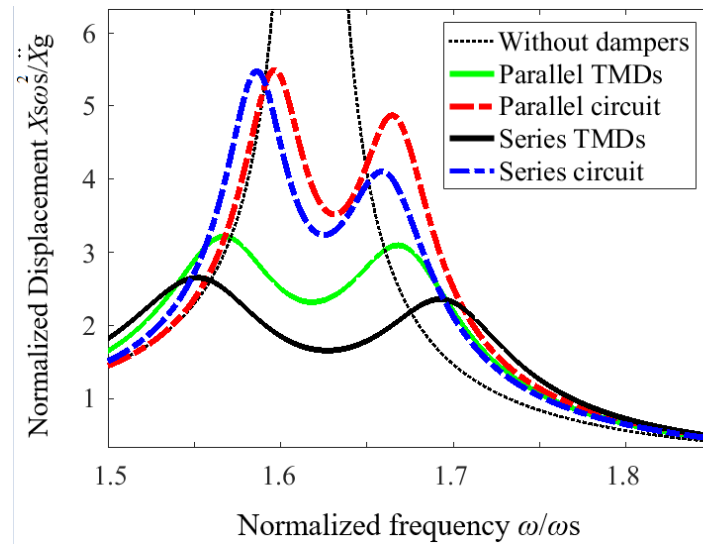
Figure 3.8 Frequency responses of multiple TMDs and multi-resonant electromagnetic shunt dampers of total stiffness ratio μ_k=5%: (a) at the first resonant frequency; (b) at the second resonant frequency.

Figure 3.8(a) shows that, at the first resonant frequency, the parallel shunt damper can achieve the best vibration suppression performance than all other types of dampers. At the second resonant frequency, as shown in Figure 3.8(b), series TMDs has the best performance while the parallel shunt damper is the least effective. However, for the Two-DOF base isolation system, the first resonant frequency is dominant, with a vibration level much larger than that of the second resonant frequency. According to the result from Table 4, the corresponding H_2 norm value for parallel shunt damper is 2.445 which is much smaller than the value 3.041 of series TMDs. Thus, we can conclude that the parallel shunt damper outperforms all other types of dampers regarding the vibration suppression of the system.

3.5 Chapter Summary

This chapter compares the effectiveness of tuned mass dampers and electromagnetic shunt dampers when combined into a primary structure which is disturbed by ground motion excitations. The result shows that, the performance of the class TMD and the electromagnetic shunt damper are similar when connected with a SDOF primary system. However, when employing multiple TMDs and multi-resonant electromagnetic shunt dampers, the effectiveness will be largely different and the difference depends on the mass ratio distribution in multiple TMDs and stiffness ratio distribution in multi-resonant electromagnetic shunt dampers. The frequency responses of the primary SDOF system when connected with the optimized multiple TMDs and multi-resonant shunt dampers of 5% total stiffness ratio show that the parallel shunt damper can achieve much better vibration suppression performance than Parallel TMDs, while series TMDs is the most effective damper among the four types of dampers. When combined into a two-DOF system, the multi-resonant mode dampers are capable of achieving enhanced vibration mitigation performance by suppressing the two vibration modes simultaneously. The frequency response of the 2DOF system shows that the parallel shunt damper can achieve the best vibration suppression performance than all other types of dampers.

4. Case Study Analysis for a Base-isolated Structure with Multi-resonant Electromagnetic Shunt Dampers

4.1 Chapter Introduction

This chapter conducted case study analysis in which a base-isolated structure is considered under earthquake ground motion excitations. The electromagnetic shunt with both parallel and series shunt circuits are applied to the base isolation system for vibration damping and simultaneous energy harvesting. The optimal design of the electromagnetic shunt circuit design is presented in detailed based on the proposed optimization method. Both frequency domain and time domain analysis are conducted to investigate the effectiveness of the electromagnetic shunt in vibration mitigation and performance in energy harvesting capabilities. In frequency domain, frequency responses of the base isolation system, including the relative displacement between the base and the primary structure, and the absolute acceleration of the primary structure are obtained. Besides, the frequency response of the harvestable power that the multi-mode shunt circuit is also presented. The performance of the parallel shunt circuit and series shunt circuit is compared in both vibration suppressing and energy harvesting. In the time domain, two real recorded earthquakes are applied to the base-isolated structure. The time history responses of the system with multi-resonant electromagnetic shunts are obtained and compared with the system with single mode shunt which is only focused on the first vibration mode. The instant power that can be collected by the multi-resonant electromagnetic shunt is obtained for both circuit branches. The analysis clearly shows the effectiveness of the multi-resonant electromagnetic shunt in both vibration mitigation and energy harvesting. In addition, the sensitivity of electrical circuit parameters of the multi-resonant electromagnetic shunt is analyzed. The robustness of the parallel and series shunt circuit regarding the parameter mistuning is also compared.

4.2 Case Study Description

Consider an eight-story base-isolated building with a primary structure mass m_s=1315417 kg and a base mass m_b=789250 kg. The stiffness of the primary structure and base are k_s=72025 kN/m and k_b=8986 kN/m, respectively. Thus, the time period of the fixed-base structure is $0.85s$ and the fundamental period of the base-isolated system is $2.5s$, which meets the recommended values for a base-isolated structure according to [63]. Assume the electromagnetic motor constants are k_v=1000 $V/(m/s)$, k_f=1000 N/A and the total stiffness ratio μ_k ($\mu_k = \mu_{k1} + \mu_{k2}$) is 0.2. We optimize the parameters of both parallel and series circuits at various stiffness ratio distributions among the two circuit branches, defined as $\gamma = \mu_{k1}/(\mu_{k1} + \mu_{k2})$. The minimal normalized H_2 norm value of relative displacement x_r between base and primary structure under earthquake excitations $\ddot{x}_g$ of unit white noise is shown in Figure 4.1. It should be noted that the damping ratio between base and primary structure is neglected. Also, the inductance and internal resistance of the electromagnetic motor is not considered in this case. Figure 4.1 shows that, with the designed parameter$s$, the parallel shunt circuit can achieve smaller normalized H_2 norm thus get better vibration suppression performance than that of the series shunt circuit.
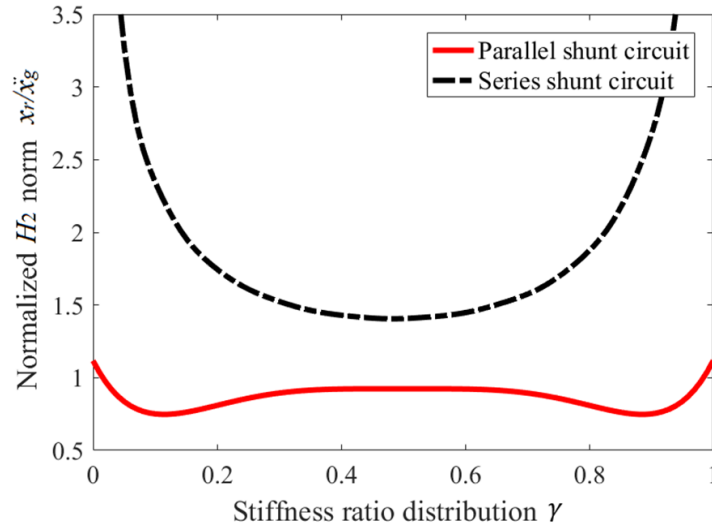
Figure 4.1 Minimal normalized H_2 norm from $\ddot{x}_g$ to x_r as a function of the stiffness distribution $\gamma = \mu_{k1}/(\mu_{k1} + \mu_{k2})$ for the base isolation system with parallel and series shunt circuits.

For the series shunt circuit, the minimum normalized H_2 norm is achieved at 1.407 for γ =0.5. For the parallel shunt circuit, the minimum is 0.797 for γ =0.1 or γ =0.9 due to the symmetric circuit structure. Given these optimal distribution values, the stiffness ratios of the two branches are selected as μ_{k1} =0.02, μ_{k2} =0.18 for the parallel shunt circuit, and μ_{k1} =0.1, μ_{k2} =0.1 for the series shunt circuit. The required inductances can thus be determined as L_1=5.56 H, L_2=0.62 H for the parallel shunt circuit and L_1=L_2=1.11H for the series shunt circuit. Such inductors are relative large. However, they are still reasonable when compared with the size of building.

Table 4.1 Analytical parameters for the case study

Optimal Parameters	Parallel shunt circuit	Series shunt circuit
Electrical tuning ratio f_{e1}, f_{e2}	1.69, 0.28	0.40, 1.19
Electrical damping ratio ξ_{e1}, ξ_{e1}	0.015, 0.21	0.16, 0.0037
Inductance L_1, L_2	5.56 H, 0.62 H	1.11 H, 1.11H
Capacitance C_1, C_2	0.0011 F, 0.36 F	0.105 F, 0.012 F
Resistance R_1, R_2	2.15 Ω, 0.55 Ω	1.03 Ω, 0.07 Ω

According to the design, the following dimensionless parameters are determined, mass ratio μ = 0.6, frequency ratio f_b= 0.46 and total stiffness ratio μ_k = 0.2. The optimal electrical tuning and damping parameters $f_{e1}, f_{e2}, \xi_{e1}, \xi_{e2}$ can thus be obtained using the H_2 criteria to minimize root-mean-square values of the relative displacement between base and the primary structure. The corresponding optimal value of circuit elements, including capacitances C_1, C_2 and resistances R_1, R_2 can thus be obtained. The obtained optimal normalized parameters and corresponding circuit element values are shown in Table 4.1.

4.3 Frequency Domain Analysis

4.3.1 Frequency response for vibration mitigation

The optimal frequency responses of the relative displacement between base and primary structure under earthquake excitation with parallel or series shunt circuits are shown in Figure

4.2(a). It clearly shows that both vibration modes of the base isolation system can be suppressed using either parallel or series shunt circuits.

(a)
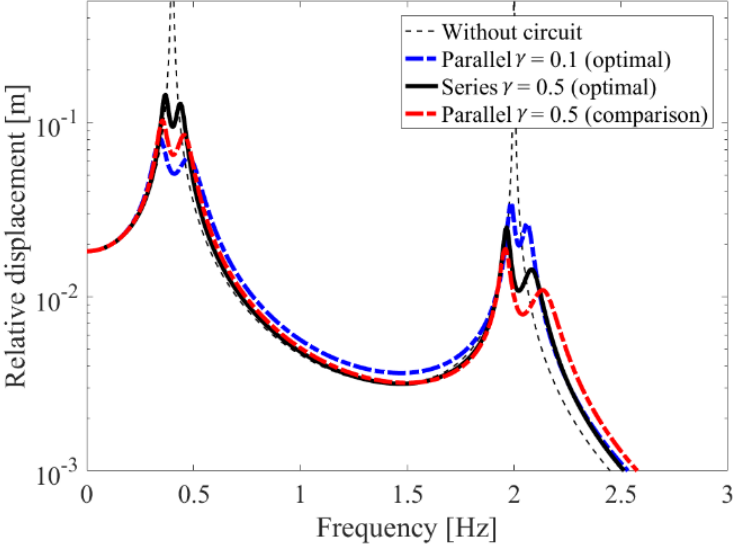
(b)
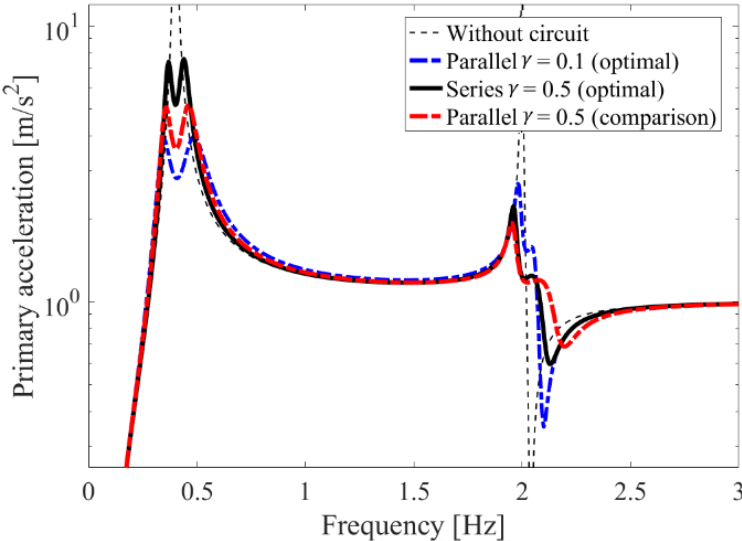
Figure 4.2 Frequency response of the base isolation system. (a) Relative displacement between base and primary structure; (b) absolute acceleration of primary structure.

Figure 4.2(a) shows that, with the same stiffness ratio distribution $\gamma = 0.5$, parallel shunt circuit outperforms series shunt circuit by mitigating both vibration modes of the base isolation system more effectively. Besides, at the optimal stiffness ratio distribution $\gamma = 0.1$, parallel shunt circuit can further improve the performance by suppressing vibration at the dominant frequency more effectively. With same set of parameters, frequency response of the absolute acceleration of the primary structure are presented in Figure 4.2(b). It shows that the primary structure acceleration can also be mitigated effectively. Same conclusion, that parallel shunt circuit is superior to series shunt circuit regarding to the acceleration suppression performance, can be drawn from the results.

4.3.2 Frequency responses of harvestable power

Multi-resonant electromagnetic shunt circuit is capable of suppressing vibration and simultaneously harvesting the vibrational energy. Assuming resistances of the shunt circuits are converters, the energy harvesting capabilities of parallel and series shunt circuits are investigated in this subsection when the system is optimized for vibration suppression. The optimal frequency response from ground excitation $\ddot{x}_g$ to the square root of the power spectrum density of the harvestable energy with parallel or series shunt circuits are shown in Figure 4.3.
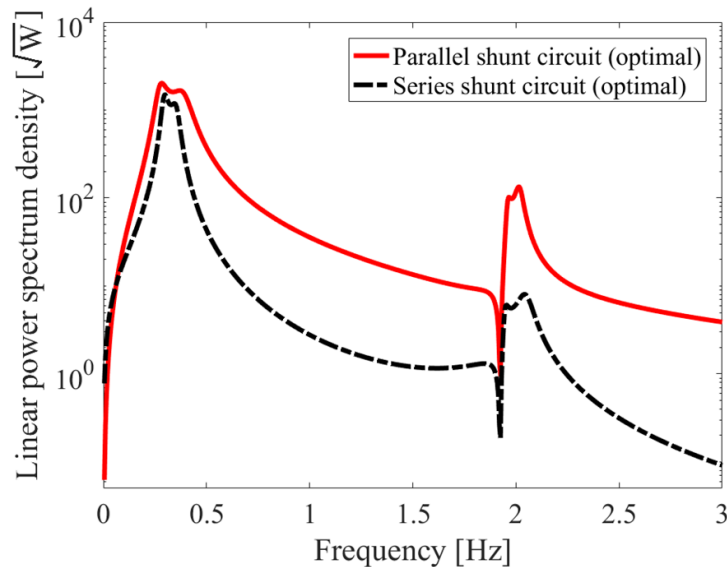
Figure 4.3 Linear power spectrum density of harvestable energy

It shows that multi-mode shunt circuit can harvest the energy from both vibration modes. The power collected from the second mode is far less than the first mode. Besides, Fig. 6 clearly shows that the parallel shunt circuit can harvest more energy than the series shunt circuit almost across the whole bandwidth.

4.4 Sensitivity of Multi-resonant Shunt Circuit Parameters

In practice, it is difficult to tune perfectly, or perhaps some parameters may change over time. Figure 4.4 and Figure 4.5 show how the optimal performance index (*PI*) value will change with the uncertainties of the tuning electrical elements C_1, C_2, R_1, R_2 in the parallel and series shunt circuits, respectively. The variation of both the capacitance and resistance are set as $\pm 20\%$ of the optimal value. The maximum PI value due to the parameter changes for the two cases are shown in Table 4.2. For parallel shunt circuit, the maximum PI value will be 3.02 times larger than the optimal value regarding changes in capacitances, and 1.025 times larger regarding changes in resistances. For series shunt circuit, the corresponding value will be 4.22 times larger than the optimal value regarding changes in capacitances, and 1.026 times larger regarding changes in resistances. The result shows that, for both parallel and series shunt circuits, the system is sensitive to the change of capacitances, but not sensitive to the change of resistances. Comparatively, parallel shunt circuit is less sensitive than series shunt circuit, which indicates that the parallel shunt circuit would be more robust in parameter tuning than the series shunt circuit.

(a)   (b)
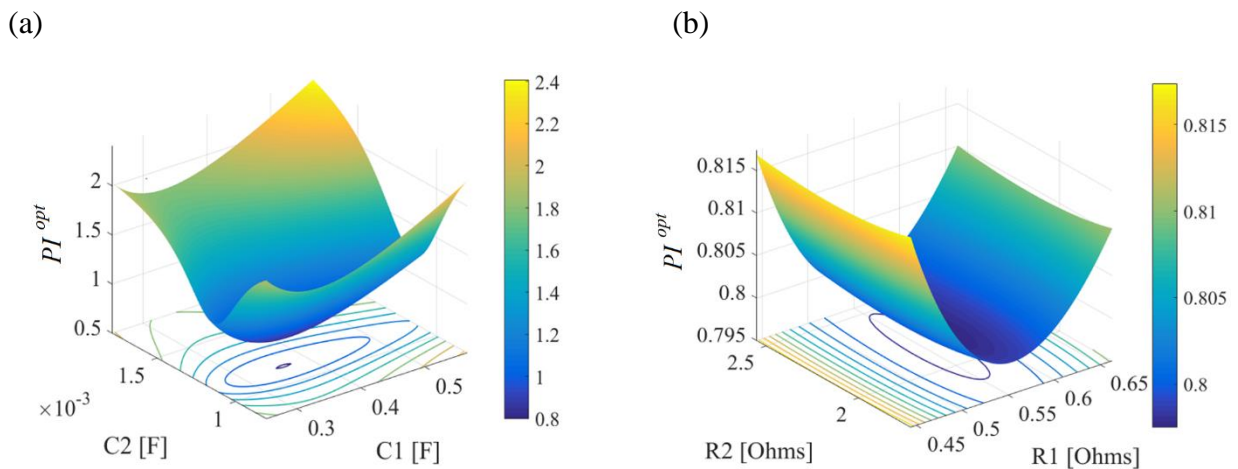
Figure 4.4 Performance index cost surface as a function of parameters in parallel shunt circuit. (a) $\pm 20\%$ changes of capacitances C_1 and C_2; (b) $\pm 20\%$ changes of resistances R_1 and R_2.
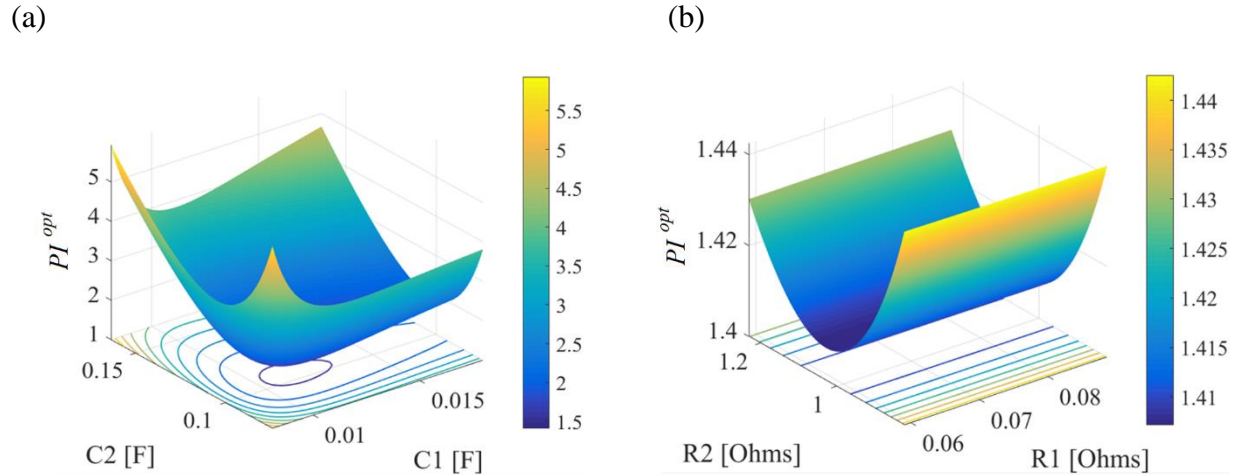
Figure 4.5 Performance index cost surface as a function of parameters in series shunt circuit. (a) $\pm20\%$ changes of capacitances C_1 and C_2; (b) $\pm20\%$ changes of resistances R_1 and R_2.

Table 4.2 Performance index comparison with changes in electrical parameters

PI	Optimal	C change ±20%	R change ±20%
Parallel shunt circuit	0.797	Max: 2.409	Max: 0.817
Series shunt circuit	1.407	Max: 5.937	Max: 1.443

4.5 Time Domain Analysis

4.5.1 Recorded earthquake excitations

To investigate the performance of the multi-mode electromagnetic shunt damper in real situations, the system is now analyzed in the time domain with two recorded earthquakes. The first earthquake signal is from the historical seismic event 1994 Northridge which occurred in Reseda, a neighborhood of Los Angeles, California. The ground acceleration is shown in Figure 4.6(a) with a peak amplitude 0.6g. The second is from Kobe earthquake, occurred on 1995 in the southern part of Hanshin, Japan. The ground acceleration is shown in Figure 4.6(b) with a peak amplitude 0.8g. Since we already concluded from frequency responses that parallel circuit outperforms series circuit in both vibration suppression and energy harvesting, only parallel shunt circuit is analyzed in the time domain analysis. The performance of the multi-mode parallel shunt circuit is presented in

comparison with the single mode shunt circuit (f_e=0.28, ξ_e=0.21), using one RLC resonant shunt circuit and focusing only on the first vibration mode.

(a)   (b)
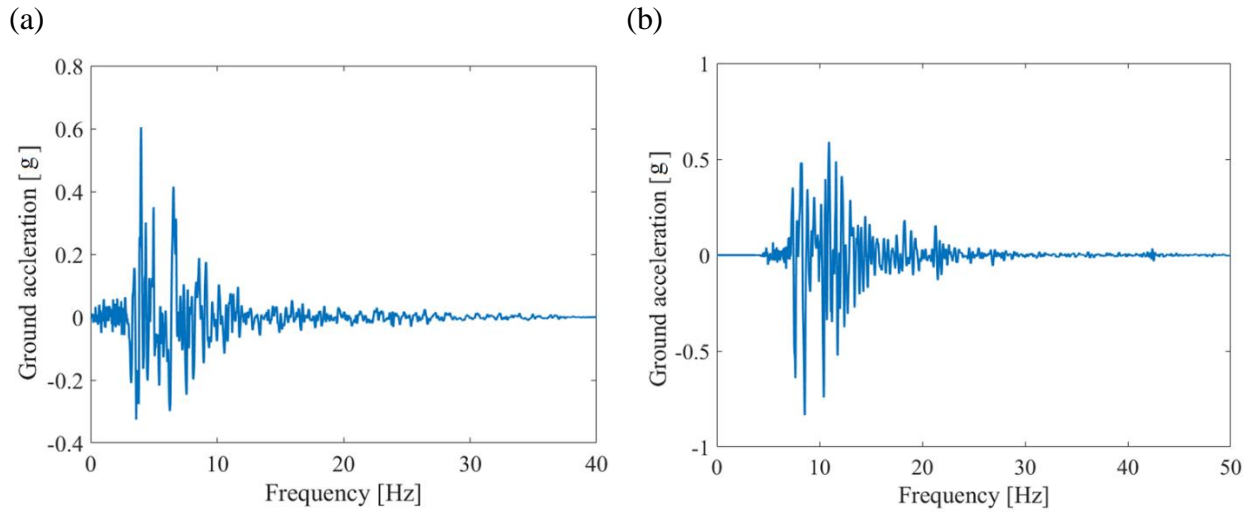
Figure 4.6 Ground acceleration of two recorded earthquakes. (a) Northridge NS 1994; (b) Kobe NS 1995.

4.5.2 Time history responses of the base isolation system

Figure 4.7 shows the time history responses of the relative displacement between base and primary structure, and absolute primary structure acceleration under the Northridge earthquake.

(a)   (b)
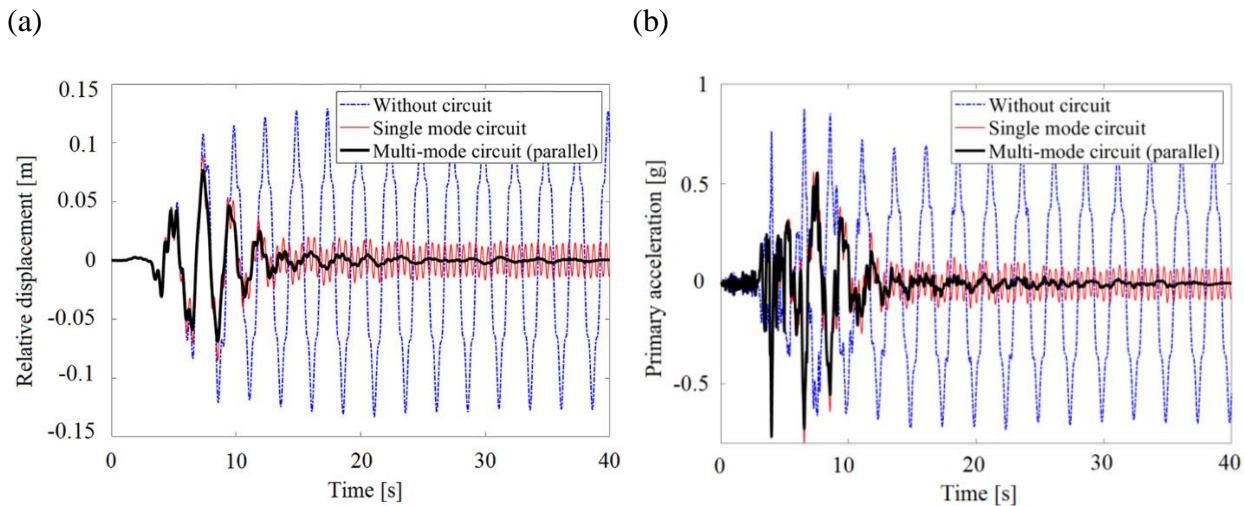
Figure 4.7 Time history responses of the base isolation system under Northridge earthquake. (a) Relative displacement response; (b) Primary acceleration responses.

It can be seen clearly that the system vibration is suppressed quickly with resonant shunt circuits. The multi-mode shunt circuit can achieve much smaller amplitude compared with single mode shunt circuit. Figure 4.8 shows the time history responses of the relative displacement and absolute primary structure acceleration under the Kobe earthquake. It shows that multi-mode shunt circuit can realize the vibration attenuation much faster than single mode shunt circuit.

(a)   (b)
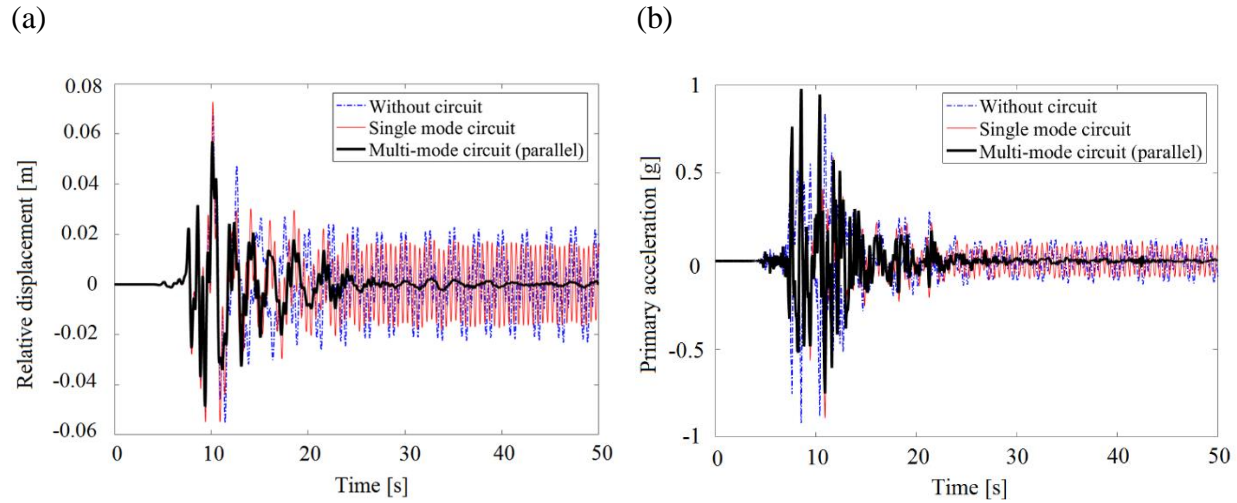
Figure 4.8 Time history responses of the base isolation system under Kobe earthquake. (a) Relative displacement response; (b) Primary acceleration responses.

4.5.3 Instant voltage generated by the multi-resonant shunt circuit

To show energy harvesting capabilities of the multi-resonant electromagnetic shunt circuit, the instant voltage generated by the two circuit branches under Northridge and Kobe earthquakes are presented in Figure 4.9, respectively. For Northridge earthquake, the first natural frequency of the base-isolated structure is dominant, thus much more voltage is generated in the first branch. The peak voltage is 359V for the first branch and 85.9V for the second branch. Comparatively, the first natural frequency of the structure is less dominant for Kobe earthquake. As a result, the second circuit branch is capable of generating relatively more voltage. The peak voltage is 748.2V for the first branch and 67.3V for the second branch.
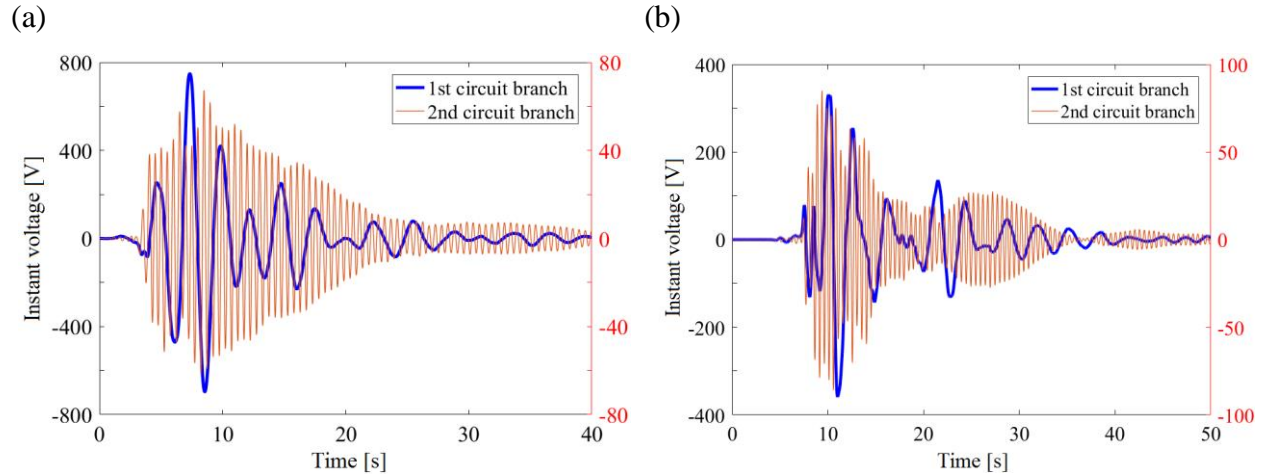
Figure 4.9 Instant voltage generated in two circuit branches of the parallel shunt circuit. (a) Under Northridge earthquake; (b) under Kobe earthquake.

4.5.4 Instant power collected by the multi-resonant shunt circuit

The instant power that can be collected by the two circuit branches under Northridge and Kobe earthquakes are presented in Figure 4.10, respectively. For Northridge earthquake, the peak instant power can reach up to 1.18 Megawatts for the first circuit branch and 3.32 Kilowatts for the second circuit branch. The total average power of the shunt circuit during the earthquake is 203.37 Kilowatts. For Kobe earthquake, the peak instant power can reach up to 0.5 Megawatts for the first circuit branch and 3 Kilowatts for the second circuit branch. The total average power of the shunt circuit under this level of earthquake is 101.26 Kilowatts.
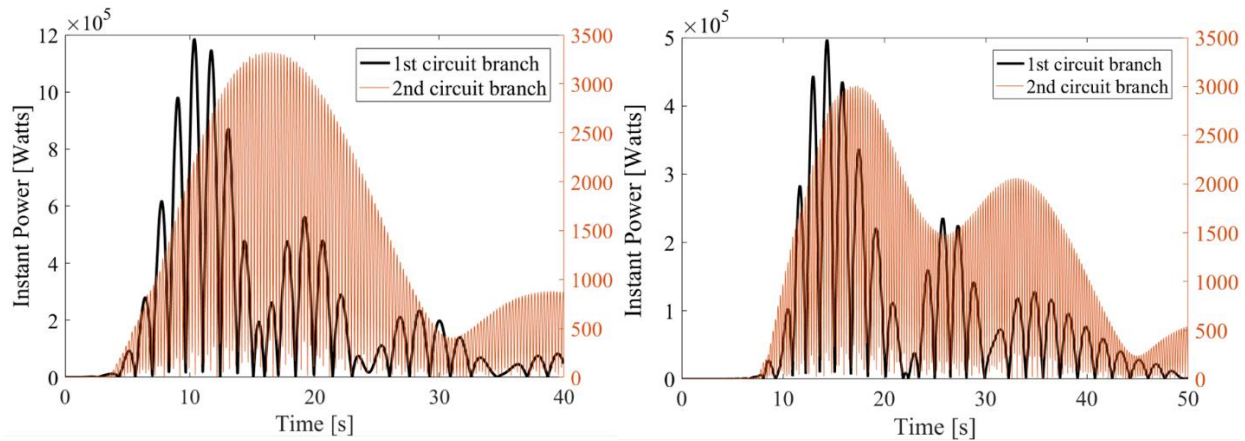
Figure 4.10 Instant power collected by two circuit branches of the parallel shunt circuit. (a) Under Northridge earthquake; (b) under Kobe earthquake.

4.6 Chapter Summary

Case study of a base-isolated structure is analyzed in both the frequency and the time domain to investigate the effectiveness of the proposed multi-resonant electromagnetic shunts. From frequency domain analysis, it shows that both vibration modes of the base isolation system can be suppressed using either the parallel or the series electromagnetic shunt. Besides, with same set of parameters, the parallel shunt circuit is superior to the series shunt circuit regarding both the vibration suppression and energy harvesting performance. From time domain analysis, it shows that the multi-mode resonant shunt circuit can achieve much smaller amplitude than single mode shunt circuit regarding the relative displacement and absolute acceleration of the primary structure when subjected to real recorded earthquakes. The instant power that can be collected by the multi-resonant electromagnetic shunt is capable of reaching the level of megawatts. Additionally, regarding the sensitivity of circuit parameters, the case study shows that for both parallel and series shunt circuits, the system is sensitive to the changes of capacitances, but not sensitive to the changes of resistances. Comparatively, parallel shunt circuit would be more robust in parameter mistuning than the series shunt circuit.

5. Experiment Verification of the Multi-resonant Electromagnetic Shunt Damper in a Base Isolation System

5.1 Chapter Introduction

This chapter conducts experimental verification of the proposed multi-resonant electromagnetic shunt circuit in base isolation system. A scaled-down base isolated structure is established. An electromagnetic linear motor is installed between the base and the ground. The experiment includes two parts. The first part is a hammer impact testing, which is conducted to verify the dynamic model by measuring frequency responses of base isolation system. Both absolute acceleration of the primary structure and relative displacement between base and primary structure are presented in comparison with their simulation results. The second part is a shake table testing, which demonstrates the dual functions of the multi-resonant electromagnetic shunt circuit, that is, enhanced vibration suppression and simultaneous energy harvesting. Two scaled-down earthquake signals, Northridge and Kobe, are applied to the base isolation system through the shake table. The acceleration of the primary structure is measured with both single mode and multi-mode resonant shunt circuits. The effectiveness of the multi-resonant electromagnetic shunt circuit is experimentally verified in both frequency and time domain responses analysis.

5.2 Experimental Setup

Figure 5.1 shows the experimental setup of a scaled-down base isolation system with the multi-resonant parallel electromagnetic shunt circuit. When the stroke is small, the motions of the primary structure and the base can be simplified as two degrees of freedom linear motions in the horizontal direction. The fundamental frequency of the base-isolated structure is 7.5 Hz and the second natural frequency is 34 Hz. A linear voice coil motor is installed between the base and a fixed table. A three dimensional positioner is used to align the coil and magnet of the motor to avoid frictions. The capacitors and external resistors are placed on the circuit board. The parallel shunt circuit is implemented due to its better dual-functional performance. The parameters of the experimental setup are listed in Table 5.1.
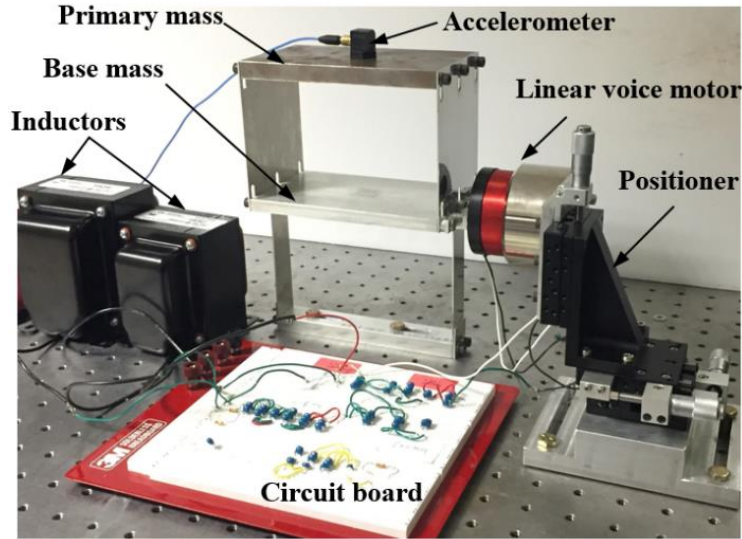
Figure 5.1 Experimental setup of the base isolation system

Table 5.1 Experimental parameters

Description	Symbol	Value
Primary structure mass	m_s	1.354 kg
Base mass	m_b	0.606 kg
Stiffness of the primary structure	k_s	16640 N/m
Stiffness of the base	k_b	5519 N/m
Inductance of linear motor	L_i	4 mH
Internal resistance of linear motor	R_i	4 Ω
Total inductance of 1st electrical resonator	L_1	170 mH
Capacitance of 1st electrical resonator	C_1	148 μF
External resistance of 1st electrical resonator	R_1	7.0 Ω
Total inductance of 2nd electrical resonator	L_2	400 mH
Capacitance of 2nd electrical resonator	C_2	940 μF
External resistance of 2nd electrical resonator	R_2	5.5 Ω

5.3 Impact Hammer Testing

5.3.1 Testing equipment and procedure

The equipment for the impact hammer testing includes,

a. Impact hammer: General purpose analysis impact hammer (model 086C03) is used. When hitting the impact hammer to the structure, and impulsive force is generated. An equal and opposite force is sensed by the load cell fitted in the head of the hammer. This generates an electric signal which is given to vibration analyzer which analyzes the signal.

b. Accelerometers: Two IEPE accelerometers (model 356A17) are used. Tri-axial accelerometers provide simultaneous measurements in three orthogonal directions, for analysis of all of the vibrations being experienced by a structure. Each unit incorporates three separate sensing elements that are oriented at right angles with respect to each other.

c. Vibration analyzer: The Crystal Instruments CoCo-80 vibration data collector is used as the vibration analyzer. Coco-80 is a portable device for vibration monitoring and data collection. The device processes and analyzes the signals received from transducers used in the vibration measurement. The device has 8 channels, which can receive number of electric signals simultaneously.

d. PC loaded with a software for modal analysis: The Engineering Data Management (EDM) software in Vibration Data Collector (VDC) Mode is applied to setup the CoCo-80 hardware and define routes before vibration measurements. After the data is downloaded to the PC, the user can use the tools in the EMD software to analyze and archive the data.
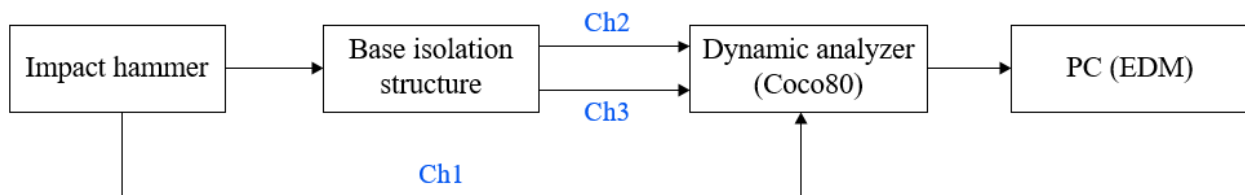
Figure 5.2 Experimental system diagram of the impact hammer testing

In this experiment, an impact force of the hammer was applied to the primary structure in the horizontal direction to emulate a broadband force excitation. Two piezoelectric accelerometers are attached to the structure to measure the absolute acceleration frequency responses of the base and the primary structure. The signal from the impact hammer is given to the vibration analyzer CoCo-80, which is then compared with the signals received from accelerometers to get the frequency response functions (FRFs) and obtain the natural frequencies of the base isolation system. The experimental system diagram is shown in Figure 5.2. The settings of measurement channels, including channels, input mode and sensitivities, are listed in Table 5.2.

Table 5.2 Settings of measurement channels for impact hammer testing

	Channel	Input Mode	Sensitivity
Impact hammer	1 (Reference)	ICP	2.25 mV/N
Accelerometer 1	2	ICP	495 mV/g
Accelerometer 2	3	ICP	500 mV/g

After getting the test result, the data is processed by using the EMD software. The frequency response of the absolute acceleration of the primary structure can be obtained directly. The frequency response of the relative displacement between the base and the primary structure can be calculated according to,

$$\left| \frac{X_r(j\omega)}{F(j\omega)} \right| = \left| \frac{\ddot{X}_s(j\omega) - \ddot{X}_b(j\omega)}{F(j\omega)} \right| \cdot \frac{1}{\omega^2} \tag{5.1}$$

5.3.2 Frequency responses of the base isolation system

Figure 5.3(a) shows theoretical and experimental acceleration frequency responses of the primary structure when excited by the impulse force. For comparison, the original system response without the electrical circuit is also presented. It shows that by using the multi-mode resonant circuit, the first resonant peak is reduced in magnitude by 27.32dB, and the second resonant peak is reduced by 22.61dB. Figure 5.3(b) shows the theoretical and experimental frequency responses of the relative displacement between the base and primary structure. The experimental results match theoretical responses closely which verifies the numerical analysis.

(a)
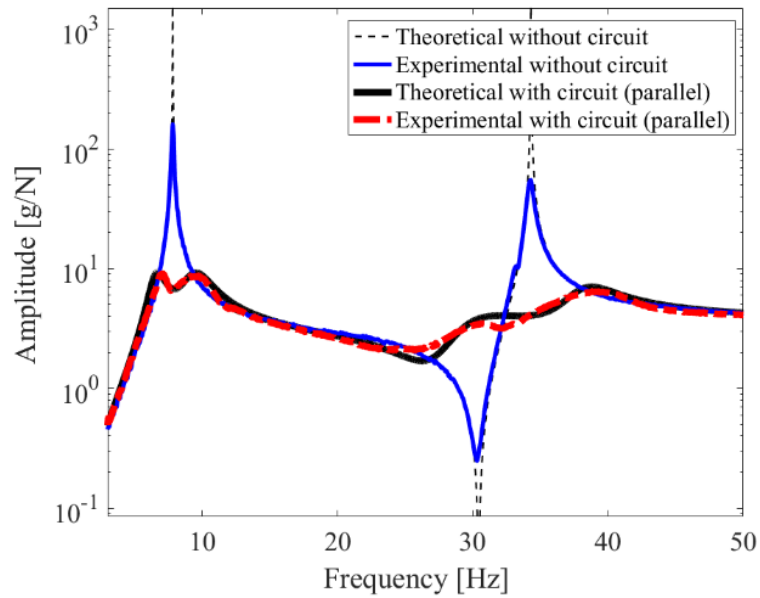
(b)
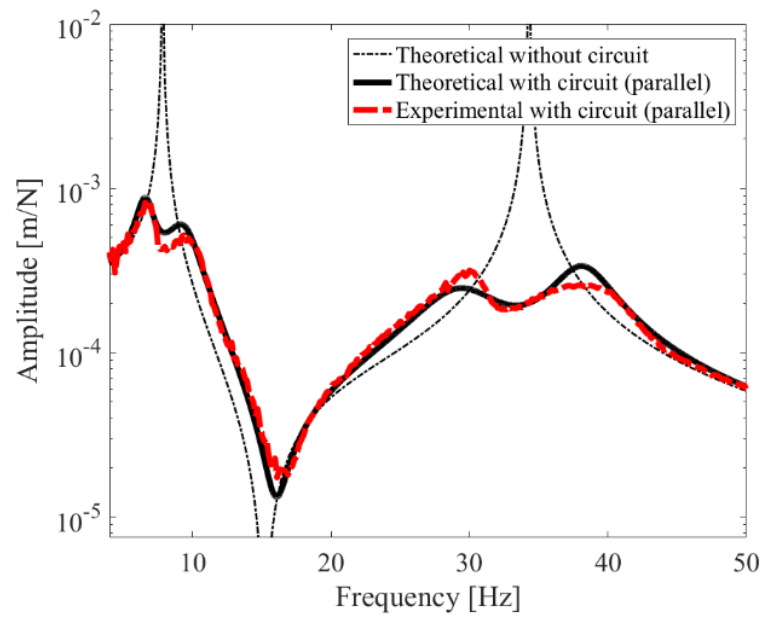
Figure 5.3 Theoretical and experimental frequency responses of the base isolation system with electromagnetic parallel shunt circuit. (a) Absolute acceleration of primary structure; (b) relative displacement between base and primary structure.

5.4 Shake Table Testing

5.4.1 Testing equipment and procedure
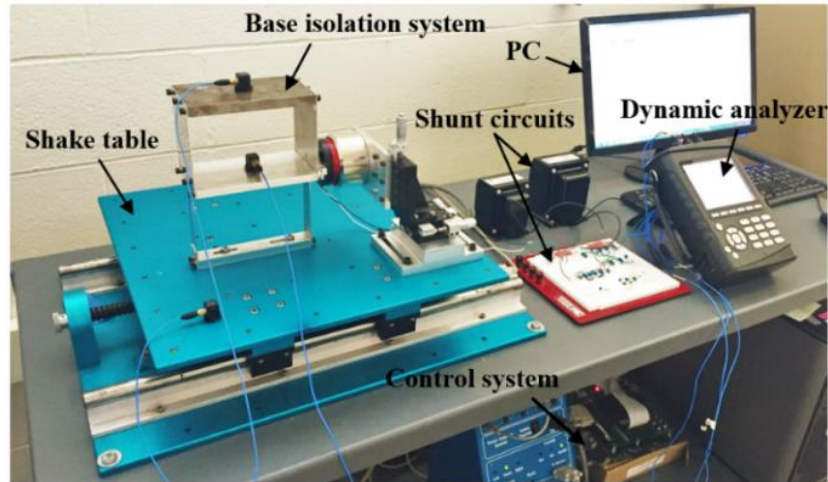
Figure 5.4 Testing system using shake table

As shown in Figure 5.4, the equipment for the shake table testing includes,

a. Quanser shake table. The top stage of the shake table is driven by a powerful motor that allow it to achieve an acceleration of 2.5g when up to 7.5kg of mass is mounted. The stage rides on two ground-hardened metal shafts using linear bearings which allows for smooth linear motions with low path deflection. When starting from center the stage is capable of moving 7.62cm, or 3 inches, on each side. It therefore has a total travel of 15.24cm.

b. Power amplifier. The Universal Power Module model UPM-180-25B is used for high-powered Quanser plants, which is capable of supplying continuous currents up to 25 A. It is consisted of a current-controlled power amplifier, an independent DC power supply, an analog input interface, and embedded safety circuitry.

c. Data acquisition (DAQ) board. Quanser's Q8 board is used, which is a powerful real-time measurement and control board offering an extensive range of hardware features and software support. With its wide range of inputs and outputs, the user can easily connect and control a variety of devices instrumented with analog and digital sensors.

d. PC loaded with real-time control software. Quanser Real-Time Control (QUARC) software is used which can run Simulink models in real-time on a PC. From the user-designed Simulink diagram, QUARC generates real-time code and creates a corresponding QUARC executable file. The users can command and measure signals to and from the shake table on a PC.

e. Accelerometers. Three IEPE accelerometers are used to measure the acceleration responses of the base isolation system. To get more accurate ground motion excitation input, one accelerometer is attached directly on the shake table.

f. Vibration analyzer. The Crystal Instruments CoCo-80 vibration data collector is still used as the vibration analyzer. In this experiment, five channels are used. The detailed settings of the measurement channel is listed in Table.5.3.

The experimental system diagram of the shake table testing is shown in Figure 5.5. By using the QUARC real-time controller on PC, the user specifies the amplitude and frequency of the input signal. The current needed to move the stage of the shake table at the desired position is calculated in QUARC and sent through the analog output channel of the DAQ board to the UPM device. The power amplifier in the UPM amplifies the current and drives the motor. The table moves back and forth at the position and frequency of the commanded sine wave. The resulting displacement and acceleration of the stage are measured by the on-board encoder sensor and the accelerometer sensor. The encoder and accelerometer are connected to the DAC board and their signals can be displayed and processed further in QUARC. Plotted data can be also be saved for later analysis.
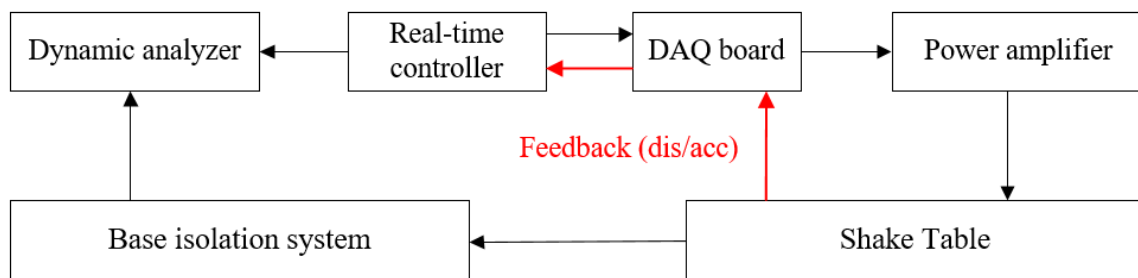
Figure 5.5 Experimental system diagram of the shake table testing

Table 5.3 Settings of measurement channels for shake table testing

Signal input	Location	Channel	Input Mode	Sensitivity
Accelerometer 1	Shake table	1	ICP	495 mV/g
Accelerometer 2	Base mass	2	ICP	500 mV/g
Accelerometer 3	Primary structure	3	ICP	497 mV/g
BNC connector 1	1st circuit branch	4	AC-Single End	1000 mV/V
BNC connector 2	2nd circuit branch	5	AC-Single End	1000 mV/V

In this experiment, Both Northridge and Kobe earthquake signal are applied to the system. However, due to the limited stroke of the motor, the actual input earthquake signal is scaled down. For Northridge earthquake signal, the displacement of the original peak movement is scaled from 16.92cm to 0.05cm. Also, since the experimental structure is a scaled-down model, the fundamental frequency of the structure (7.5Hz) is actually enlarged around 15 times than a real base-isolated structure. Considering this, the time duration of the excitation signal is scaled from original 39.98s to 2.66s. By the same token, for Kobe earthquake signal, the peak displacement is scaled from original 3.09cm to 0.05cm. The time duration is scaled from original 77.98s to 5.19s. The scaled earthquake input signal is presented in Figure 5.6.

(a)   (b)
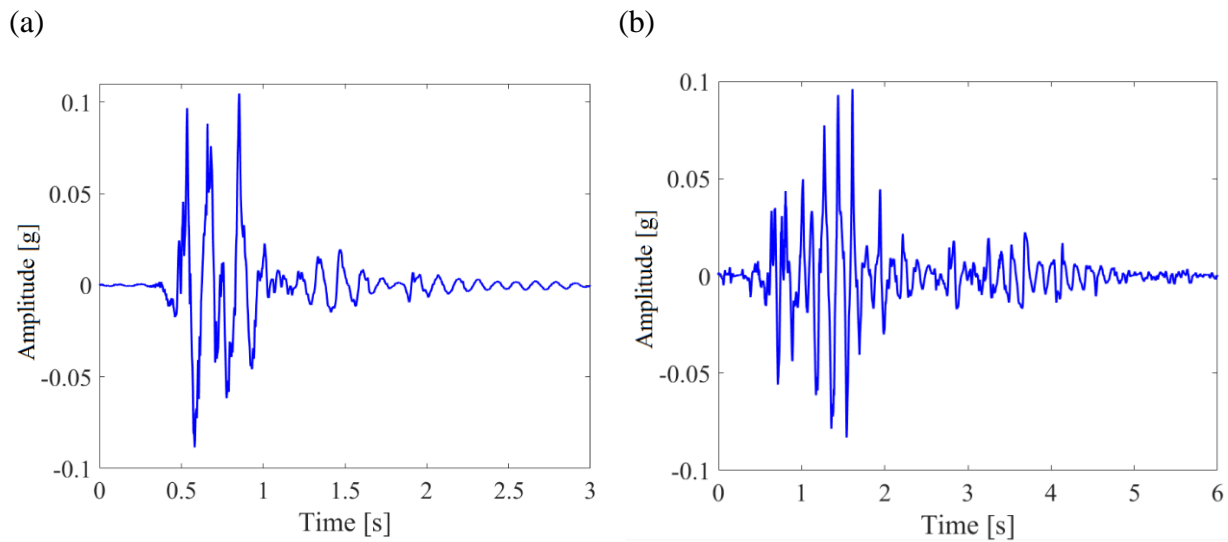
Figure 5.6 Ground accelerations under scaled earthquake signals. (a) Northridge; (b) Kobe.

5.4.2 Time history responses of the base isolation system

The time domain acceleration responses of the primary mass under scaled Northridge and Kobe earthquake excitations are shown in Figure 5.7.

(a)
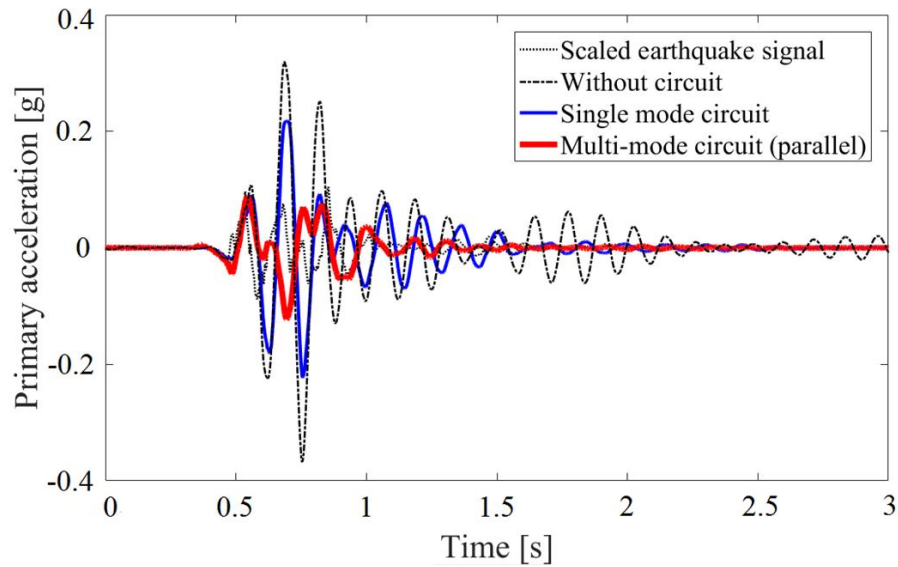
(b)
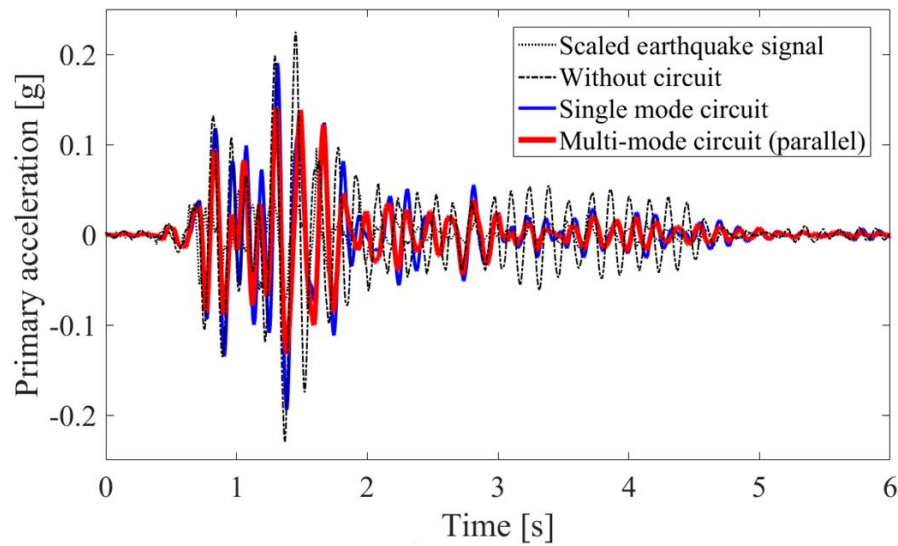
Figure 5.7 Time domain acceleration responses of the primary structure under scaled earthquake signals. (a) Northridge; (b) Kobe.

For comparison, responses of the system with single mode shunt circuit, which is only tuned to the first natural frequency of the base-isolated structure, are also tested and presented. It shows that under scaled Northridge earthquake signal, single mode shunt circuit can effectively suppress the vibration, reducing the peak value by 31.72%. The multi-mode shunt circuit outperforms the single mode shunt circuit by reducing the peak value by 72.81%. Under scaled Kobe earthquake signal, single and multi-mode shunt circuit can realize vibration suppression by reducing the peak value by 15.25% and 37.72%, respectively. The results also show that the vibration amplitude in multi-mode shunt circuit case decreases much faster than that of the single mode shunt circuit.

5.4.3 Instant voltage generated by the multi-resonant shunt circuit

The voltages simultaneously generated in the two branches of the multi-mode shunt circuit under the two scaled earthquakes. Since most vibration energy exist in the fundamental vibration mode, the generated voltage in the second circuit branch is much less than the first circuit.
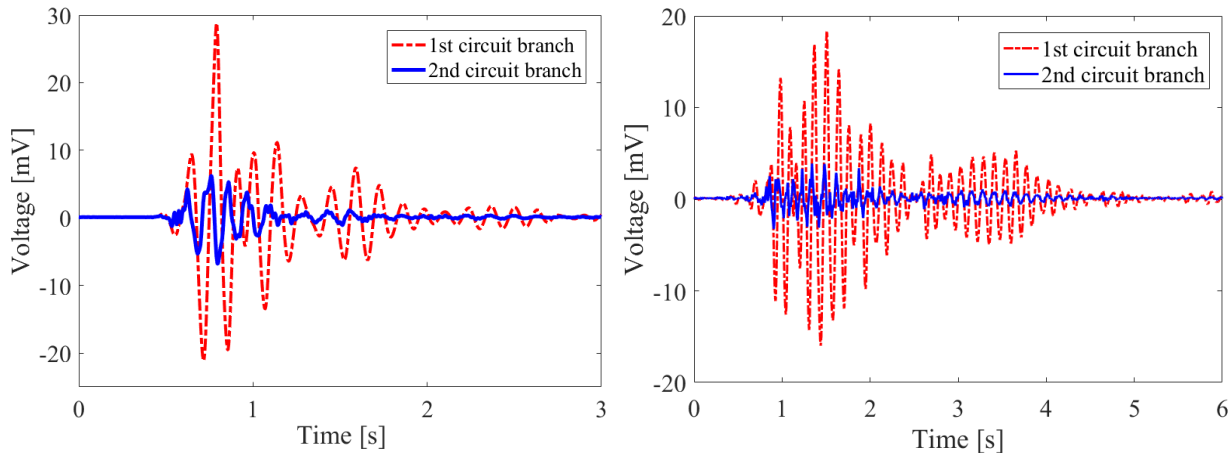
Figure 5.8 Output voltage across on external resistive loads in two circuit branches of the parallel shunt circuit under scaled earthquake signals. (a) Northridge; (b) Kobe.

Figure 5.8 shows that, under scaled Northridge earthquake, the peak voltage is around 30mV for the first branch and 6mV for the second branch. Under scaled Kobe earthquake, the peak voltage is around 18mV for the first branch and 4mV for the second branch. Figure 5.7 and Figure 5.8 clearly demonstrated the dual functions of the multi-mode shunt circuit in base isolation systems, that is,

achieving enhanced vibration suppression effectiveness and simultaneously harvesting the vibrational energy.

5.5 Summary

This chapter conducted experimental study on a scaled-down building base isolation system with multi-resonant electromagnetic shunt circuits. The dual-functions of the multi-mode electromagnetic shunt circuit in both vibration damping and energy harvesting are validated through experimental tests. The frequency response analysis from the impact hammer test shows that by using the multi-mode resonant circuit, the first resonant peak of the absolute acceleration of the primary structure is reduced by 27.32dB and the second resonant peak is reduced by 22.61dB. The experimental results match theoretical responses closely which verifies the numerical analysis. The time history response analysis from the shake table test shows that under the scaled earthquake excitations, multi-mode shunt circuit is more effective in suppressing the vibration of the base isolation system than that of the single mode shunt circuit. It shows that, under scaled Kobe and Northridge earthquake signals, the multi-resonant electromagnetic shunt is capable of suppressing the resonant peak of the vibration by 37.72% and 72.81%, respectively. In addition, the voltages simultaneously generated in the two branches of the multi-mode shunt circuit are also obtained, which demonstrated the dual functions of the multi-mode electromagnetic shunt circuit in base isolation system.

6. Conclusion and Future Work

6.1 Conclusions of the Thesis

This thesis developed multi-resonant electromagnetic shunts for dual-functional vibration damping and energy harvesting in the building base isolation system. The following conclusions can be drawn from the work completed.

1. The proposed parallel and series electromagnetic shunt dampers outperform the single mode electromagnetic shunt damper by suppressing both vibration modes of the base isolation system effectively. Under the same stiffness ratio, the parallel electromagnetic shunt is more effective and robust than the series electromagnetic shunt regarding both vibration damping and energy harvesting. In addition, parallel electromagnetic shunt damper can achieve better vibration mitigation performance than equivalent parallel TMDs and series TMDs with the same total mass ratio in the base isolation system.

2. The multi-resonant electromagnetic shunt circuit can be optimized using the H_2 criteria to minimize the RMS relative displacement between the base and the primary structure thus achieve the best effectiveness in enhancing the building safety. The optimal design of the circuit is related to four tuning parameters: electrical tuning ratios f_{e1}, f_{e2} and electrical damping ratios ξ_{e1}, ξ_{e2}. The optimization process provides a schematic way to determine the optimal parameters for the electromagnetic shunt circuits when the base isolation system is subjected to wind or earthquake induced excitations.

3. The dual functions of the multi-resonant electromagnetic shunt in vibration damping and energy harvesting are experimentally validated on a scaled-down building base isolation system. The impact hammer testing result shows that the multi-resonant electromagnetic shunt can effectively mitigate the vibrations by suppressing the first resonant peak by 27.32dB and the second resonant peak by 22.61dB regarding the primary structure acceleration. The shake table testing demonstrates that the multi-resonant electromagnetic shunt is superior to the single resonant shunt and is capable of energy harvesting simultaneously.

6.2 Recommendations for Future Work

The recommendations for future work are summarized as follows,

1. The multi-resonant electromagnetic shunt damper can be further designed to suppress higher vibration modes of multi-floor buildings. For buildings with inter-story isolation systems, the electromagnetic shunt damper can be employed to save the space and harvest the potential energy. In addition to civil structure, the multi-resonant electromagnetic shunt circuit can also be applied to traditional base isolation system which is used for protection of the precision machine and instrumentations.

2. Building performances involve building safety, people comfort and energy harvesting, related to the relative displacement, absolute acceleration of the primary structure, and the electrical current in the harvesting circuit, respectively. In this thesis, building safety is considered as it is the highest priority for practice when extreme situation happens. However, for other cases when people comfort or energy harvesting are the major concern, the performance index can be chosen accordingly. The performance of the multi-resonant electromagnetic shunt for other considerations can be further investigated.

3. The multi-mode electromagnetic shunt circuit with external resistors is employed in this thesis to represent an ideal energy harvesting circuit. The energy dissipated in the resistors is regarded as the harvested energy. In the future, practical high-efficiency energy harvesting circuits are expected to be developed for powering the wireless sensing networks or structural control systems in the civil engineering applications. By connecting the circuit to the building's power grid, a complete semi-active self-powered vibration control system can be realized.

References

[1] Shanmuga, P.D., Cinitha, A., Umesha, P.K., and Nagesh, R.I., "Enhancing the Seismic Response of Buildings with energy dissipation methods - An Overview," *Journal of Civil Engineering Research*, vol. 4, no. 2, pp. 17-22, 2014.

[2] Stephen, N.G., "On energy harvesting from ambient vibration," *Journal of Sound and Vibration*, vol. 293, no. 1, pp. 409-425, 2006.

[3] Park, G., Rosing, T., Todd, M.D., Farrar, C.R., and Hodgkiss, W., "Energy harvesting for structural health monitoring sensor networks," *Journal of Infrastructure Systems*, vol. 14, no. 1, pp. 64-79, 2008.

[4] Shen, W., Zhu, S., and Zhu, H., "Electromagnetic energy harvesting from structural vibrations during earthquakes," *Smart Structures and Systems,* vol. 18, pp. 449-470, 2016.

[5] Zhu, S., Shen, W., and Xu, Y., "Linear electromagnetic devices for vibration damping and energy harvesting," *Engineering Structures*, vol. 34, pp. 198-212, 2012.

[6] Tang, X., and Zuo, L., "Simultaneous energy harvesting and vibration control of structures with tuned mass damper," *Journal of Intelligent Material Systems and Structures*, vol. 23, no. 18, pp. 2117-2127, 2012.

[7] Skinner, R.I., Robinson, W.H., and McVerry, G.H., An introduction to seismic isolation. Wiley, Chichester, England, 1993.

[8] Moheimani, S.O.R., and Fleming, A.J., Piezoelectric transducers for vibration control and damping, London: Springer-Verlag, pp. 73-84, 2006.

[9] Inoue, T., Ishida Y., and Sumi M., "Vibration suppression using electromagnetic resonant shunt damper," *Journal of Vibration and Acoustics*, vol. 130, no. 4, pp. 041003, 2008.

[10] Zhang, X., Niu, H., and Yan, B., "A novel multimode negative inductance negative resistance shunted electromagnetic damping and its application on a cantilever plate," *Journal of Sound and Vibration*, vol. 331, no. 10, pp. 2257-2271, 2012.

[11] Buckle, I.G., and Ronald, L.M., "Seismic isolation: history, application, and performance-A world view," *Earthquake Spectra*, vol. 6, no. 2, pp. 161-201, 1990.

[12] Islam, A., Ahmad, S., Jameel, M., and Zamin, M., "Seismic base isolation for buildings in regions of low to moderate seismicity: Practical Alternative Design," *Practice Periodical on Structural Design and Construction*, vol. 17, no. 1, pp. 13-20, 2012.

[13] http://www.did.org.tr/eng/?page_id=47

[14] Jangid, R.S., and Datta, T.K., "Seismic behavior of base-isolated buidlings: a state-of-the art review," *Proceedings of the Institution of Civil Engineers: Structures and Buildings*, vol. 110, no. 2, pp. 186-203, 1995.

[15] James, M.K., "Base Isolation: Linear Theory and Design," *Earthquake Spectra*, vol. 6, no. 2, pp. 223-244, 1990.

[16] Symans, M.D., Charney, F.A., and Whittaker, A.S., "Energy dissipation systems for seismic applications: current practice and recent developments," *Journal of Structural Engineering*, vol. 134, no. 1, pp. 3-21, 2008.

[17] Wu, T.C., "Design of base isolation system for buildings," Master Thesis, Massachusetts Institute of Technology, 2001.

[18] Manarbek, S., "Study of base isolation systems," Master Thesis, Massachusetts Institute of Technology, 2013.

[19] Nagarajaiah, S. and Sun, X., "Seismic performance of base isolated buildings in the 1994 northridge earthquake," *Eleventh World Conference on Earthquake Engineering*, no. 598, 1996.

[20] Farzad, N., and James, M.K., Design of seismic isolated structures: From Theory to Practice, John Wiley & Sons, Inc., 1999.

[21] James, M.K., "Aseismic base isolation: review and bibliography," *Soil Dynamics and Earthquake Engineering*, vol. 5, no. 3, pp. 202-216, 1986.

[22] Spencer, Jr, B.F., and Sain, M.K., "Controlling buildings: A new frontier in feedback," *IEEE Control System Magazine*, vol. 17, no. 6, pp. 19-35, 1997.

[23] Reinhorn, A.M., and Riley, M., "Control of bridge vibrations with hybrid devices," *Proceedings of the First World Conference on Structural Control*, pp. 50-59, Los Angeles, 1994.

[24] Ramallo, J.C., Johnson, E.A., and Spencer, Jr, B.F., "Smart Base Isolation Systems", *Journal of Engineering Mechanics*, vol. 128, no. 10,pp. 1088-1099, 2002.

[25] Spencer, Jr, B.F., and Soong, T.T., "New applications and development of active, semi-active and hybrid control techniques for seismic and non-seismic vibration in the USA," *Proceedings of International Post-SMiRT Conference Seminar on Seismic Isolation*, Cheju, Korea, August 23-25, 1999.

[26] Matsagar, V.A., and Jangid, R.S., "Viscoelatic damper connected to adjacent structures involving seismic isolation," *Journal of Civil Engineering and Management,* vol. 11, no. 4, pp. 309-322, 2005.

[27] Yoshioka, H., Ramallo, J.C., and Spencer, Jr, B.F., "Smart base isolation strategies employing magnetorheological dampers," *Journal of Engineering Mechanics*, vol. 128, no. 5, pp. 540-551, 2002.

[28] Etedali, S., Sohrabi, M. R., and Tavakoli, S., "Optimal PD/PID control of smart base isolated buildings equipped with piezoelectric friction dampers," *Earthquake Engineering and Engineering Vibration*, vol. 12, no. 1, pp. 39-54, 2013.

[29] Niu, H., Zhang, X., Xie, S., and Wang, P., "A new electromagnetic shunt damping treatment and vibration control of beam structures," *Smart Materials and Structures*, vol.18, no.4, pp. 045009, 2009.

[30] Khaligh, A., Zeng, P., and Zheng, C., "Kinetic energy harvesting using piezoelectric and electromagnetic technologies—state of the art," *IEEE Transactions on Industrial Electronics*, vol. 57, no. 3, pp. 850-860, 2010.

[31] Zuo L., and Tang X., "Large-scale vibration energy harvesting," *Journal of Intelligent Material Systems and Structures*, vol, 24, no. 11, pp. 1405-1430, 2013.

[32] Behrens, S., Fleming, A.J., and Moheimani, S.O.R., "Electromagnetic shunt damping," *Proceedings of the 2003 IEEE/ASME International Conference on Advanced Intelligent Mechatronics*, pp. 1145-1150, 2003.

[33] Cui, W., Tang, X., and Zuo, L., "H_2 optimization of electricity-generating tuned mass dampers for simultaneous vibration control and energy harvesting," *SPIE Smart Structures and Materials: Nondestructive Evaluation and Health Monitoring*, pp. 86880U-86880U, 2013.

[34] Sodano, H.A., Magliula, E.A., Park, G., and Inman, D.J., "Electric power generation using piezoelectric materials," *Proceedings of the 13th International Conference Adaptive Structural Technology*, Potsdam, Germany, pp. 153-161, 2002.

[35] Shearwood, C., and Yates, R.B., "Development of an electromagnetic microgenerator," *Electronics Letters*, vol. 33, no. 22, pp. 1883-1884, 1997.

[36] Large Shaker Model V53-64/DSA4 [Online]. Available: http://www.gearing-watson.com

[37] Behrens, S., Fleming, A.J. and Moheimani, S.O.R., "Vibration isolation using a shunted electromagnetic transducer," *Smart Structures and Materials*, vol. 5386, pp. 506-515, 2004.

[38] Palomera-Arias R, "Passive electromagnetic damping device for motion control of building structures," Ph.D. Dissertation, Massachusetts Institute of Technology, 2005.

[39] Cheng, T.H., and Oh, I.K., "A current-flowing electromagnetic shunt damper for multi-mode vibration control of cantilever beams," *Smart Materials and Structures*, vol. 18, no. 9, pp. 095036, 2009.

[40] Zhang, C., and Ou, J., "Control structure interaction of electromagnetic mass damper system for structural vibration control," *Journal of Engineering Mechanics*, vol. 134, no. 5, pp. 428-437, 2008.

[41] Zuo, L., and Cui, W., "Dual-functional energy-harvesting and vibration control: electromagnetic resonant shunt series tuned mass dampers," *Journal of Vibration and Acoustics,* vol. 135, pp. 051018, 2012.

[42] Tang, X., Liu, Y., Cui, W., and Zuo, L., "Analytical solutions to H2 and H∞ optimizations of resonant shunted electromagnetic tuned mass damper and vibration energy harvester," *Journal of Vibration and Acoustics*, vol. 138, pp. 011018, 2016.

[43] Liu, Y., Lin, C.C., Parker J., and Zuo L., "Exact H2 Optimal Tuning and Experimental verification of energy-harvesting series electromagnetic tuned-mass dampers," *Journal of Vibration and Acoustics,* vol. 138, pp. 061003, 2016.

[44] Viana, F.A.C., and Steffen, Jr, V., "Multimodal vibration damping through piezoelectric patches and optimal resonant shunt circuits," *Journal of the Brazilian Society of Mechanical Sciences and Engineering*, vol. 28, no. 3, pp. 293-310, 2006.

[45] Fleming, A.J., and Moheimani, S.O.R., "Adaptive piezoelectric shunt damping," *Smart Materials and Structures*, vol. 12, no. 1, pp. 36-48, 2003.

[46] Lesieutre, G.A., "Vibration damping and control using shunted piezoelectric materials," *The Shock and Vibration Digest*, vol. 30, no. 3, pp. 187-195, 1998.

[47] Forward, R.L., "Electronic Damping of Vibrations in Optical Structures," *Applied Optics*, vol. 18, no. 5, pp. 690-697, 1979.

[48] Hagood, H.W., and Von Flotow, A., "Damping of Structural Vibrations with Piezoelectric Materials and Passive Electrical Networks," *Journal of Sound and Vibration*, vol. 146, no. 2, pp. 243-268, 1991.

[49] Behrens, S., and Moheimani, S.R., "Optimal resistive elements for multiple mode shunt-damping of a piezoelectric laminated beam," *IEEE Conference on Decision and Control*, vol. 4, pp. 4018-4023, 2000.

[50] Edberg, D.L., Bicos, A.S., Fuller, C.M. Tracy, J.J, and Fechter, J.S., "Theoretical and Experimental Studies of a Truss Incorporating Active Members," *Journal of Intelligent Material Systems and Structures*, vol. 3, pp. 333-347, 1992.

[51] Wu, S.Y., "Method for multiple mode shunt damping of structural vibration using a single PZT transducer," *SPIE Conference on Passive Damping*, vol. 3327, pp. 159-168, 1998.

[52] Hollkamp, J.J., "Multimodal passive vibration with piezoelectric materials and resonant shunts," *Journal of Intelligent Material Systems and Structures*, vol. 5, no. 1, pp. 49-57, 1994.

[53] Behrens, S., Moheimani, S. O. R., and Fleming, A.J., "Multiple mode current flowing passive piezoelectric shunt controller," *Journal of Sound and Vibration*, vol. 266, no. 5, pp. 929-942, 2003.

[54] Fleming, A.J., Moheimani, S.O.R., and Behrens, S., "Reducing the inductance requirements of piezoelectric shunt damping circuits," *Smart Materials and Structures*, vol. 12, no. 1, pp. 57-64, 2003.

[55] Niederberger, D., Fleming, A., Moheimani, S. and Morari, M., "Adaptive multi-mode resonant piezoelectric shunt damping," *Smart Materials and Structures*, vol. 13, no. 5, pp. 1025-1035, 2004.

[56] Cao, M., and Zuo, L., "Energy harvesting from building seismic isolation with multi-mode resonant shunt circuits," *ASME 2014 Dynamic Systems and Control Conference*, San Antonio, Texas, USA, October 2014.

[57] Cheng, T., and Oh, I., "A current-flowing electromagnetic shunt damper for multi-mode vibration control of cantilever beams," *Smart Materials and Structures*, vol. 18, no. 9, pp. 095036, 2009.

[58] Zhang, X., Niu, H., and Yan, B., "A novel multimode negative inductance negative resistance shunted electromagnetic damping and its application on a cantilever plate," *Journal of Sound and Vibration,* vol. 331, no. 10, pp. 2257-2271, 2012.

[59] Liu, Y., Lin, C.C., and Zuo, L., "Evaluation and optimum design of dual-functional electromagnetic tuned mass dampers," *12th International Conference on Motion and Vibration Control*, Hokkaido, Japan, August 2014.

[60] Zuo, L., "Effective and robust vibration control using series multiple tuned-mass dampers," *Journal of Vibration and Acoustics*, vol. 131, no. 3, pp. 031003, 2009.

[61] Firestone, F.A., "A new analogy between mechanical and electrical systems*," Journal of the Acoustical Society of America*, vol. 4, no. 3, pp. 249-267, 1933.

[62] Hubert, M.J., Nathaniel, B.N., and Ralph, S.P., Theory of servomechanisms. New York: McGraw-Hill, pp. 333-339, 1947.

[63] Kircher, C.A., Seismically Isolated Structures, NEHRP Recommended Provisions: Design Examples (FEMA P-751), Building Seismic Safety Council, Washington, D.C., pp. 1201-1263, 2012.

Appendix

MS response integration of an eighth order system

$$I_8 = \frac{1}{2\pi j} \int_{-\infty}^{\infty} \frac{g_8(x)}{h_8(x)h_8(-x)} dx = \frac{M_7}{2a_0\Delta_7}$$

where $h_n(x) = a_0 x^8 + a_1 x^7 + a_2 x^6 + a_3 x^5 + a_4 x^4 + a_5 x^3 + a_6 x^2 + a_7 x^1 + a_8$, $g_n(x) = b_0 x^{14} + b_1 x^{12} + b_2 x^{10} + b_3 x^8 + b_4 x^6 + b_5 x^4 + b_6 x^2 + b_7$,

and the roots of $h_n(x)$ all lie in the upper half plane.

$$M_7 = b_0 m_0 + a_0 b_1 m_1 + a_0 b_2 m_2 + a_0 b_3 m_3 + a_0 b_4 m_4 + a_0 b_5 m_5 + a_0 b_6 m_6 + a_0 b_7 m_7$$

in which,

$$
\begin{aligned}
m_0 = &(a_6 a_7^3 - a_5 a_8 a_7^2)a_0^2 \\
&+ (a_3^2 a_5 a_8^2 - 2a_3 a_4 a_5 a_7 a_8 - a_3 a_5^2 a_6 a_8 + a_3 a_5 a_6^2 a_7 + 2a_2 a_3 a_7^2 a_8 \\
&- 2a_1 a_3 a_7 a_8^2 + a_4^2 a_5 a_7^2 + a_4 a_5^3 a_8 - a_4 a_5^2 a_6 a_7 - 2a_2 a_4 a_7^3 + 2a_1 a_4 a_7^2 a_8 \\
&- a_2 a_5^2 a_7 a_8 - a_1 a_5^2 a_8^2 + a_2 a_5 a_6 a_7^2 + 3a_1 a_5 a_6 a_7 a_8 - 2a_1 a_6^2 a_7^2)a_0 - a_1^3 a_8^3 \\
&+ 3a_1^2 a_2 a_7 a_8^2 + a_1^2 a_3 a_6 a_8^2 + 2a_1^2 a_4 a_5 a_8^2 - 3a_1^2 a_4 a_6 a_7 a_8 - a_1^2 a_5 a_6^2 a_8 \\
&+ a_1^2 a_6^3 a_7 - 3a_1 a_2^2 a_7^2 a_8 - 3a_1 a_2 a_3 a_5 a_8^2 + a_1 a_2 a_3 a_6 a_7 a_8 - a_1 a_2 a_4 a_5 a_7 a_8 \\
&+ 3a_1 a_2 a_4 a_6 a_7^2 + 2a_1 a_2 a_5^2 a_6 a_8 - 2a_1 a_2 a_5 a_6^2 a_7 - a_1 a_3^2 a_4 a_8^2 + 2a_1 a_3 a_4^2 a_7 a_8 \\
&+ a_1 a_3 a_4 a_5 a_6 a_8 - a_1 a_3 a_4 a_6^2 a_7 - a_1 a_4^3 a_7^2 - a_1 a_4^2 a_5^2 a_8 + a_1 a_4^2 a_5 a_6 a_7 + a_2^3 a_7^3 \\
&+ 3a_2^2 a_3 a_5 a_7 a_8 - 2a_2^2 a_3 a_6 a_7^2 - a_2^2 a_4 a_5 a_7^2 - a_2^2 a_5^3 a_8 + a_2^2 a_5^2 a_6 a_7 + a_2 a_3^3 a_8^2 \\
&- 2a_2 a_3^2 a_4 a_7 a_8 - a_2 a_3^2 a_5 a_6 a_8 + a_2 a_3^2 a_6^2 a_7 + a_2 a_3 a_4^2 a_7^2 + a_2 a_3 a_4 a_5^2 a_8 \\
&- a_2 a_3 a_4 a_5 a_6 a_7
\end{aligned}
$$

$$
\begin{aligned}
m_1 = &(a_8 a_5^2 a_7 - a_6 a_5 a_7^2 + a_4 a_7^3 - a_3 a_8 a_7^2)a_0^2 + (-a_1^2 a_7 a_8^2 + 2a_1 a_2 a_7^2 a_8 + 2a_1 a_3 a_5 a_8^2 \\
&- a_1 a_3 a_6 a_7 a_8 - a_1 a_4 a_6 a_7^2 - a_1 a_5^2 a_6 a_8 + a_1 a_5 a_6^2 a_7 - a_2^2 a_7^3 - 3a_2 a_3 a_5 a_7 a_8 \\
&+ 2a_2 a_3 a_6 a_7^2 + a_2 a_4 a_5 a_7^2 + a_2 a_5^3 a_8 - a_2 a_5^2 a_6 a_7 - a_3^3 a_8^2 + 2a_3^2 a_4 a_7 a_8 \\
&+ a_3^2 a_5 a_6 a_8 - a_3^2 a_6^2 a_7 - a_3 a_4^2 a_7^2 - a_3 a_4 a_5^2 a_8 + a_3 a_4 a_5 a_6 a_7)
\end{aligned}
$$

$$
\begin{aligned}
m_2 = &(a_2 a_7^3 - a_5^3 a_8 - a_1 a_7^2 a_8 - a_3 a_6 a_7^2 - a_4 a_5 a_7^2 + a_5^2 a_6 a_7 + 2a_3 a_5 a_7 a_8)a_0^2 + (-a_1^2 a_5 a_8^2 \\
&+ a_1^2 a_6 a_7 a_8 + a_1 a_3^2 a_8^2 - 2a_1 a_3 a_4 a_7 a_8 - a_1 a_3 a_5 a_6 a_8 + a_1 a_3 a_6^2 a_7 + a_1 a_4^2 a_7^2 \\
&+ a_1 a_4 a_5^2 a_8 - a_1 a_4 a_5 a_6 a_7 + a_1 a_2 a_5 a_7 a_8 - a_1 a_2 a_6 a_7^2)
\end{aligned}
$$

$$
\begin{aligned}
m_3 = &-a_7^3 a_0^2 + (-a_8 a_3^2 a_7 + a_8 a_3 a_5^2 - a_6 a_3 a_5 a_7 + a_4 a_3 a_7^2 - 2a_1 a_8 a_5 a_7 + 2a_1 a_6 a_7^2)a_0 \\
&+ (a_1^2 a_5 a_6 a_8 - a_1^2 a_6^2 a_7 + a_4 a_1^2 a_7 a_8 - a_3 a_1^2 a_8^2 - a_2 a_1 a_5^2 a_8 + a_2 a_1 a_5 a_6 a_7 \\
&- a_2 a_4 a_1 a_7^2 + a_2 a_3 a_1 a_7 a_8)
\end{aligned}
$$

$$m_4 = a_5 a_7^2 a_0^2 + (-a_8 a_3^2 a_5 + a_6 a_3^2 a_7 - a_2 a_3 a_7^2 + 2a_1 a_8 a_3 a_7 + a_1 a_8 a_5^2 - a_1 a_6 a_5 a_7$$
$$- a_1 a_4 a_7^2) a_0 + (a_1^3 a_8^2 - 2a_1^2 a_2 a_7 a_8 + a_4 a_6 a_1^2 a_7 - a_4 a_5 a_1^2 a_8 + a_1 a_2^2 a_7^2$$
$$- a_3 a_6 a_1 a_2 a_7 + a_3 a_5 a_1 a_2 a_8)$$

$$m_5 = (a_3 a_7^2 - a_5^2 a_7) a_0^2$$
$$+ (a_8 a_1^2 a_7 - a_6 a_1 a_3 a_7 - 2a_5 a_8 a_1 a_3 - a_2 a_1 a_7^2 + 2a_4 a_5 a_1 a_7 + a_8 a_3^3 - a_4 a_3^2 a_7$$
$$+ a_2 a_5 a_3 a_7) a_0 + (a_1^2 a_2 a_5 a_8 - a_1^3 a_6 a_8 - a_1 a_2 a_3^2 a_8 - a_1 a_2^2 a_5 a_7 - a_1^2 a_4^2 a_7$$
$$+ a_1^2 a_2 a_6 a_7 + a_1^2 a_3 a_4 a_8 + a_1 a_2 a_3 a_4 a_7)$$

$$m_6 = (a_5^3 - 2a_3 a_5 a_7 + a_1 a_7^2) a_0^2$$
$$+ (a_8 a_1^2 a_5 - 2a_6 a_7 a_1^2 - a_8 a_1 a_3^2 + 3a_6 a_1 a_3 a_5 - 2a_4 a_1 a_5^2 + a_2 a_7 a_1 a_5 - a_6 a_3^3$$
$$+ a_4 a_3^2 a_5 + a_2 a_7 a_3^2 - a_2 a_3 a_5^2) a_0 + (-a_8 a_1^3 a_4 + a_1^3 a_6^2 + a_8 a_1^2 a_2 a_3$$
$$+ a_7 a_1^2 a_2 a_4 - 2a_1^2 a_2 a_5 a_6 - a_1^2 a_3 a_4 a_6 + a_1^2 a_4^2 a_5 - a_7 a_1 a_2^2 a_3 + a_1 a_2^2 a_5^2$$
$$+ a_1 a_2 a_3^2 a_6 - a_1 a_2 a_3 a_4 a_5)$$

$$m_7 = (a_7^3 a_0^3 + (a_8 a_3^2 a_7 - a_8 a_3 a_5^2 + 3a_6 a_3 a_5 a_7 - 2a_4 a_3 a_7^2 - a_6 a_5^3 + a_4 a_5^2 a_7 - a_2 a_5 a_7^2$$
$$+ 2a_1 a_8 a_5 a_7 - 3a_1 a_6 a_7^2) a_0^2 + a_1^2 a_3 a_8^2 - 2a_1^2 a_4 a_7 a_8 - 2a_1^2 a_5 a_6 a_8 + 3a_1^2 a_6^2 a_7$$
$$- 3a_1 a_2 a_3 a_7 a_8 + 3a_1 a_2 a_4 a_7^2 - a_1 a_2 a_5 a_6 a_7 + a_1 a_3^2 a_6 a_8 + 2a_1 a_3 a_4 a_5 a_8$$
$$+ a_1 a_3 a_4 a_6 a_7 - 3a_1 a_3 a_5 a_6^2 - 2a_1 a_4^2 a_5 a_7 + 2a_1 a_4 a_5^2 a_6 + a_2^2 a_3 a_7^2 + a_2 a_3^2 a_5 a_8$$
$$- 2a_2 a_3^2 a_6 a_7 - a_2 a_3 a_4 a_5 a_7 + a_2 a_3 a_5^2 a_6 - a_3^3 a_4 a_8 + a_3^3 a_6^2 + a_3^2 a_4^2 a_7$$
$$- a_3^2 a_4 a_5 a_6) a_0 - a_1^3 a_2 a_8^2 + 2a_1^3 a_4 a_6 a_8 - a_1^3 a_6^3 + 2a_1^2 a_2^2 a_7 a_8 - a_1^2 a_2 a_3 a_6 a_8$$
$$- 3a_1^2 a_2 a_4 a_6 a_7 + 2a_1^2 a_2 a_5 a_6^2 - a_1^2 a_3 a_4^2 a_8 + a_1^2 a_3 a_4 a_6^2 + a_1^2 a_4^3 a_7 - a_1^2 a_4^2 a_5 a_6$$
$$- a_1 a_2^3 a_7^2 - a_1 a_2^2 a_3 a_5 a_8 + 2a_1 a_2^2 a_3 a_6 a_7 + a_1 a_2^2 a_4 a_5 a_7 - a_1 a_2^2 a_5^2 a_6$$
$$+ a_1 a_2 a_3^2 a_4 a_8 - a_1 a_2 a_3^2 a_6^2 - a_1 a_2 a_3 a_4^2 a_7 + a_1 a_2 a_3 a_4 a_5 a_6)/a_8$$

$$\Delta = a_7^4 a_0^3 + (2a_8 a_3^2 a_7^2 - 4a_8 a_3 a_5^2 a_7 + 3a_6 a_3 a_5 a_7^2 - 2a_4 a_3 a_7^3 + a_8 a_5^4 - a_6 a_5^3 a_7 + a_4 a_5^2 a_7^2$$
$$- a_2 a_5 a_7^3 + 4a_1 a_8 a_5 a_7^2 - 3a_1 a_6 a_7^3) a_0^2$$
$$+ (4a_1^2 a_3 a_7 a_8^2 - 3a_1^2 a_4 a_7^2 a_8 + 2a_1^2 a_5^2 a_8^2 - 5a_1^2 a_5 a_6 a_7 a_8 + 3a_1^2 a_6^2 a_7^2$$
$$- 5a_1 a_2 a_3 a_7^2 a_8 + 3a_1 a_2 a_4 a_7^3 + a_1 a_2 a_5^2 a_7 a_8 - a_1 a_2 a_5 a_6 a_7^2 - 4a_1 a_3^2 a_5 a_8^2$$
$$+ a_1 a_3^2 a_6 a_7 a_8 + 4a_1 a_3 a_4 a_5 a_7 a_8 + a_1 a_3 a_4 a_6 a_7^2 + 3a_1 a_3 a_5^2 a_6 a_8$$
$$- 3a_1 a_3 a_5 a_6^2 a_7 - 2a_1 a_4^2 a_5 a_7^2 - 2a_1 a_4 a_5^3 a_8 + 2a_1 a_4 a_5^2 a_6 a_7 + a_2^2 a_3 a_7^3$$
$$+ 3a_2 a_3^2 a_5 a_7 a_8 - 2a_2 a_3^2 a_6 a_7^2 - a_2 a_3 a_4 a_5 a_7^2 - a_2 a_3 a_5^3 a_8 + a_2 a_3 a_5^2 a_6 a_7$$
$$+ a_3^4 a_8^2 - 2a_3^3 a_4 a_7 a_8 - a_3^3 a_5 a_6 a_8 + a_3^3 a_6^2 a_7 + a_3^2 a_4^2 a_7^2 + a_3^2 a_4 a_5^2 a_8$$
$$- a_3^2 a_4 a_5 a_6 a_7) a_0 + a_1^4 a_8^3 - 3a_1^3 a_2 a_7 a_8^2 - a_1^3 a_3 a_6 a_8^2 - 2a_1^3 a_4 a_5 a_8^2$$
$$+ 3a_1^3 a_4 a_6 a_7 a_8 + a_1^3 a_5 a_6^2 a_8 - a_1^3 a_6^3 a_7 + 3a_1^2 a_2^2 a_7^2 a_8 + 3a_1^2 a_2 a_3 a_5 a_8^2$$
$$- a_1^2 a_2 a_3 a_6 a_7 a_8 + a_1^2 a_2 a_4 a_5 a_7 a_8 - 3a_1^2 a_2 a_4 a_6 a_7^2 - 2a_1^2 a_2 a_5^2 a_6 a_8$$
$$+ 2a_1^2 a_2 a_5 a_6^2 a_7 + a_1^2 a_3^2 a_4 a_8^2 - 2a_1^2 a_3 a_4^2 a_7 a_8 - a_1^2 a_3 a_4 a_5 a_6 a_8 + a_1^2 a_3 a_4 a_6^2 a_7$$
$$+ a_1^2 a_4^3 a_7^2 + a_1^2 a_4^2 a_5^2 a_8 - a_1^2 a_4^2 a_5 a_6 a_7 - a_1 a_2^3 a_7^3 - 3a_1 a_2^2 a_3 a_5 a_7 a_8$$
$$+ 2a_1 a_2^2 a_3 a_6 a_7^2 + a_1 a_2^2 a_4 a_5 a_7^2 + a_1 a_2^2 a_5^3 a_8 - a_1 a_2^2 a_5^2 a_6 a_7 - a_1 a_2 a_3^3 a_8^2$$
$$+ 2a_1 a_2 a_3^2 a_4 a_7 a_8 + a_1 a_2 a_3^2 a_5 a_6 a_8 - a_1 a_2 a_3^2 a_6^2 a_7 - a_1 a_2 a_3 a_4^2 a_7^2$$
$$- a_1 a_2 a_3 a_4 a_5^2 a_8 + a_1 a_2 a_3 a_4 a_5 a_6 a_7$$